NATIONAL COOPERATIVE HIGHWAY RESEARCH PROGRAM
REPORT **66**

IDENTIFICATION OF FROST-SUSCEPTIBLE PARTICLES IN CONCRETE AGGREGATES

REFER TO:	Action	Info	Int
Mat'ls & Resh Engr.			
Mat'ls Engr.			
Asst. Mat'ls Engr.		✓	
Research Engr.			
Assoc Resh Engr.			
Soils Engr.		✓	WJ
Geologist		✓	BB
Testing Engr.		✓	
Office Mgr.			
Quality Control		✓	W
Project Devlp.			
E. I. T.			

HIGHWAY RESEARCH BOARD
NATIONAL RESEARCH COUNCIL
NATIONAL ACADEMY OF SCIENCES—NATIONAL ACADEMY OF ENGINEERING

NATIONAL COOPERATIVE HIGHWAY RESEARCH PROGRAM
REPORT 66

IDENTIFICATION OF FROST-SUSCEPTIBLE PARTICLES IN CONCRETE AGGREGATES

T. D. LARSON AND P. D. CADY
THE PENNSYLVANIA STATE UNIVERSITY
UNIVERSITY PARK, PENNSYLVANIA

RESEARCH SPONSORED BY THE AMERICAN ASSOCIATION
OF STATE HIGHWAY OFFICIALS IN COOPERATION
WITH THE BUREAU OF PUBLIC ROADS

SUBJECT CLASSIFICATION:
CEMENT AND CONCRETE
MINERAL AGGREGATES

HIGHWAY RESEARCH BOARD
DIVISION OF ENGINEERING NATIONAL RESEARCH COUNCIL
NATIONAL ACADEMY OF SCIENCES—NATIONAL ACADEMY OF ENGINEERING 1969

NATIONAL COOPERATIVE HIGHWAY RESEARCH PROGRAM

Systematic, well-designed research provides the most effective approach to the solution of many problems facing highway administrators and engineers. Often, highway problems are of local interest and can best be studied by highway departments individually or in cooperation with their state universities and others. However, the accelerating growth of highway transportation develops increasingly complex problems of wide interest to highway authorities. These problems are best studied through a coordinated program of cooperative research.

In recognition of these needs, the highway administrators of the American Association of State Highway Officials initiated in 1962 an objective national highway research program employing modern scientific techniques. This program is supported on a continuing basis by funds from participating member states of the Association and it receives the full cooperation and support of the Bureau of Public Roads, United States Department of Transportation.

The Highway Research Board of the National Academy of Sciences-National Research Council was requested by the Association to administer the research program because of the Board's recognized objectivity and understanding of modern research practices. The Board is uniquely suited for this purpose as: it maintains an extensive committee structure from which authorities on any highway transportation subject may be drawn; it possesses avenues of communications and cooperation with federal, state, and local governmental agencies, universities, and industry; its relationship to its parent organization, the National Academy of Sciences, a private, nonprofit institution, is an insurance of objectivity; it maintains a full-time research correlation staff of specialists in highway transportation matters to bring the findings of research directly to those who are in a position to use them.

The program is developed on the basis of research needs identified by chief administrators of the highway departments and by committees of AASHO. Each year, specific areas of research needs to be included in the program are proposed to the Academy and the Board by the American Association of State Highway Officials. Research projects to fulfill these needs are defined by the Board, and qualified research agencies are selected from those that have submitted proposals. Administration and surveillance of research contracts are responsibilities of the Academy and its Highway Research Board.

The needs for highway research are many, and the National Cooperative Highway Research Program can make significant contributions to the solution of highway transportation problems of mutual concern to many responsible groups. The program, however, is intended to complement rather than to substitute for or duplicate other highway research programs.

This report is one of a series of reports issued from a continuing research program conducted under a three-way agreement entered into in June 1962 by and among the National Academy of Sciences-National Research Council, the American Association of State Highway Officials, and the U. S. Bureau of Public Roads. Individual fiscal agreements are executed annually by the Academy-Research Council, the Bureau of Public Roads, and participating state highway departments, members of the American Association of State Highway Officials.

This report was prepared by the contracting research agency. It has been reviewed by the appropriate Advisory Panel for clarity, documentation, and fulfillment of the contract. It has been accepted by the Highway Research Board and published in the interest of an effectual dissemination of findings and their application in the formulation of policies, procedures, and practices in the subject problem area.

NCHRP Project 4-3(2) FY '66
NAS-NRC Publication 1740
Library of Congress Catalog Card Number: 78-602410

FOREWORD

By Staff

Highway Research Board

The problem of determining the acceptability of aggregates for use in portland cement concrete that is to be subjected to freezing and thawing, plus other forms of exposure in cold climates, continues to plague highway agencies. Although the tests described in this report and the companion *NCHRP Report 65* are not a panacea for all of the problems associated with concrete where freezing conditions prevail, they do provide a basis for an initial screening to determine the acceptability of new aggregate sources and for identifying the particular undesirable aggregate fractions that might be removed to provide improved concrete performance. It is hoped that the suggested use of a battery of tests will permit a more discriminate use of aggregate with resulting improved utilization of current aggregate supplies and improved performance of concrete pavements and structures. Both reports will be of primary interest and value to highway materials and testing engineers. Concrete researchers and bridge engineers concerned with the problem of bridge deck deterioration should also find the report of special interest.

The durability of exposed concrete is influenced by several factors but performance records indicate that, as the predominant constituent of the mix, the qualities of the coarse aggregate significantly affect the ability of concrete to successfully resist damage caused by alternate freezing and thawing. Excessive volume change of the coarse aggregate particles is considered the primary physical factor contributing to early concrete deterioration. For this reason, the objective of NCHRP Projects 4–3(1) and 4–3(2), begun in 1963 at Virginia Polytechnic Institute and The Pennsylvania State University, respectively, was to develop a quick test or tests for identifying aggregates which undergo destructive volume change when frozen in concrete.

Curently used aggregate tests can be grouped in two general categories. Some tests are based on a correlation between some identifiable and measurable aggregate property characteristic and known field performance of the aggregate. Others depend on simulating the service environment to which the concrete will be exposed as a method of predicting field performance. Such tests can be performed either on individual aggregate particles or on the sample representative of an aggregate source.

From the practicing highway engineer's point of view, the ideal solution to the problem would involve a "black box" with dials that could be set for the environment and structure form under consideration. Aggregates would be funneled in, some sort of separation or modification would occur and out would come streams of acceptable and rejected aggregates. However, a single basic aggregate property that could be used to trigger a black box mechanism has not been found.

In view of the importance of tests both on individual aggregate particles or fractions and on the entire sample from a source, two separate studies were under-

taken. The work at Virginia Polytechnic Institute under Project 4–3(1), published as *NCHRP Report 65,* concentrated on development of a one-cycle freeze test for predicting the durability or performance of concrete using coarse aggregates as produced from a particular source. The interim report was published as *NCHRP Report 12,* "Identification of Aggregates Causing Poor Concrete Performance When Frozen." The companion study at The Pennsylvania State University under Project 4–3(2), reported herein, dealt with individual aggregate fractions, both from the standpoint of correlation with known field performance and the simulating of field environmental conditions. The Pennsylvania State University interim report was published as *NCHRP Report 15,* "Indentification of Concrete Aggregates Exhibiting Frost Susceptibility."

The V.P.I. One-Cycle Slow-Freeze Test

During the V.P.I. program, a one-cycle slow-freeze test was developed and evaluated by correlating results with durability factor obtained from ASTM Method C290 (the standard freezing and thawing test in water). The one-cycle test involves fabrication of 3 x 3 x 16-inch concrete specimens using aggregates representative of the aggregate source and, after 7-day curing, placing the specimens in a conventional household deep freeze chamber. Strain measurements are made with a Whittemore strain gauge at 5- to 15-minute intervals over a 4-hour cooling period. From the data collected, the cumulative length change is plotted vs time and the time slope, b_t, determined as the minimum slope that can be found within a $\frac{1}{3}$-hour or greater time range.

Nineteen coarse aggregates from different parts of the country and representing varying performance histories were used to fabricate 336 specimens during the evaluation program. A sufficiently strong relationship was found between the time slope and the durability factor at 100 freeze-thaw cycles to indicate that the one-cycle test could be used as a screening test where durability factor can be considered as a measure of potential field performance. The method has the advantages of simplicity, minimal equipment requirements, and relative rapidity. It is described in detail in *NCHRP Report 65.*

The Pennsylvania State University Program

Several methods of identifying frost-susceptible aggregate particles were evaluated using two approaches. First, a test method simulating field conditions was investigated with the objective of providing a test that would directly indicate probable field performance. This method was developed from the T. C. Powers' concept of a field exposure test first published in 1955. It involves the casting of specimens using the aggregate under study and, after curing, cooling at 5 F per hour while automatically recording temperatures and dilation (strain). Test cycles are run every two weeks until expansion beyond the elastic limit occurs. A means was developed to determine the period of frost immunity that could be expected for the aggregate under study. The work on development and evaluation of the slow cooling method was performed with carefully selected homogeneous aggregate fractions because it was felt that beneficiation of an aggregate would be by removal of deleterious fractions. Also, only by evaluating relatively homogeneous fractions can reproducible results amenable to statistical interpretation be obtained. A complete description of the slow-cooling method is contained in this report in a generalized form so that it may be used to identify particles or fractions to be removed

through beneficiation or for aggregate source acceptance testing. It requires expensive, sophisticated equipment and takes a relatively long time to perform; however, it appears to have the ability to distinguish between "marginal" aggregates—a very significant asset.

The second approach by Pennsylvania State consisted of an investigation of several rapid techniques for obtaining relative frost-susceptibility ratings of individual particles or fractions. It was found that a skilled petrographer, although untrained in concrete technology, could rate the relative frost susceptibility of homogeneous aggregate fractions by megascopic examination and could be of invaluable service in preparing aggregates for testing and in evaluating the test results. A combination of permeability coefficient and volumetric particle expansion provided good relative rating of the aggregate fractions, and vacuum saturated absorption resulted in only a slightly inferior rating.

The use of the petrographer or a single particle test to provide a "good" or "poor" rating for an aggregate fraction requires minimal equipment and time, but this approach lacks the ability to discriminate in the "intermediate" performance range. It will be useful in identifying deleterious particles that should be removed in beneficiation. For the acceptance of an aggregate source, field correlation of performance with the amount of a particular aggregate fraction under consideration must be obtained.

Application of Findings

On the basis of research conducted under these two projects and supported by field experience, it is apparent that no single test having the attributes of speed and simplicity is available or likely to be developed in the immediate future for predicting the performance of coarse aggregate in portland cement concrete that is subjected to freezing and thawing exposure. A systematic approach to acceptance testing, taking advantage of a trained petrographer and using a battery of tests, seems to be indicated. There is also a need for an accumulation and evaluation of field performance under a variety of exposure conditions for correlation with test data on aggregate sources and individual fractions.

The accompanying figure indicates the test possibilities applicable to aggregate acceptance programs and how they might be used to meet varying objectives. A petrological examination of all sources is suggested as a first step. The left branch of the figure covers the large number of cases where general acceptance of a source is to be determined. If field performance information is available on aggregates with similar characteristics, a relative rating by two or more of the methods listed may be sufficient. The slow cooling (Powers) method may be used for cases where a period of frost resistance is desirable or no field experience is available for similar aggregates.

The right branch of the chart is appropriate for cases where economical aggregate sources in the "intermediate" field performance range must be evaluated. The sample is separated into relatively homogeneous fractions and the performance of each rated by single-particle tests and the slow cooling method when a determination of frost resistance is desired. The effect on performance of the deleterious fractions should be evaluated and beneficiation required if the source material is not considered suitable for the exposure anticipated.

It is hoped that this study of available and recently developed aggregate test

methods will result in a reduction of unnecessary testing and the saving of time and money in some instances where a rapid screening approach will be adequate for acceptance or rejection of an aggregate source. In addition, the more sophisticated method for predicting coarse aggregate performance in concrete under simulated field conditions should provide a basis for better utilization of marginal aggregate sources and improving the performance of highway pavements and structures under a variety of exposure conditions.

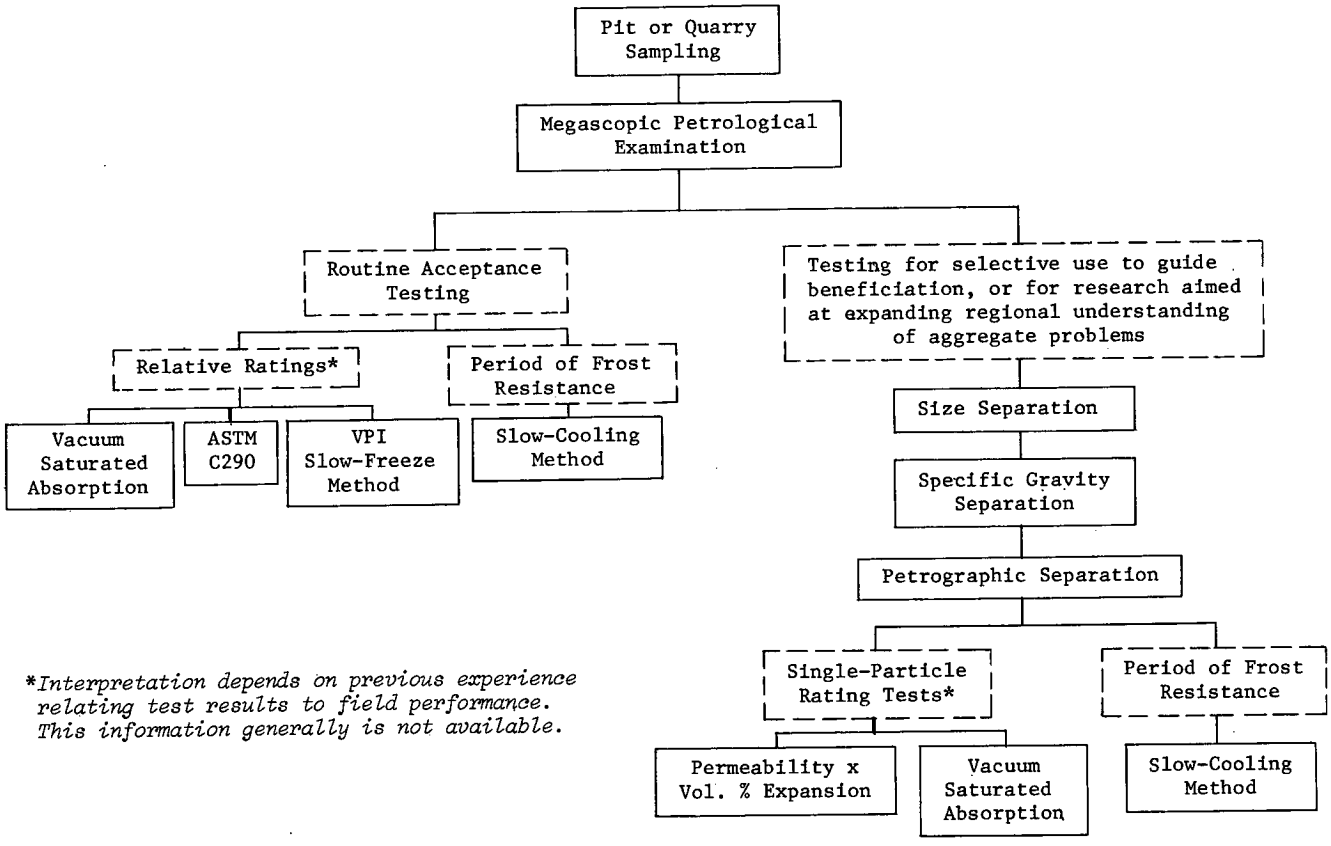

Procedural approaches to frost-susceptibility tests.

CONTENTS

ACKNOWLEDGMENTS

The research reported herein was done under NCHRP Project 4-3(2) by The Pennsylvania State University, with Thomas D. Larson, Associate Professor of Civil Engineering, as Principal Investigator. The laboratory work and data analyses were performed by P. D. Cady, Research Assistant, and T. A. Bakr, R. M. Eshbach, and S. C. Woo, Graduate Assistants in Civil Engineering. Petrographic analysis was done by F. B. Galas, Graduate Assistant in Mineralogy.

The facilities and equipment of the Department of Civil Engineering were employed, and the project was under the general administration of Dr. E. F. Osborn, Vice President for Research, The Pennsylvania State University.

IDENTIFICATION OF FROST-SUSCEPTIBLE PARTICLES IN CONCRETE AGGREGATES

CHAPTER ONE

INTRODUCTION

The research reported herein consists largely of extensive evaluation of test methods that are described in *NCHRP Report 15* (*7*). That report and *HRB Special Report 80* (*8*) are considered to be a necessary preface to this one since they treat the philosophy and problems of aggregate testing in detail.

Two approaches to the problem of identifying frost-susceptible aggregate particles were followed. In one, relatively homogeneous aggregate fractions were tested in concrete under simulated field conditions, with two objectives: (1) to develop a rational test method incorporating elements of field exposure conditions, and (2) to establish meaningful bases of aggregate performance against which other test methods could be compared. The second approach explored the potentialities of single aggregate particle tests as simple, quick, and economical means of identifying frost-susceptible aggregates.

The basic mechanisms of frost action were also investigated. This work, which has less direct application than the other studies, was aimed toward supplying information needed to develop and interpret any practical test method. However, it was made particularly appropriate by some current research that appeared to contradict the principal existing theory of frost action in aggregates.

All of the experimental work carried out by the project employed aggregate test particles and fractions that were carefully sorted according to mineralogical type and structure. This procedure evolved from the major assumption of the test rationale: that in most aggregates displaying poor frost resistance in concrete, only a small percentage of the particles is involved in the destructive process. There are, of course, aggregates in which virtually all of the particles are frost-sensitive, but they behave so poorly that their deleterious nature is easily exposed by normal characterization testing. Of primary concern here is the vast majority of aggregates, which display their deleterious tendencies only upon occasion and can be beneficiated if the offending particles can be identified.

Because of their nature, the test methods that are evaluated in this report require the services of a trained petrographer to identify and separate the many petrographic subtypes that are present in most problem-causing mass aggregate samples.

CHAPTER TWO

RESEARCH FINDINGS

The results of the investigations that are outlined in Chapter One are briefly reviewed here.

The test data and detailed analyses for each case are given in Appendix A through Appendix F.

PETROLOGICAL STUDIES

Petrological Fractionation of Aggregates

The as-received aggregates were subjected to three fractionation processes to obtain relatively uniform test frac-

tions. This procedure was employed so that findings could be related to characteristics, and so that processes for beneficiation might ultimately be developed. By mechanical analysis each aggregate was classified into two size groups—½ to ¾ in., and ¾ to 1 in. Each size group was then separated by heavy-medium flotation into two specific gravity fractions—less than or equal to 2.50, and greater than 2.50. Finally, each of the four specific gravity and size fractions was handpicked into mineralogical groupings by a trained petrographer, but one who was unfamiliar with the specific problems of aggregates in concrete.

Prediction of Frost Sensitivity

On the basis of mineralogical type, structural characteristics, and weathering, the petrographer attempted to rate the fractions of each aggregate in terms of frost sensitivity. In two-thirds of the cases his predictions proved to be correct. The lack of agreement in the other third of the cases is not considered serious, because the behavior of the aggregate fractions in these was essentially similar and ratings were therefore meaningless.

Petrology of Failed Concrete Specimens

Twenty-two of the concrete specimens tested by the slow-cooling method (see next section) were sliced longitudinally with a diamond saw and submitted to petrological examination. The specimens selected had displayed exceptionally large dilations during freezing. The purpose was to determine which particles were instrumental in producing the dilations. The offending particles usually constituted less than one-third of the total number of particles in the specimen. In several cases, one or two particles (5 to 10 percent of the total exposed) were effective in disrupting the concrete. These observations indicate that even finer petrological segregation of the test aggregates may sometimes be warranted.

Four modes of failure were observed in the failed specimens: aggregate shattering, bed-plane splitting, aggregate-paste bond failure, and general disintegration of the paste matrix. The last mode occurred in combination with one or more of the first three, and apparently depended upon the degree of damage incurred by the concrete. It was predicted that aggregate shattering and bed-plane splitting would be prevalent in rocks of low permeability, and that aggregate-paste bond failures would occur primarily with highly permeable aggregates. Investigation supported this assumption.

SLOW-COOLING METHOD

The slow-cooling method, formerly referred to as the Powers method, was evaluated in the research reported in *NCHRP Report 15* (*7*). Because of its flexibility and rational base, it was believed to be the most reliable indicator of the field performance of aggregates. One of the goals of the study reported herein was to write a test specification for the method, but additional information had to be secured before that could be done. The following subsections summarize the related research findings.

Applicability of Test Method

To determine the ability of the slow-cooling method to differentiate between the relatively homogeneous aggregate fractions, described previously, with respect to their frost susceptibility, a statistical analysis of variance was performed on the test data for 21 aggregate fraction types. The analysis showed that this test is capable of differentiating between aggregates at the 95 percent significance level for any given number of freeze-thaw (F-T) cycles.

Effect of Mixture Variability

The reproducibility of the test method as related to concrete mixture was investigated statistically. Analysis of variance of the test data revealed that mixture is not a significant source of variation, but aggregate type is significant at the 95 percent confidence level.

Number of F-T Cycles vs Soaking Period

The effect of the frequency of F-T cycles for a given period of soaking was investigated in a specially designed experiment. Two levels of F-T frequency were employed, differing by a factor of ten. The length of the soaking period exerts the dominant effect on frost susceptibility. The effect of F-T frequency varied from none to moderate. Considering the extreme range of the experimental F-T frequencies, differences between the number of cycles employed in the laboratory and the number encountered in the field should have negligible effect on the test results.

Effect of Specimen Drying

Specimens soaked and then dried at 75 F and 50 percent relative humidity for seven days were much less susceptible to frost damage than those that were soaked continuously. On the average, even after 11 weeks of F-T testing the dried specimens dilated only 3 percent as much during freezing.

Determination of Test End Point

One purpose of the experiments was to develop a technique for determining the end of the period of frost immunity in the slow-cooling test. In *NCHRP Report 15* it was pointed out that dilation during cooling increases linearly with soaking time, up to a certain point. Beyond this point—termed the *critical point*—dilation increases exponentially with increased soaking time. The critical point was therefore believed to signify the end of the period of frost immunity. It was also suggested that the frost-induced stress equals the tensile strength of the concrete at the critical point. Since the same mixture-proportioning criteria were used for all of the test specimens, the tensile strength of the concrete should have been nearly constant. Hence, the dilation at the critical point (critical dilation) should be constant, regardless of aggregate type.

The critical points for 124 test specimens were determined by computerized curved fitting, and the critical dilation was indeed found to be relatively constant at about 422 μin. The theoretical critical dilation, based on the

principles of elasticity and estimated elastic constants, was 420 μin. When the length of the period of frost immunity and the critical dilation were correlated with the last-cycle dilation, the critical dilation failed to correlate even at the 90 percent significance level. This supports the contention that critical dilation is independent of aggregate type. The period of frost immunity correlated significantly at better than the 99.9 percent level, indicating the dependence of this variable on the frost sensitivity of the aggregate.

Number of Test Specimens Needed

The number of specimens needed to assure statistical integrity depends upon the confidence interval and significance level chosen. It is a function of the inherent variability of the slow-cooling method. For the experiments conducted in this research, an average of eight specimens would be required for a confidence interval of the mean of $\pm$ 20 percent at the 95 percent significance level.

RAPID TEST METHODS

Single-particle tests were investigated to determine if a test possessing the attributes of speed, simplicity, and economy could be found that would reliably indicate frost susceptibility. Two of the techniques—pore studies and linear particle expansion—were developed in the work reported in *NCHRP Report 15* (7), but both needed further evaluation covering a wide range of aggregate types. A third method—volumetric particle expansion—was initiated and evaluated in the work discussed here.

Pore Studies

Permeability, porosity, and absorption data were collected for particles representing 24 aggregate fractions of widely varying frost susceptibility and mineralogical type, using the techniques described in *NCHRP Report 15*. Correlation of the test data with a measure of frost susceptibility (average dilation per cycle in the slow-cooling test) revealed that vacuum saturated absorption values of less than 1 percent indicate highly durable aggregates; values greater than 5 percent indicate highly susceptible aggregates. For vacuum saturated absorption between 1 and 5 percent, a combination of permeability and absorption, or permeability and apparent porosity, is the best indicator of frost susceptibility.

Preliminary tests were carried out to evaluate some of the variables in the permeability test method. The nature of the permeating fluid (nitrogen or air), drying of the specimens, and extended periods of percolation at high pressure (150 psi for 1 hr) had no observable effect on the test results.

Linear Particle Expansion Tests

The method of testing linear particle expansion described in *NCHRP Report 15* showed considerable promise. The most attractive features of the method were its simplicity and low cost, inasmuch as simple dial gauges were found to be capable of differentiating particle expansions with sufficient accuracy. In the earlier evaluation, however, few aggregate types having an exceptionally wide range of frost susceptibility were used. To determine whether the linear particle expansion test was capable of producing data that correlated with the frost susceptibility of concrete made with the aggregates, tests were run on 22 aggregate fractions of varying frost susceptibility and mineralogical type. The data collected included dilation and permanent length change during freezing as measured by linear variable differential transformers (transducers), and permanent length change measured with 0.0001-in. dial gauges. The average dilation per cycle in concrete specimens that were made with the aggregate was taken as the measure of frost susceptibility.

All three of the measured test variables were found to correlate with frost susceptibility at the 99 percent significance level or higher, thus supporting the results of the earlier work. However, one of the faults of that work was still present in this analysis. Two of the samples displayed extremely high frost sensitivity; the other 20 ranged from very durable to moderately sensitive. Because of the obvious effect of two such outliers on the correlation, the analyses were repeated without the highly sensitive aggregates. None of the three measured variables then correlated at the 99 percent significance level, and only permanent length change as measured with transducers was found to correlate at the 95 percent level.

An important defect of existing unconfined-particle tests is their failure to take into account the effect of permeability. Aggregates with high permeability coefficients show little expansion in unconfined tests because excess water is easily expelled from them during freezing. The same aggregates encased in concrete could be very deleterious, owing to excessive stresses produced by water expelled into the relatively impermeable paste surrounding them. Each of the measured variables was therefore multiplied by $\log_{10}$ (permeability $\times 10^6$) and the correlations were rerun, again without the two exceptional aggregates. The dilation and the transducer permanent length change measurements modified by permeability were then found to correlate at the 99 percent significance level, but the dial-guage permanent length change measurements still failed to yield a significant correlation coefficient even at the 95 percent level.

Comparison of the dilations measured along the predicted axes of maximum dilation with those measured along orthogonal axes revealed that the amount of expansion of saturated aggregate particles differs significantly along preferred axes. This test also showed that the petrographer had been able to predict quite accurately the performance and the direction of maximum expansion of single aggregate particles.

Volumetric Particle Expansion Tests

In linear particle expansion tests the aggregate particles do not expand equally in all directions during freezing. Although a trained petrographer usually can predict the direction of maximum expansion, this factor still contributes to the variability of the test method. In the work reported herein the volumetric expansion of saturated aggregate particles was investigated as a possible means of reducing this source of variability.

The equipment developed for the volumetric particle expansion test consisted of a cooling bath, in which the temperature was maintained at 15 ± 0.5 F, and a mercury-displacement dilatometer. Saturated aggregate particles were placed in the dilatometer at room temperature. The dilatometer was then lowered into the cold bath, and changes in the volume of the dilatometer and its contents were observed as changes in the level of mercury in a capillary tube over a 25-min period. Five particles each of 22 different aggregate fractions were tested in this manner. Precalibration of the dilatometer permitted conversion of the test data into volumetric changes in the aggregate particles. The volumetric dilations were converted to percentage volumetric dilation to eliminate the effect of the varying size of aggregate particles.

The percentage volumetric dilation correlated significantly at better than the 99.9 percent level with frost susceptibility as measured by the average dilation per cycle of concrete specimens made with the aggregates. Even without the two outliers mentioned before, a significant correlation existed at the 99.9 percent level, although the correlation coefficient was considerably diminished (from 0.960 to 0.685).

To take into account aggregate permeability, the percentage volumetric dilations were multiplied by $\log_{10}$ (permeability $\times 10^6$). With the two outliers eliminated, these data again correlated significantly with frost susceptibility at the 99.9 percent level, and a marked improvement in the correlation coefficient was obtained (0.864).

Comparison of the Rapid Test Methods

To determine which of the rapid test methods is the best indicator of frost susceptibility, each was correlated with frost susceptibility as measured by the average dilation per cycle in the slow-cooling test. Only the data from aggregates in the intermediate frost-susceptibility range (5 to 100 μin. dilation per cycle) were used in these analyses, because highly durable and highly susceptible aggregates are easy to detect by simple absorption tests. Aggregates in the intermediate range are difficult to discriminate and require more elaborate tests. The correlations in Table 1 suggest that the combination of permeability and volumetric particle expansion provides the best indication of frost susceptibility.

It should be pointed out that all of the rapid methods are capable only of rating aggregate particles. To obtain estimates of concrete performance under various exposure conditions, a rational approach such as the slow-cooling method must be used.

BASIC MECHANISMS OF FROST ACTION IN CONCRETE

Because all of the standardized methods that are now used to test frost susceptibility have a degree of empiricism, they provide only qualitative indications of frost susceptibility. Quantitative test methods demand a rational approach; that is, simulation of field conditions in the laboratory. The validity of model-prototype relationships depends on a clear understanding of the basic mechanisms involved.

Current Theories

The hydraulic pressure theory, proposed by Powers (*9*), was found to agree well with observed phenomena in laboratory freeze-thaw tests (*7*). In 1965, however, Dunn and Hudec (*3*) suggested an entirely different mechanism of frost destruction, based on research conducted at Rensselaer Polytechnic Institute (RPI). Using differential thermal analysis techniques on clay-bearing dolomitic limestones, they found that frost susceptibility varied inversely with the percentage of freezable water, an apparent contradiction of the hydraulic pressure theory. To account for this the RPI researchers proposed a destructive mechanism based on the temperature-dependent volume change of adsorbed water. Because of the short range of the physicochemical forces involved in adsorption phenomena, this mechanism would be operative only in minute intergranular spaces of the aggregates. In further support of their theory, Dunn and Hudec showed that frost susceptibility varied directly with the percentage of the contained water in the adsorbed state.

Experiments

Two sets of experiments were carried out to evaluate the conflicting hypotheses of Powers and of Dunn and Hudec regarding the basic mechanisms of frost action. First, adsorption isotherms were determined for duplicate specimens of 31 aggregate subfractions at two temperatures—35 F and 75 F. The second phase consisted of determining by differential thermal analysis (DTA) techniques the amount of freezable water contained in nine different saturated aggregate fractions encased in concrete. The tests were run in duplicate, and up to seven freeze-thaw cycles were run on each specimen.

When the adsorption data were compared with frost susceptibility as measured by the average dilation per cycle in the slow-cooling test, the correlation was not significant at the 95 percent level; this indicated that the mechanism proposed by Dunn and Hudec was not the predominant destructive effect for the aggregates in this study. In the differential thermal analysis tests, the amount of water frozen correlated directly with frost susceptibility at the 99.9 percent significance level, but the percent of freezable water failed to correlate with susceptibility even at the 90 percent level. Both of these results favor the hydraulic pressure mechanism and oppose the adsorbed water theory. Further evidence of the dependence of destruction on freezing was observed in the invariable coincidence of the onset of freezing with expansion of the specimens.

Dual-Mechanism Theory

From the experimental results, the hydraulic pressure theory appears adequate to account for the destructive mechanism of frost action. It was observed, however, that the concrete specimens continued to dilate after the DTA equipment indicated that freezing had ceased. Although the post-freezing expansions were usually only a small percentage of the total dilation, their presence points to the existence of a second destructive mechanism that is not related to freezing.

That mechanism is believed to be the "ordering" or adsorption of unfrozen bulk water on ice and pore surfaces, an idea similar to Dunn and Hudec's postulation, but with one major difference. Dunn and Hudec explained the destructive effect as being the result of the temperature-dependent volume change of adsorbed water. The theory set forth here is that the destructive effect is the result of hydraulic pressure generated by an increase in the specific volume of water during the change of state from bulk water to adsorbed water. This hypothesis was found to be compatible with experimental observations and thermodynamic theory.

Apparently, then, in the frost-destruction of concrete two mechanisms are involved, in varying degrees. The extent to which one or the other will predominate depends on the pore and sorption characteristics of the aggregate. Dunn and Hudec's findings can thus be explained by the fact that all of the aggregates they tested were clay-bearing dolomitic limestones, which favor the adsorption mechanism.

TABLE 1

CORRELATION OF RAPID TEST METHODS WITH SLOW-COOLING METHOD FOR AGGREGATES IN INTERMEDIATE FROST-SUSCEPTIBILITY RANGE

RAPID TEST AND VARIABLE	SIGNIFICANCE LEVEL (%)
Linear particle expansion test:	
Log_{10} (permeability $\times 10^6$) $\times$ permanent length change	<90
Pore studies:	
Log_{10} (permeability $\times 10^6$) $\times$ vacuum saturated absorption	<90
Vacuum saturated absorption	95-98
Volumetric particle expansion test:	
Percent volumetric expansion	<90
Log_{10} (permeability $\times 10^6$) $\times$ percent volumetric expansion	99-99.9

CHAPTER THREE

INTERPRETATION, APPRAISAL, AND APPLICATION

PETROLOGICAL EVALUATION OF AGGREGATES

The percentage of deleterious particles in a frost-susceptible aggregate is usually small; therefore, for test purposes, the frost-sensitive particles must be identified and concentrated into relatively homogeneous test fractions. A trained petrographer's services are indispensable for this task, as was demonstrated in this research. His job was to establish fractionation criteria for the test aggregates and to perform megascopic petrologic separations. Although time limitations precluded examination of aggregate thin sections, it is believed that a catalog of microscopic characteristics could be a valuable diagnostic tool, at least on a local or regional basis (*NCHRP Report 15* contains thin section analyses that support this view).

When frost-sensitive particles have been identified, the fractionation criteria and the test results can provide guidelines for the beneficiation of aggregates. The economics of beneficiation would be indicated by the amount of deleterious material to be removed.

APPRAISAL OF TEST METHODS

Slow-Cooling Method

The slow-cooling method is the most realistic approach to testing aggregates for frost susceptibility, because the test conditions can be varied to approximate field conditions. Developmental work on the method was done using hand-picked, relatively homogeneous aggregate fractions. In field applications this procedure will yield valuable information concerning selective aggregate usage and will guide beneficiation processing. For those situations where it is desired that testing be performed on conventional samples, the procedure is equally applicable, however. An earlier problem with this method was defining the end of the period of frost immunity. Experiments now indicate that this point is reached when the dilation of the concrete equals the elastic strain limit of the concrete in tension. The critical dilation can be calculated from the specimen dimensions and the elastic constants of the concrete, or it can be approximated in microinches by 70 times the specimen length in inches.

The slow-cooling method is time consuming and expensive in terms of equipment and labor, but it is the only technique now available for evaluating the performance of marginal aggregates under simulated field conditions. The advantage of being able to choose the most economical aggregates that this method shows to be satisfactory for specific uses will far outweigh the cost and time factors in most cases, especially in locations where sources of high quality aggregates are scarce.

Detailed test specifications for the slow-cooling method are given in Appendix B.

Rapid Test Methods

The percentage volumetric expansion of aggregate particles in combination with permeability is the best rapid indicator of frost susceptibility. The indicating variable in this pro-

cedure is volume percent expansion multiplied by $\log_{10}$ (permeability coefficient $\times 10^6$). For vacuum saturated specimens, values of this variable up to 0.75 indicate durable aggregates. Aggregates of low-to-moderate frost susceptibility range from 0.75 to 2.00. Values above 2.00 are highly susceptible aggregates. Although this method readily detects the low-to-moderate range of frost susceptibility, it provides only a relative rating of the aggregates. Estimates of actual field behavior cannot be made by this or any other rapid method now known.

As others have long suggested, vacuum saturated absorption, one of the simplest tests, is an excellent indicator of highly durable and highly frost-sensitive aggregates. Absorption values below 1 percent invariably identify durable aggregates; those above 5 percent seem to always indicate poor frost resistance.

RECOMMENDED APPLICATION PROCEDURES

Test procedures for determining the frost susceptibility of concrete aggregates will vary with the objectives of the testing agency and the intended use of the data. These objectives might range from developing relative frost-susceptibility ratings to predicting performance under specified field conditions of pit or quarry samples. In another instance the objective might be to identify frost-susceptible particles from various aggregate sources to investigate the economics and means of beneficiation. Clearly, a different approach is required for each purpose.

From the experience gained in this research, the procedures shown in Figure 1 are recommended for various objectives. Regardless of the approach, the services of a trained petrographer are essential.

INTERPRETATION OF FROST-ACTION MECHANISMS

Hydraulic pressure generated by a restricted flow of bulk water ahead of an advancing ice front in aggregate or paste pores is usually the dominant mechanism in frost destruction of concrete. Hydraulic pressure resulting from an increase in the specific volume of water during adsorption of water on ice and mineral surfaces can also produce distress in some aggregates, and in certain cases it may be the dominant cause of damage. The clay-bearing dolomitic limestones studied by Dunn and Hudec were of such a nature as to be more vulnerable to the effects of the latter mechanism. One of the nine aggregate fractions tested in this research behaved similarly.

The experiments indicated that in any given case the dominance of one or the other of the two mechanisms depends upon four properties of the aggregate: relative adsorption, total pore volume, average pore size, and pore size distribution.

Four basic curve patterns for freezing vs time or temperature (differential thermograms) were observed, and these appear to be related to pore size distribution. Further experimentation is required to verify this observation. If the existence of such a relationship can be proved, the DTA technique could be used as a diagnostic tool for evaluating aggregate performance as it relates to pore characteristics.

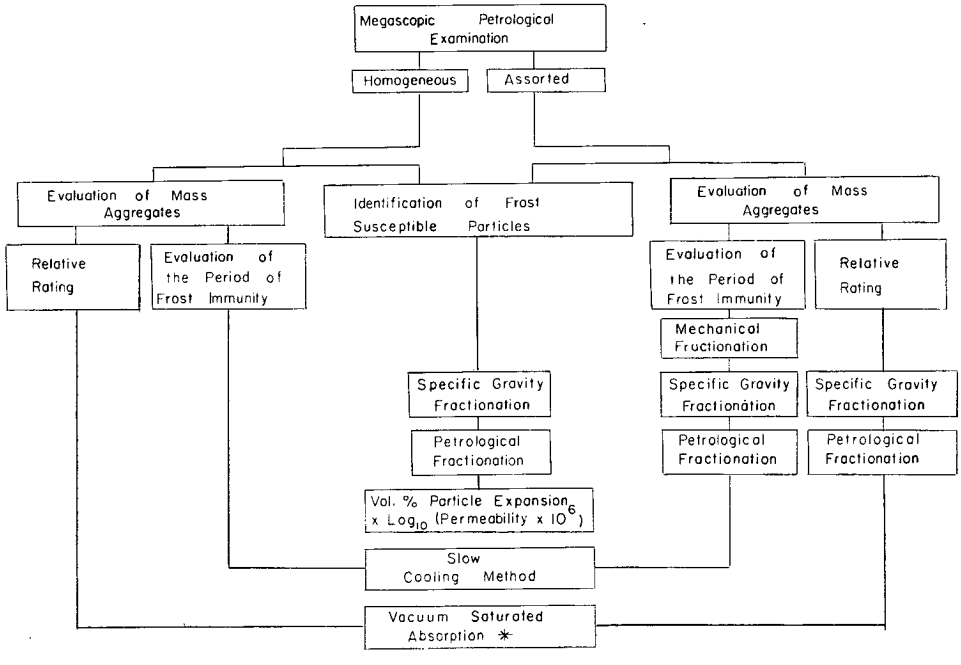

*Recommended alternatives: ASTM C290 rapid freeze-thaw test or VPI slow-freeze method.

Figure 1. Procedural approaches to frost-susceptibility tests.

CHAPTER FOUR

CONCLUSIONS AND SUGGESTED RESEARCH

CONCLUSIONS

The following specific conclusions are drawn from the total research effort of this project:

1. A reliable quantitative evaluation of aggregate frost susceptibility can be achieved by the slow-cooling method, originally proposed by Powers and extensively investigated in this research.
2. The more economical rapid test methods yield relative ratings of aggregates with respect to frost susceptibility. The single-particle test of permeability and volume change during cooling is the most discriminating of the rapid methods studied. Vacuum saturated absorption is only slightly inferior as a basis for performance rating.

Several general conclusions may also be stated. The prospects are poor of finding a single quick, simple, economical and reliable method of identifying frost-susceptible aggregate particles. As Powers noted in 1955, frost susceptibility is not a basic property of an aggregate. The degree of saturation and the prevailing environmental conditions are as important as the deleterious characteristics of the aggregate. "Frost susceptibility" is therefore meaningless unless it is defined in conjunction with the environmental conditions related to freezing and accessibility to water.

Except in extreme cases, rapid tests are not likely to provide a sound basis for accepting or condemning aggregates with respect to their frost susceptibility. They can be employed to make a relative choice from among several aggregates, but they give only the assurance of knowing which of those aggregates has the best chance of resisting frost action. The question of whether that aggregate will perform satisfactorily under specified conditions in the field must be answered by field experience or by a laboratory test, such as the slow-cooling method, that closely simulates the anticipated conditions of field exposure.

The services of a trained petrographer are an absolute necessity for any agency that is responsible for passing judgment on aggregate durability. Untried or less desirable aggregates will often need beneficiation before they can be used in concrete construction, and selection of a beneficiation process depends on identification of the deleterious particles and determination of the pertinent physical properties. This procedure entails professional judgment in the realm of petrology. The role of the petrographer in routine frost-susceptibility testing is equally important. The research carried out by this project has shown conclusively that petrological fractionation of raw aggregate materials is necessary for meaningful evaluation of frost susceptibility.

SUGGESTED RESEARCH

Further research on rapid methods for identifying frost-susceptible aggregate particles does not appear to be warranted at this time. Significant progress has been made in defining the basic mechanisms of frost destruction of concrete containing frost-susceptible aggregates. Future research should be directed toward extending this knowledge and exploiting it to devise more rational test methods. If a reliable, quick, and economical test is ever to be found, it must evolve from a better understanding of aggregate characteristics, failure mechanisms, and environmental factors.

Because testing conditions for meaningful laboratory tests must be related to field exposure conditions, it is recommended further that research be carried out to develop environmental exposure indices.

REFERENCES

1. CORDON, W. A., "Freezing and Thawing of Concrete—Mechanisms and Control." *Am. Conc. Inst. Monograph 3* (1966).
2. CROW, E. L., DAVIS, F. A., and MAXFIELD, M. W., *Statistics Manual.* Dover (1960).
3 DUNN, J. R., and HUDEC, P. P., "The Influence of Clay on Water and Ice in Rock Pores." *Physical Research Report RR 65-5,* New York State Dept. of Public Works (1965).
4. DUNN, J. R., and HUDEC, P. P., "Rock Deterioration—Frost Versus Sorption Sensitivity." Paper presented at HRB meeting, Washington, D. C. (Jan. 1967).
5. HELMUTH, R. A., "Capillary Size Restrictions on Ice Formation in Hardened Portland Cement Pastes." *Monograph 43,* Vol. II, Nat. Bur. Standards (1960) pp. 855-869.
6. HELMUTH, R. A., "Dimensional Changes of Hardened Portland Cement Pastes Caused by Temperature

Changes." *Proc. HRB,* Vol. 40 (1961) pp. 315-336.
7. LARSON, T. D., BOETTCHER, A., CADY, P. D., FRANZEN, M., and REED, J. R., "Identification of Concrete Aggregates Exhibiting Frost Susceptibility." *NCHRP Report 15* (1965).
8. LARSON, T. D., CADY, P. D., FRANZEN, M., and REED, J. R., "A Critical Review of Literature Treating Methods of Identifying Aggregates Subject to Destructive Volume Change When Frozen in Concrete, and a Proposed Program of Research." *HRB Spec. Report 80* (1964).
9. POWERS, T. C., "Basic Considerations Pertaining to Freezing and Thawing Tests." *Proc. ASTM,* Vol. 55 (1955) pp. 1132-1155.
10. POWERS, T. C., and BROWNYARD, T. L., "Studies of the Physical Properties of Hardened Portland Cement Paste." *Jour. Am. Conc. Inst.,* Vol. 18 (1946) pp. 469-504.
11. POWERS, T. C., and HELMUTH, R. A., "Theory of Volume Changes in Hardened Portland Cement Paste During Freezing." *Proc. HRB,* Vol. 32 (1953) pp. 285-297.
12. SCHOLER, C. H., "The Durability of Concrete." *Proc. HRB,* Vol. 10 (1930) pp. 132-163.
13. VALORE, R. C., "Volume Changes in Small Concrete Cylinders During Freezing and Thawing," *Jour. Am. Conc. Inst.,* Vol. 21, No. 6 (1950) pp. 417-434.
14. VERBECK, G., and LANDGREN, R., "Influence of Physical Characteristics of Aggregates on Frost Resistance of Concrete." *Proc. ASTM,* Vol. 60 (1960) pp. 1063-1079.
15. WALKER, R. D., "Identification of Aggregates Causing Poor Concrete Performance When Frozen." *NCHRP Report 12* (1965).
16. WENDLANDT, W. W., *Thermal Methods of Analysis.* John Wiley & Sons (1964).

APPENDIX A

TEST AGGREGATES

SOURCES OF TEST AGGREGATES

In *NCHRP Report 15* (7) it was recommended that more aggregate types covering a wide range of durability should be used for further evaluation of frost-susceptibility tests. The initial step in the research here reported was to contact state highway departments and other agencies in 38 states in the U.S.A. for information on sources of aggregates of intermediate-to-high frost susceptibility. The area that was covered by this survey is shaded in Figure A-1. From the information received, test aggregates were obtained from 15 sources in 12 states, indicated by the code numbers in Figure A-1. Each pair of code numbers represents one aggregate source, as is explained in the next section.

Aggregate selection was based primarily on the following criteria (in order of decreasing importance): (1) known or suspected frost susceptibility; moderately susceptible aggregates given preference; (2) mineralogical type; wide variety of types sought; (3) geographical distribution; wide distribution preferred.

IDENTIFICATION AND CLASSIFICATION

To deal with the great number and variety of aggregates and fractions used for testing, a complex classification system was developed. It evolved directly from the handling and treatment that the aggregate received in the course of testing.

Each unsorted aggregate was given a source code-number pair on its arrival at the laboratory. The aggregate labeled "River Gravel, Wyoming," for example, was designated 05-06. The sample was then put through a sieve analysis from which two size fractions, ¾ to 1 in. and ½ to ¾ in., were retained and labeled A and B, respectively. The A and B fractions were individually vacuum-saturated and subjected to specific gravity separation, using a heavy-liquid medium adjusted to 2.50 sp gr. The "sink" retained the even integer of the number pair, and the "float" retained the corresponding odd integer. The resulting test aggregate would thus have four fractions, each with its own sieve size and specific gravity separation characteristics and each labeled according to a matrix like that shown in Figure A-2.

The four fractions for a given aggregate were hand-sorted into petrologic types and subtypes according to the following procedure. Each aggregate particle was initially classified as igneous, sedimentary, or metamorphic and given the corresponding symbol I, S, or M. For particles that were undifferentiable and fractions with few particles (so that subdivision was impractical), the symbol X was used. Each petrologic type was then subdivided according to specific rock types identified by two-letter symbols added to the first letter. In the designation SSs, for example, the first S indicates that the rock is sedimentary, and the symbol Ss indicates a sandstone. Similarily, the symbol MQz indicates a metamorphic quartzite, the symbol SDl indicates a sedimentary dolomite.

The igneous rocks were classified according to a slightly different procedure. The phaneritic (coarse grained) and presumably intrusive igneous rocks were given a two-letter

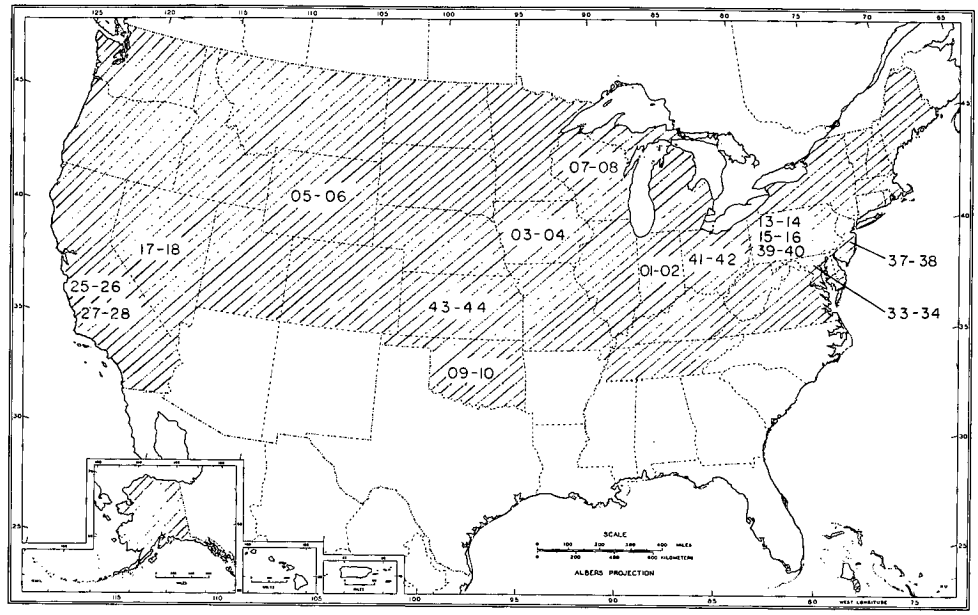

Figure A-1. Sources of test aggregates.

symbol in addition to the initial designation I. For the aphanitic (fine-grained to glassy) and presumably extrusive igneous rocks, a one-letter symbol was added to the initial I. A granite would thus be labeled IGr, and a scoria would be labeled IS. A complete list of the rock types encountered, and their corresponding symbols, is given in Table A-1.

Occasionally, a given rock type could be realistically subdivided into two or more subtypes on the basis of unique weathering or textural, mineralogical, or structural characteristics. In such cases, the subtypes were numbered 1, 2, 3, etc., in the supposed order of increasing frost susceptibility.

This classification system, although more elaborate than is usually considered ideal, enabled unambigous labeling of every test aggregate fraction handled in the laboratory. A fraction labeled B05SSs3, for example, could be unmistakably identified as follows:

B	Particle size	½ to ¾ in.
05	Odd number	< 2.50 sp gr
SSs	Petrological type	Sedimentary sandstone
3	Specific designation	Cherty sandstone

FRACTION	SIZE (IN.)	FLOAT <2.50 SP GR	SINK >2.50 SP GR
A	3/4 to 1	A-05	A-06
B	1/2 to 3/4	B-05	B-06

Figure A-2. Classification matrix example, river gravel, Wyoming.

The petrographic breakdown of the test aggregates as received is given in Table A-2. Percentage data like those in the table could be a valuable aid in judging beneficiation processes and their cost.

The petrographer was capable of visually rating aggregate subfractions with respect to their frost susceptibility (1, 2, 3, etc.). In two-thirds of the cases, the order he predicted proved to be correct; in the remaining third, the susceptibility of the subfractions was so nearly the same that the rating was meaningless anyway.

PETROLOGY OF THE TEST FRACTIONS

The megascopic petrology of each of the aggregate fractions selected for testing is described in the following paragraphs.

02SLs1. Relatively pure calcitic limestone, well indurated, medium to dark gray; massive, finely laminated in part, slightly dolomitic in part. A few particles are lithographic, essentially nonfossiliferous, only slightly vuggy or fractured, and generally fresh. Occurs as angular chips and fragments.

02SLs2. Very pure calcitic limestone, pale gray to white, slightly leached, and porous or vuggy. Some particles are oolitic, stained with oxidized limonite. Occurs as subangular to subrounded particles.

03SLs1. Relatively pure calcitic limestone, well indurated, medium to dark gray; massive, some particles finely laminated, dolomitic in part, lithographic in part; essentially nonfossiliferous, partly encrinal; only slightly vuggy or fractured. Occurs as angular chips.

04SLs4. Clastic limestone, medium to dark gray, encrinal; coarse to finely clastic matrix, often sandy, sometimes finely bedded; slightly crumbly particles. Occurs as rounded to subrounded particles.

05SSs1 + 2 and *06SSs1 + 2.* SSs1, buff, tan, or pale gray

TABLE A-1

CODE SYMBOLS FOR ROCK TYPES

Igneous (I)		*Sedimentary* (S)	
ICc	Travertine, etc.	SAk	Arkose
IGr	Granitic	SBr	Breccia
IL	Lava	SCc	Calcite, coarse vein and vug
IMf	Mafic	SCg	Conglomerate
IP	Pumice	SCh	Chert
IQ	Chalcedony, opal, etc.	SCl	Claystones (bentonites, etc.)
IS	Scoria	SDl	Dolomite
IT	Tuff	SGw	Graywacke
IVQ	Vein quartz	SLm	Limonite concretions
Metamorphic (M)		SLs	Limestone
MAm	Amphibolite	SMc	Miscellaneous
MGn	Gneiss	SSh	Shale
MMb	Marble	SSs	Sandstone
MMc	Miscellaneous	SSt	Siltstone
MPl	Phyllite		
MQz	Metaquartzite	*Other*	
MSh	Schist	ASg	Slag
MSl	Slate	X	Undifferentiated
MVQ	Vein quartz		

medium to fine-grained sandstone, including low-grade orthoquartzite and metaquartzite and uniform tough siltstone; only banding is opaques and manganese stains, some oxidation; tough, coherent, well indurated; some with carbonate cement. SSs2, red sandstone, including some metaquartzite and siltstone; medium to fine grained, tough and coherent; occurs mostly as pebbles, some chips.

06SSs3 + SCh. SSs3, cherty sandstone and siltstone; tough pebbles, highly cherty but variable in chert content; some highly fractured, weathered, or vuggy. SCh, chert; fractured, dense, angular fragments.

08SDl2. Weathered dolomite, generally massive and well indurated, very little fracturing; fossiliferous in part; moderately to strongly weathered to buff color; generally quite vuggy. All are recrystallized.

10SLs1. Coarse clastic limestone, medium to dark gray, brownish in part; medium to coarse clastic texture, clastic material largely broken shell material; very coarse grained, recrystallized in part, slightly argillaceous; occasional subtle and sporadic contorted fine bedding and stylolite zones; generally tough and well indurated. Occurs as subangular to subrounded particles.

14SStl 1 + 2. SStl, green sandstone and siltstone, including low-grade phyllites, shales, and slates; mostly fine grained, slightly argillaceous; pronounced fine bedding or fissility; occurs as tablets and plates. SSt2, red sandstone and siltstone, highly argillaceous or ferruginous; mostly fine-grained siltstone, usually very fissile; occurs as tablets and plates.

14SSs3 + SAk. SSs3, weathered sandstone, including all sandstone-like rocks such as siltstone, phyllite, and arkose; generally highly porous. SAk, arkose and conglomerate, highly variable and mostly felsic; generally highly weathered.

16SSs1. Sandstone and siltstone, gray, greenish gray, red, buff; only slightly weathered; medium to fine grained (some coarse grained), some with uniform grain size; generally tough, indurated, and coherent; more or less equant or elongate particles, some slightly platy. Occurs as rounded pebbles, pebble fragments, and angular chips.

16SSs2. Argillaceous siltstone and sandstone, greenish gray, buff, red, and brown; medium to fine grained, many crumbly, tough; some rich in clay. Occurs invariably as plates, tablets, and wafers; most particles highly rounded to subrounded.

18IS + IT. IS, scoriaceous and pumiceous lava, black, dark gray, purple, and red; scoriaceous fragments red with jagged fracture surfaces; pumiceous fragments rounded to subrounded; generally massive, aphanitic and vitrophyric, contains a few phenocrysts; variable vesicularity. IT, tuff and tuff-lapillite, well indurated, red or red and black; angular, uneven fragments; includes crystalline tuffs.

25IL1. Hornblende andesite, somewhat variable color: pale gray, dark gray, purplish gray, and grayish black. Generally massive and structureless, occasionally shows flow banding; rich in hornblende (phenocryst), sometimes oxidized; slightly pumiceous in part. Occurs as angular to subangular fragments.

25IP1. Pumice, a hornblende andesite in composition; highly vesicular (pumiceous), crumbly, and generally brittle; often fractured. Occurs as rounded to subrounded pebbles.

28MSh. Biotite schist; fresh, weathered, and deuterically altered fragments, all very rich in biotite. Includes fragments of biotite adamellite, in which biotite exceeds half the total volume.

28IGr1. Biotite adamellite; fresh, generally rich in biotite, but it is less than half the total volume. Contains minor hornblende and pyrite. Equant angular fragments; slightly gneissic.

34MAm1. Hornblende amphibolite; tough, fresh, angular to subangular, very slightly schistose; irregular banding, mostly granulose; essentially monominerallic hornblende, but with traces of felsic and carbonate minerals and iron sulfides.

34MAm2. Hornblende amphibolite, quite schistose; minor plagioclase, biotite, and chlorite. Contains quartz veins and accessory pyrite.

38MGn2. Gneiss, poor quality, medium to coarse grained; quartzofeldspathic but (1) very low in quartzofeldspathic minerals (relatively rich in micas and amphibolites), or (2) very strongly weathered and altered (clays, iron oxides), or (3) generally coarse to very coarse grained and porous, occasionally schistose.

40SSs2. Shaly sandstone and siltstone, greenish gray, fine grained; some moderately weathered; very few contain calcareous cement; generally quite fissile. Occurs as subrounded to rounded lenticular platy particles.

42SLs2. Clastic and weathered limestone, pale gray to grayish buff; largely clastic, fragmental, and encrinal; moderately weathered, slightly leached in part. Includes fragments containing porous cherts, also large coral frag-

TABLE A-2

PETROGRAPHIC BREAKDOWN OF AGGREGATES AS RECEIVED

SOURCE	AGGREGATE	WEIGHT % BY SIZE AND SP GR 3/4 to 1 IN. <2.5	3/4 to 1 IN. >2.5	1/2 to 3/4 IN. <2.5	1/2 to 3/4 IN. >2.5
01-02	SLs1 Limestone	1.2	23.8	1.5	54.8
	SLs2 Weathered limestone	1.5	4.8	2.2	9.6
	SCc Coarse vein calcite	0.0	0.2	0.0	0.0
	SCh Chert	0.1	0.1	0.1	0.3
03-04	SLs1 Massive limestone	1.6	32.4	2.4	36.3
	SLs2 Lithographic limestone	0.0	3.1	0.0	2.2
	SLs3 Encrinal limestone	0.0	1.8	0.0	3.0
	SLs4 Clastic limestone	0.2	3.6	0.2	3.8
	SLs5 Conglomeritic limestone	0.1	2.9	0.1	3.5
	SLs6 Weathered limestone	0.0	1.4	0.0	1.3
	SLs7 Coral	0.0	0.0	0.0	0.0
05-06	SSs1 Buff sandstone	9.8	26.2	8.7	19.2
	SSs2 Red sandstone	1.4	5.4	1.1	4.5
	SSs3 Cherty sandstone, siltstone	1.1	1.9	1.8	5.4
	SCh Chert	0.2	1.5	0.5	2.3
	SGw Graywacke	0.3	1.5	0.3	1.3
	SCl Claystone	0.1	0.0	0.2	0.0
	SMc Miscellaneous	0.4	0.0	0.5	0.0
	SAk Arkose	0.0	1.2	0.0	0.8
	MGn Gneiss	0.0	0.1	0.0	0.2
	MQz Metaquartzite	0.0	0.8	0.0	0.6
	IGr Igneous	0.0	0.4	0.0	0.2
07-08	SD11 Dolomite	0.0	54.0	0.0	38.6
	SD12 Weathered dolomite	0.0	3.6	0.0	3.7
	X Undifferentiated	0.1	0.0	0.1	0.0
09-10	SLs1 Coarse clastic limestone	0.0	33.2	0.0	36.9
	SLs2 Bedded massive to clastic limestone	0.0	13.0	0.0	11.5
	SLs3 Weathered limestone	0.0	1.8	0.0	3.7
13-14	SSs1 Massive sandstone	0.0	10.6	0.0	22.7
	SSt1 Green sandstone, siltstone	0.0	7.1	0.0	15.8
	SSt2 Red sandstone, siltstone	0.0	4.3	0.0	8.7
	SSs2 Orthoquartzite	0.0	3.3	0.0	5.4
	SSs3 Weathered sandstone	0.0	1.5	0.0	5.7
	SAk Arkose and conglomerate	0.0	0.5	0.0	2.0
	SCh Chert	0.0	0.2	0.0	1.4
	MQz Pink metaquartzite	0.0	0.6	0.0	0.5
	MGn Gneiss	0.0	0.7	0.0	2.3
	IGr Igneous	0.0	0.2	0.0	0.6
	X Undifferentiated	1.1	0.0	4.7	0.0
15-16	SSs1 Sandstone and siltstone	8.4	20.8	5.4	10.0
	SSs2 Argillaceous sandstone, siltstone	4.1	8.5	2.4	4.1
	SSs3 Weathered sandstone	2.1	3.8	1.7	1.2
	SLs Limestone	0.0	1.2	0.0	0.3
	SAk Arkose and conglomerate	0.0	1.0	0.0	0.3
	ASg Slag	0.1	0.0	0.0	0.0
	SCh Chert	1.5	1.7	2.9	2.2
	SLm Limonite concretion	0.4	1.5	0.2	0.6
	MQz Quartzite	0.0	1.2	0.0	0.5
	MGn Gneiss	0.0	3.0	0.0	1.0
	MPh Phyllite	1.3	0.7	1.4	0.7
	IGr Felsic igneous	0.0	1.8	0.0	0.7
	IMf Mafic igneous	0.0	0.6	0.0	0.5
17-18	IL Lava	1.6	12.6	1.3	6.6
	IS Scoriaceous and pumiceous lava	5.0	25.9	4.4	21.3
	IT Tuff and tuff-lapillite	0.5	2.7	0.6	3.3
	ICc Travertine	0.6	3.7	1.6	7.7
	IQ Chalcedony, opal	0.0	0.2	0.0	0.2
25-26	IL1 Hornblende andesite	24.8	3.4	12.5	3.9
	IL2 Hornblende andesite, oxidized	11.1	0.5	13.1	0.7
	IP1 Pumice	11.1	0.0	8.9	0.0
	IP2 Pumice, oxidized	1.9	0.0	3.9	0.0
	IX Miscellaneous	1.5	0.6	1.8	0.3
27-28	IGr1 Biotite adamellite, fresh	0.0	38.5	0.0	28.3
	IGr2 Biotite adamellite, altered	0.0	9.6	0.0	4.4
	MSh Biotite schist	0.0	11.7	0.0	7.5
33-34	MAm1 Amphibolite	0.0	50.0	0.0	30.9
	MAm2 Schistose amphibolite	0.0	10.5	0.0	7.8
	MVQ Vein quartz	0.0	0.3	0.0	0.3
37-38	SSs1 Pure sandstone	0.0	4.1	0.0	4.2
	SSs2 Shaly sandstone	0.0	3.5	0.0	4.9
	SGw Graywacke	0.0	1.7	0.0	1.3
	SCg Conglomerate and arkose	0.0	4.4	0.0	5.4
	SCh Chert	0.0	0.1	0.0	0.1
	MQz Metaquartzite	0.0	0.4	0.0	0.1
	MGn1 Gneiss, fresh	0.0	15.3	0.0	12.3
	MGn2 Gneiss, poor quality	0.0	16.5	0.0	16.8
	IGr Igneous, mostly granite	0.0	3.8	0.0	3.7
	X Undifferentiated	0.4	0.0	0.9	0.0
39-40	SSs1 Massive sandstone, siltstone	2.1	28.3	1.5	16.9
	SSs2 Shaly sandstone, siltstone	2.2	14.4	2.0	17.4
	SLs Limestone	0.0	3.2	0.0	1.4
	SAk Arkose and conglomerate	0.0	0.4	0.0	0.4
	SSh Shale	0.0	0.1	0.1	0.1
	SCh Chert	0.3	0.4	0.3	0.5
	SMc Miscellaneous	0.2	0.2	0.2	0.2
	MQz Metaquartzite	0.0	1.6	0.0	1.2
	MGn Gneiss	0.0	2.0	0.0	1.0
	IGr Igneous	0.0	0.8	0.0	0.4
41-42	SLs1 Massive fresh limestone	0.0	18.1	0.0	36.1
	SLs2 Clastic weathered limestone	0.0	13.0	0.0	19.4
	SLs3 Strongly weathered limestone	0.0	4.8	0.0	4.8
	SCh Chert	0.0	2.9	0.0	0.1
	X Undifferentiated	0.4	0.0	0.4	0.0
43-44	SLs1 Massive compact limestone	0.0	11.7	0.0	4.7
	SLs2 Massive granular limestone	0.0	25.4	0.0	19.6
	SLs3 Stylolitic limestone	0.0	7.9	0.0	7.2
	SLs4 Fine clastic bedded limestone	0.0	13.8	0.0	8.8
	X Undifferentiated	0.2	0.0	0.4	0.0

ments and fragments of coarse calcitic fracture fillings. Generally not vuggy, but somewhat porous. Chemically quite reactive to HCl. Occurs as subangular to subrounded particles.

44SLs3 + 4. SLs3, stylotitic limestone, medium to dark gray; massive, compact, nearly lithographic to granular (clastic); occurs in angular fragments and chips. SLs4, clastic bedded limestone, fine to very fine grained, finely bedded; contains thin carbonaceous layers; occurs as subangular fragments, occasionally as medium-grained clastic coquinoidal limestone.

PETROLOGY OF FAILED CONCRETE SPECIMENS

Twenty-two of the concrete specimens tested by the slow-cooling method were sliced longitudinally with a diamond saw and subjected to megascopic petrological examination. The specimens selected were those that displayed exceptionally high frost susceptibility, as evidenced by dilation during cooling and by fracturing. The purposes of this study were to ascertain which particles were instrumental in producing failure and to determine whether they possessed petrologically distinguishable characteristics. The various modes of failure were also observed and recorded.

Deleterious Characteristics

Twelve of the specimens examined involved three of the aggregate test fractions: 02SLs1, 05SSs1 + 2, and 40SSs2. Comparison of the aggregate particles that were exposed by sectioning these specimens produced some interesting observations regarding the deleterious characteristics of frost-sensitive aggregates. Usually, only a few particles were instrumental in producing the destruction, and these were readily identifiable by the crack patterns.

Specimens that contained the 02SLs1 aggregate tended to display bond failure at the aggregate-paste interface, as shown in Figure A-3. This indicates the ability of the aggregate to accommodate freezing stress elastically, and points to expulsion of water from the aggregate as the cause of failure. With this aggregate such a result would be expected, in view of its high permeability and absorption (3.353×10^{-4} darcys and 3.848 percent, respectively). There are, however, a few petrologic subtypes of this limestone that are susceptible to internal failure during freezing. These subtypes include very fine-grained particles with a microconglomeratic or microbreccia fabric, very fine-bedded particles, and less well-indurated and more porous particles. An example of a very fine-bedded particle that was fractured by freezing stresses is shown in Figure A-4.

In aggregate 05SSs1 + 2 the distress was usually traceable to a few sensitive particles. Close inspection revealed that these particles invariably were fine to very fine grained, massive, poorly consolidated, and extensively weathered. Apparently, they are near the lowest limit of the textural range designating sandstones, making it difficult to determine whether they are well-sorted sandstones. In general, deleterious particles of this type produced bond and paste fractures, as shown in Figure A-5. Again, the high permeability and absorption (1.658×10^{-3} darcys and 5.692 percent, respectively) would have led to prediction of the observed results. In one specimen (No. 106) failure was produced by extensive internal fracturing of a single particle composed of siltstone and chert. This exception is shown in Figure A-6. The chert is the dark portion of the particle.

Aggregate 40SSs2, like 05SSs1 + 2, owes its deleterious tendency to a small percentage of its constituents. Examination of the sectioned specimens showed that about 90 percent of the particles were very well bonded and only about 20 percent of them suffered internal fracturing. Particles that were damaged, apparently by frost action, invariably fractured along very fine bedding planes. The fractures usually occurred in sets and traversed the entire length of the particle. These fracture zones were usually found along the finer-grained bedding planes of the particles, which were often oxidized or cemented by calcite. The fine bedding planes can be seen on the marked aggregate particles in Figure A-7, but evidence of failure is almost totally absent in these particles. As would be expected from the internal fracturing of the aggregates, 40SSs2 has low permeability (1.394×10^{-6} darcys) and moderate absorption (3.016 percent).

Modes of Failure

Four modes of failure were observed: shattering of aggregates, bed-plane splitting, aggregate-paste bond failure, and disruption of the paste matrix. All four modes are illustrated in the photographs of deleterious particles (Figs. A-1 through A-7). Additional striking examples of the first two modes are shown in Figures A-8 and A-9. Aggregate 44SLs3 + 4 (permeability, 1.005×10^{-5} darcys; absorption, 2.343 percent) is shown in Figure A-8. Figure A-9 is aggregate 16SSs1 (permeability, 2.053×10^{-5} darcys; absorption, 2.432 percent). An example of extensive aggregate-paste bond failure and disruption of the paste matrix is shown in Figure A-10, which is aggregate 04SLs4 (permeability, 2.227×10^{-4} darcys; absorption, 3.604 percent). Notice that in each case the observed mode of failure might have been anticipated from the permeability and absorption values.

Thin Sections

Time limitations prevented examination of thin sections of the aggregates as was done for *NCHRP Report 15* (*1*). Careful petrological fractionation, hand-picking of the test aggregates, and petrological examination of failed specimens were considered to be of greater importance. As was pointed out in *NCHRP Report 15*, however, thin-section examination might prove to be a valuable means of defining microscopic deleterious characteristics, a catalog of which could be useful in identifying frost-susceptible aggregates at least locally or regionally.

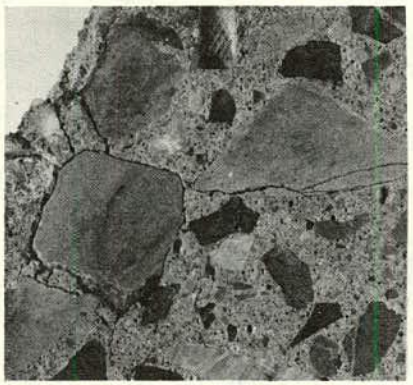

Figure A-3. Aggregate 02SLs1, specimen 140.

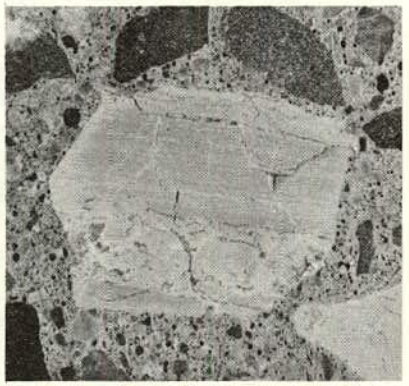

Figure A-4. Aggregate 02SLs1, specimen 112.

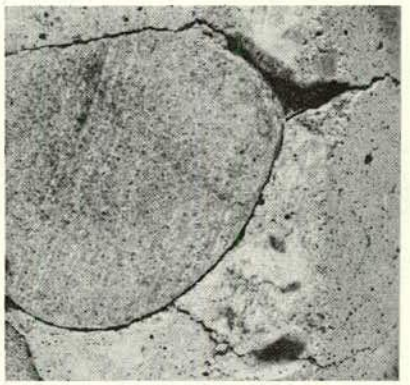

Figure A-5. Aggregate 05SSs1+2, specimen 110.

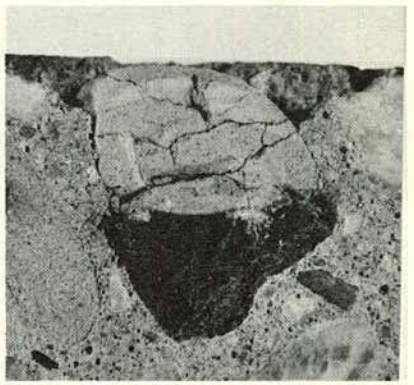

Figure A-6. Aggregate 05SSs1+2, specimen 106.

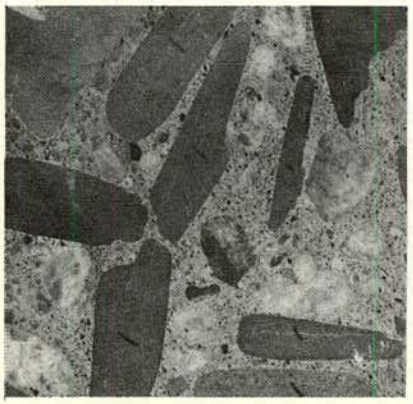

Figure A-7. Aggregate 40SSs2, specimen 160.

Figure A-8. Shattered particle, 44SLs3+4.

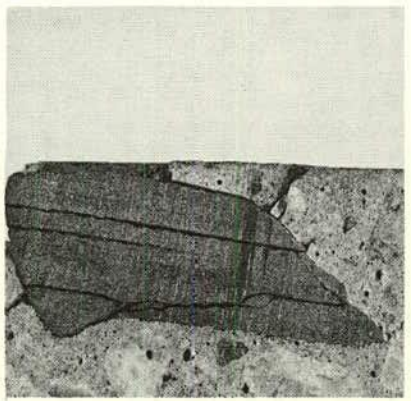

Figure A-9. Bed-plane splitting, 16SSs1.

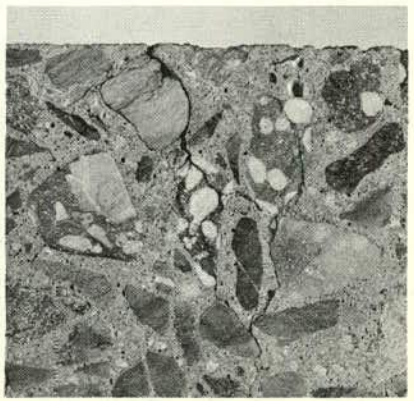

Figure A-10. Extensive bond failure, 04SLs4.

APPENDIX B

THE SLOW-COOLING METHOD

The slow-cooling method is based on the slow freeze-thaw test procedure proposed by Powers in 1955 (*9*). The Powers test and earlier evaluations of its applicability are reviewed in *NCHRP Report 15* (*7*). Proceeding from the results of that work, experiments were carried out for the dual purpose of clarifying several unexplored or incongruous aspects of previous research and probing the mechanisms of frost destruction. Although the experiments reported in *NCHRP Report 15* provided answers to many questions about equipment and test variables, many information gaps prevented the construction of meaningful test specifications.

With regard to the destructive mechanisms involved, the earlier experiments generally lent support to Powers' theory, but could not be considered proof of it. A mathematical model was developed for frost damage vs soaking time (in terms of freeze-thaw cycles) and was shown to be appropriate. This model, termed the "deterioration function," was believed to be a measure of the period of frost resistance. However, the limited experimental data with respect to specimen conditioning and length of the soaking period prevented developing the model to the point of providing a specification for the end point of the test.

Experimentation subsequent to the work described in *NCHRP Report 15* centered on two objectives. The first was to bridge the remaining technological gaps so that a meaningful test specification could be written; the second was to examine in greater detail the basic mechanisms of frost action.

DEVELOPMENT OF TEST SPECIFICATION

Before a specification for the slow-cooling test could be developed, the following areas of uncertainty had to be investigated:

1. Applicability of the test method to a wide variety of aggregate types.
2. Effects of mixture variability.
3. Effects of number of freeze-thaw cycles vs length of soaking period.
4. Effects of specimen drying.
5. Defining the end point of the test.
6. Specimen variability.

Experiments

To provide the information required to write a meaningful test procedure, experiments were carried out in three phases. Phase I was designed to evaluate the effect of varying numbers of freezing cycles per unit soaking time and the effect of a drying period on the frost susceptibility of concrete specimens made with the test aggregates. Phase II was designed to determine the ability of the test method to provide significant discrimination of aggregate fractions according to frost susceptibility. Phase III was designed to show the effects of long-term soaking and to evaluate the reproducibility of the test method. The data from all three phases were used to evaluate the deterioration-function concept, leading to definition of the test end point and a means of interpreting the test results. The experimental designs for the three test phases are shown in Figure B-1.

For all concrete mixtures the proportioning criteria were the same as those given in *NCHRP Report 15* (*7*). The fine aggregate and cement were also as described in *Report 15*. A single specimen size, 3 in. in diameter and 6 in. long, was used throughout.

The measured test variables included the following:

1. Permanent length change during the cooling and thawing cycle (except in Phase III).
2. Weight change during the cooling and thawing cycle (except in Phase III).
3. Total evaporable water content after the last cycle.
4. Dilations during cooling.
5. Temperatures at which dilations occurred.
6. Rate of length change with respect to temperature change before and after freezing.

The last three of these measurements were obtained from continuous recordings made during the cooling cycles. Detailed descriptions of the recording equipment and instrumentation are given in *NCHRP Report 15*.

EXPERIMENTAL RESULTS

Summaries of the measured data from the three test phases appear in Tables B-1 through B-3. The statistical analyses of these data were performed on Penn State's 7074/360 electronic computer system, using existing library programs. A special program was written to evaluate the deterioration-function concept. The data analyses relevant to each of the six problem areas are discussed in the following subsections.

Applicability of Test Method

The applicability of the test method refers to its ability to differentiate between aggregates with respect to frost susceptibility. The primary source of information relative to this point was Phase II, in which 21 different aggregate fractions were tested. Single-classification analysis of variance computations was executed for each of nine measured cycles, with total dilation as the test variable. The total dilation was found to be a significant source of variation at the 95 percent confidence level in each instance. The

TABLE B-1

DATA SUMMARY, PHASE I EXPERIMENTS

AGGREGATE AND MIX	INTERMED. CYC.	SPECIMEN NO.	NO. MEAS. CYCS.	LAST CYCLE MEASUREMENT TOTAL DIL. (μin.)	DIL. TEMP. (F)	SLOPE (μin./°F) INIT.	SLOPE (μin./°F) FIN.	ΔW (g)	ΔL (μin.)	EVAP. WATER (g)	AVERAGE MEASUREMENT TOTAL DIL. (μin.)	DIL. TEMP. (F)	SLOPE (μin./°F) INIT.	SLOPE (μin./°F) FIN.	ΔW (g)	ΔL (μin.)
40SSs2																
Mix 1	Yes	148	9	665	26.8	42	51	+0.3	-20	103.6	305	26.8	41	57	+0.7	-12
wet		150	9	805	26.6	46	49	+0.6	+20	108.3	430	26.6	41	57	+0.8	+9
		152	9	730	26.2	38	52	+0.4	+92	100.6	390	26.9	39	58	+0.8	+13
	No	154	11	940	27.4	44	35	+0.3	+24	105.3	535	27.2	42	54	+0.9	+5
		156	12	1000	27.6	40	37	+0.4	-2	101.0	540	27.2	42	50	+0.8	+6
		158	12	730	27.8	39	51	+0.4	-14	103.3	420	27.4	41	53	+0.7	+2
Mix 1	Yes	149	9	70	26.5	41	57	+0.1	+12	97.8	55	26.7	43	56	+3.9	-1
dry		151	9	50	26.2	41	55	+0.2	+25	91.3	45	26.9	39	57	+3.6	+1
		153	9	45	26.6	43	50	+0.1	+11	88.1	50	26.6	41	56	+3.5	+2
	No	155	9	80	25.6	37	60	+0.4	--	90.3	50	26.7	38	61	+3.8	-3
		157	9	70	26.3	41	59	+0.2	-10	91.4	40	26.8	41	58	+3.9	-2
		159	9	45	26.3	42	60	+0.4	--	97.3	45	26.9	42	62	+3.9	-15
Mix 2	Yes	160	9	1350	26.1	39	38	+0.1	+87	104.0	695	27.1	41	50	+0.1	-20
wet		162	9	1150	25.3	40	38	+0.6	+41	108.6	560	26.9	43	53	+0.3	+5
		164	8	550	26.9	39	65	+0.4	+5	108.3	330	26.8	40	61	+0.9	+5
	No	166	12	1320	27.5	44	38	+0.3	+12	105.3	685	27.4	42	43	+0.8	+1
		168	12	--	27.2	42	54	--	--	107.1	510	27.1	42	54	+0.9	-4
		170	12	760	27.4	39	57	+0.5	+8	105.3	390	25.7	40	56	+0.9	-1
Mix 2	Yes	161	9	60	26.5	39	54	+0.2	+6	97.2	55	27.0	40	61	+3.8	-15
dry		163	9	70	26.0	39	56	+0.3	+10	94.5	65	26.9	40	61	+4.0	-5
		165	9	40	26.8	40	55	+0.4	+37	96.8	55	26.7	42	62	+7.1	-4
	No	167	9	50	26.5	39	54	+0.1	+15	97.3	40	27.0	39	60	+4.1	-6
		169	9	60	26.4	38	56	-0.1	+12	94.5	40	27.1	40	59	+4.1	-18
		171	9	50	26.5	42	59	+0.2	+15	97.4	35	27.2	44	62	+4.2	-8
05SSs1+2																
Mix 1	Yes	124	9	2670	27.4	38	52	+0.5	+110	108.3	1400	27.0	44	56	+1.0	+72
wet		126	3	4140	27.0	49	39	+0.8	+495	105.5	2855	27.3	55	49	+2.3	+253
		128	5	4220	26.3	42	47	+0.8	+310	105.4	2420	26.7	48	51	+1.7	+177
	No	130	11	1000	27.5	43	45	-0.1	+18	111.3	645	27.2	43	54	+0.9	+17
		132	11	1670	27.4	42	39	+0.4	+31	107.4	850	24.4	42	50	+0.9	+20
		134	11	550	27.6	41	50	--	+24	--	840	27.2	43	57	+0.8	+6
Mix 1	Yes	125	9	60	26.6	35	55	+0.2	-10	86.9	65	26.6	41	56	+3.1	+8
dry		127	9	60	25.5	41	56	+0.5	-5	83.9	50	26.4	44	57	+2.9	+6
		129	9	80	26.1	42	62	+0.3	-6	84.9	60	26.8	44	60	+3.5	+10
	No	131	9	50	27.0	43	55	+0.2	-1	85.9	45	27.0	40	57	+3.6	+10
		133	9	25	27.2	43	58	+0.5	-1	87.3	50	27.3	44	56	+3.2	-2
		135	9	40	26.9	41	62	+0.1	+6	85.4	50	27.0	43	59	+3.5	+6
Mix 2	Yes	100	4	4630	26.0	43	35	+0.2	+513	107.9	2695	26.6	41	51	+2.0	+254
wet		102	4	3970	25.8	40	40	2.6	+180	108.4	2460	26.5	41	53	+2.4	+142
		104	4	3310	26.5	43	52	+0.7	+302	107.6	1985	26.7	41	58	+1.6	+165
	No	106	6	4030	27.5	44	41	+0.7	+105	112.4	2855	27.2	43	44	+1.5	+89
		108	10	1530	27.5	38	37	+0.9	+46	--	770	26.9	40	48	+0.9	+2
		110	7	3900	27.6	40	50	+0.2	+81	108.6	2750	27.3	38	52	+1.1	+61
Mix 2	Yes	101	9	50	25.7	49	54	+0.1	+30	84.8	70	26.5	40	57	+2.6	-7
dry		103	9	60	25.5	48	51	+0.3	+25	86.8	65	26.5	41	52	+3.0	-6
		105	9	40	26.5	52	56	+0.2	+11	87.3	55	26.6	43	60	+2.7	-7
	No	107	9	50	26.2	41	56	+0.3	+3	84.5	40	26.9	39	57	+2.5	-6
		109	9	40	26.2	42	52	+0.2	+1	85.6	40	27.1	39	58	+2.7	-10
		111	9	50	26.3	41	57	+0.2	+11	85.4	45	26.9	41	60	+2.8	-5
02SLs1																
Mix 1	Yes	112	9	3380	27.1	38	35	+0.9	+172	113.3	1635	26.3	34	43	+1.3	+113
wet		114	9	3800	27.2	38	41	+0.9	+227	116.3	1995	26.4	37	45	+1.2	+194
		116	9	4670	27.2	37	43	+1.1	+402	112.7	1880	26.5	35	48	+2.0	+189
	No	118	10	4200	27.5	32	35	+0.8	+96	106.5	1795	27.1	34	45	+1.3	+59
		120	12	2490	27.7	38	36	+1.0	+50	111.7	945	27.0	34	47	+1.2	+27
		122	12	1445	27.6	35	44	+0.5	+16	107.2	535	27.3	32	50	+1.1	+16
Mix 1	Yes	113	9	50	26.5	35	53	-0.2	+2	94.9	55	26.4	32	50	+3.7	+8
dry		115	9	75	27.0	37	52	+0.3	+35	98.0	55	26.5	35	52	+4.2	+1
		117	9	65	26.9	37	52	+0.4	+1	96.6	70	26.4	36	52	+4.0	+4
	No	119	9	50	27.0	32	45	+0.3	+25	91.0	40	27.0	32	49	+3.8	+5
		121	9	40	26.7	29	43	+0.5	+5	91.6	35	27.0	32	49	+4.1	+4
		123	9	30	26.3	34	45	+0.5	+1	93.1	35	27.1	35	50	+3.7	+1
Mix 2	Yes	136	9	3610	27.0	37	36	-0.3	+185	109.7	1910	26.9	35	42	+1.1	+139
wet		138	9	3900	26.0	33	34	+0.4	+283	111.1	1950	26.9	36	40	+1.3	+189
		140	9	4290	26.6	33	42	+0.9	+348	109.5	2245	26.9	33	44	+1.5	+174
	No	142	12	--	--	--	--	+0.2	+19	131.1	440	27.4	37	54	+1.0	+9
		144	12	--	--	--	--	+0.4	+32	107.4	510	27.1	36	50	+0.9	+13
		146	12	--	--	--	--	+0.2	+37	108.5	555	27.2	34	53	+0.9	+19
Mix 2	Yes	137	9	65	25.8	33	53	+0.3	-4	94.6	55	26.6	33	49	+3.8	+5
dry		139	9	40	26.0	33	57	+0.3	-9	94.9	35	26.9	33	51	+3.6	+7
		141	9	50	26.7	34	56	+0.4	-27	97.2	50	26.8	35	54	+4.5	-3
	No	143	9	50	26.5	33	46	+0.5	--	90.7	30	27.0	32	48	+4.4	+4
		145	9	35	27.5	32	47	+0.3	+10	90.8	25	27.2	34	49	+3.9	+1
		147	9	40	25.9	36	52	+0.3	+17	91.8	40	26.9	37	51	+4.4	-1

TABLE B-2

DATA SUMMARY, PHASE II EXPERIMENTS

AGGREGATE	SPECIMEN NO.	NO. MEAS. CYCS.	LAST CYCLE MEASUREMENT TOTAL DIL. (μin.)	DIL. TEMP. (F)	SLOPE (μin./°F) INIT.	SLOPE (μin./°F) FIN.	ΔW (g)	ΔL (μin.)	EVAP. WATER (g)	AVERAGE MEASUREMENT TOTAL DIL. (μin.)	DIL. TEMP. (F)	SLOPE (μin./°F) INIT.	SLOPE (μin./°F) FIN.	ΔW (g)	ΔL (μin.)
34MAm1	172	12	80	27.5	34	53	-2.0	+11	95.6	65	26.6	35	54	+0.1	-15
	173	12	110	27.0	31	51	-0.1	+51	94.8	95	26.7	34	51	+0.2	-13
	174	12	100	26.4	33	54	-0.2	+2	92.2	90	26.5	35	51	+0.2	-7
34MAm2	175	12	220	27.6	33	52	-0.3	-10	94.1	135	26.8	35	51	+0.2	-32
	176	12	670	27.7	35	47	+1.0	+31	97.6	340	27.0	33	46	+0.5	-1
	177	12	180	28.0	35	56	+0.5	-7	94.1	140	26.6	36	51	+0.4	-5
06SSs3+SCh	178	12	300	28.5	48	53	--	+15	96.4	190	26.9	42	59	+0.4	-18
	179	12	550	27.4	40	46	-0.1	+20	88.1	405	26.7	39	51	+0.3	+8
	180	12	370	28.3	47	53	--	+26	93.1	250	27.0	43	56	+0.5	-9
06SSs1+2	184	12	700	28.1	46	59	--	+64	101.7	380	27.0	44	64	+0.5	+7
	185	12	630	28.1	46	61	+0.1	+52	102.5	430	26.9	40	60	+0.5	-43
	186	12	1360	28.0	52	60	+0.1	+69	97.9	300	26.7	45	58	+0.6	+24
08SD12	196	12	140	27.0	36	47	--	+13	102.4	105	26.6	35	60	+0.5	-3
	197	12	340	26.8	33	50	+0.2	+7	106.8	205	26.8	33	60	+0.5	0
	198	12	590	26.8	36	57	-0.2	-292	105.3	630	26.1	37	62	+0.5	-82
38MGn2	214	12	250	27.6	41	48	+0.2	+26	101.3	190	26.8	39	55	+0.7	-13
	215	12	465	27.5	40	45	-0.2	+28	103.7	335	27.2	36	52	+0.5	0
	216	11	310	27.8	34	49	-0.2	-68	101.3	225	26.6	39	55	+0.5	-18
16SSs1	187	12	340	27.7	45	43	+0.4	-3	92.8	240	26.8	44	54	+0.5	-3
	188	12	1820	27.2	38	57	+0.5	+6	98.9	1265	26.9	39	46	+0.5	+23
	189	12	1230	27.4	42	33	+0.6	+34	95.0	520	26.6	44	52	+0.5	+12
16SSs2	193	12	1530	26.6	39	40	+0.4	+46	96.4	850	27.0	43	47	+0.6	+25
	194	12	1280	27.1	35	38	--	+86	99.7	655	27.0	39	46	+0.5	+16
	195	12	2700	26.5	31	22	-0.3	+74	100.1	1315	26.8	42	44	+0.5	+25
18IS+IT	217	12	130	27.0	33	46	-0.1	+20	109.8	100	27.2	33	53	+0.4	-5
	218	12	940	27.0	33	35	-0.6	+143	112.6	430	27.2	32	47	+0.5	-2
	219	12	960	26.4	33	34	--	+4	107.0	535	26.7	32	46	+0.7	+7
14SSs3+SAk	205	12	940	29.0	35	38	-0.2	+24	101.4	660	27.5	41	47	+0.2	+14
	206	12	550	29.0	36	45	+0.1	+18	94.7	430	27.3	39	50	+0.1	+2
	207	12	1080	28.0	32	40	+0.4	+41	97.4	730	27.0	41	46	+0.2	+8
14SStl+2	208	12	1870	28.5	45	47	+0.6	+26	101.1	1185	27.4	42	52	+0.3	-7
	209	12	1570	28.6	40	47	+0.2	+36	102.2	855	27.5	40	53	+0.3	+15
	210	12	440	28.0	44	60	-0.1	-5	103.5	240	26.7	42	62	+0.3	-8
28IGr1	202	12	160	28.0	28	43	+0.3	+5	99.1	155	27.1	35	48	+0.2	-2
	203	12	220	29.0	30	40	+0.3	+8	98.2	190	27.1	33	46	+0.2	-28
	204	12	270	28.5	30	37	+0.4	+1	97.5	220	27.1	36	46	+0.2	-4
28MSh	211	12	150	27.5	34	60	-0.2	-12	103.7	130	27.2	34	51	+0.3	-7
	212	12	150	27.5	33	55	+0.3	-24	99.3	145	27.1	32	49	+0.4	-10
	213	12	170	26.8	39	56	+0.6	-21	103.7	155	26.9	35	51	+0.4	-7
02SLs2	181	9	4080	27.0	31	39	+1.0	+325	118.4	2010	27.0	34	42	+1.1	+175
	182	6	4970	27.5	36	36	+1.3	+359	112.2	225	27.3	34	46	+1.0	+171
	183	7	4960	26.6	40	35	+0.8	+570	112.9	2435	26.9	38	44	+1.4	+279
04SLs4	190	7	4070	27.0	35	34	+1.3	+340	101.3	2215	27.0	33	40	+1.0	+204
	191	8	3730	26.6	34	34	+0.6	+278	107.7	2000	26.8	33	40	+0.8	+179
	192	5	4050	26.8	38	34	+0.3	+425	102.4	2075	26.9	32	44	+1.3	+232
03SLs1	199	5	2930	27.3	37	32	--	+25	113.4	1015	27.1	32	46	+1.3	+29
	200	8	4860	26.7	32	37	+1.9	+493	111.7	1570	26.8	32	48	+1.2	+154
	201	8	3250	26.9	33	38	-4.0	+210	103.2	1180	26.7	35	52	+0.0	+85
10SLs1	229	9	450	28.7	34	41	--	+31	115.9	220	28.2	33	36	+0.5	-2
	230	9	720	28.6	33	36	+0.1	+42	106.5	360	28.3	27	34	+0.7	+14
	231	9	290	28.7	30	46	+0.4	+27	107.5	160	27.9	32	40	+0.6	-10
25IL1	223	2	4340	28.1	37	31	+2.5	+350	117.8	2740	28.1	35	34	+1.9	+230
	224	5	4480	28.9	28	16	-1.0	+275	124.7	2145	28.2	28	30	+6.1	+234
	225	5	4640	28.7	23	11	+1.0	+242	124.2	2760	28.0	28	30	+1.4	+216
25IP1	226	2	3240	28.0	36	29	+4.2	+411	141.6	2490	28.0	34	34	+2.9	+266
	227	2	15,000	28.2	33	23	+5.7	+2450	148.7	9600	28.1	29	23	+3.8	+2450
	228	2	17,000	27.6	34	17	+9.1	+3560	161.3	11000	27.6	34	24	+5.7	+2076
42SLs2	220	9	1580	29.6	38	43	--	--	111.0	650	27.9	33	45	+0.7	+24
	221	9	1010	29.7	37	44	--	--	111.4	425	28.2	32	49	+0.8	+21
	222	9	2670	28.8	33	29	--	--	112.8	1260	27.6	33	41	+0.9	+33
44SLs3+4	232	9	3250	29.5	36	35	-1.3	+241	116.6	1690	28.5	31	31	+0.5	+92
	233	9	1220	28.3	33	41	+0.9	+171	114.6	460	28.3	30	39	+0.7	+5
	234	9	2560	28.3	36	40	--	+169	116.1	1245	27.9	33	39	+0.7	+89

TABLE B-3

DATA SUMMARY, PHASE III EXPERIMENTS

AGGREGATE	SPECIMEN	DILATION (μIN.) PER CYCLE[a] 1	2	3	4	5
02SLs1						
Mix 1	1	240	220	190	400	1210
	2	160	180	160	300	850
	3	210	350	1000	1060	2560
	4	150	250	270	470	1020
Mix 2	1	370	300	220	420	1560
	2	350	220	200	340	1240
	3	320	270	130	200	530
	4	280	200	190	290	770
Mix 3	1	180	90	400	1350	2950
	2	150	90	140	400	1390
	3	210	120	230	450	1240
	4	200	130	180	390	1220
14SSt1+2						
Mix 1	1	120	390	350	460	790
	2	100	270	260	290	400
	3	110	270	200	260	490
	4	230	740	740	1050	1410
Mix 2	1	180	300	220	200	450
	2	260	360	240	330	800
	3	220	370	260	280	430
	4	280	330	310	370	640
Mix 3	1	340	250	270	250	440
	2	520	540	760	950	1400
	3	440	600	570	650	930
	4	380	360	230	470	810
42SLs2						
Mix 1	1	170	200	230	210	460
	2	180	220	160	140	240
	3	220	190	160	130	260
	4	220	190	190	260	600
Mix 2	1	210	180	180	120	400
	2	290	220	380	480	970
	3	250	160	220	220	410
	4	200	140	110	130	380
Mix 3	1	180	120	400	400	860
	2	330	240	140	160	620
	3	270	390	230	420	560
	4	270	280	170	200	570
44SLs3+4						
Mix 1	1	210	310	720	1350	1740
	2	170	100	170	280	840
	3	230	260	510	1120	1680
	4	140	160	220	440	1090
Mix 2	1	150	120	200	220	770
	2	360	400	640	930	1620
	3	340	130	100	190	500
	4	240	140	150	230	840
Mix 3	1	120	340	230	370	830
	2	300	130	160	190	460
	3	220	190	200	260	890
	4	220	200	260	520	1500

[a]Soaking time: between cycles 1 through 4, 1 week; between cycles 4 and 5, 14 weeks.

analyses of variance are summarized under "Aggregate type" in Table B-4.

The ability of the slow-cooling method to differentiate aggregate fractions with respect to frost resistance was also demonstrated in an analysis of variance of the Phase III data. In this instance the sources of variation were aggregate type and cycle number. The results are given in Table B-4.

Effects of Mixture Variability

The reproducibility of the test method as related to concrete mixture variability was investigated by means of an analysis of variance of the Phase III test data. In this analysis, aggregate type and concrete mixture were examined as sources of variation in the fifth (last) measured cycle. Aggregate type, as shown previously, was a significant source of variation at the 95 percent level, but mixture was not. The results are summarized in Table B-4.

Number of Freeze-Thaw Cycles vs Soaking Period

The effect of the number of cooling cycles during a given period of time in which the concrete remained continuously saturated was examined by means of the Phase I data. Two levels of cooling cycles per unit time were used in these experiments—ten cycles per two weeks, and one cycle per two weeks.

If the rate of deterioration depended only on the number of cooling cycles, the ratio of the dilations at ten cycles per two weeks and one cycle per two weeks for any given soaking period would be shown by curve (A) in Figure B-2. In the sixth week of soaking, for example, 31 cycles would have been completed in the first case and four in the latter, and the ratio of cycles would be 31/4, or 7.75. However, if dilation were totally independent of the number of cooling cycles, the ratio would correspond to curve (B) in Figure B-2. The average values of the ratios for the three aggregates used in Phase I are shown in Figure B-2, and it appears that in the case of aggregate 40SSs2 the number of cycles had no effect at all. For the other two aggregates, the intermediate cycles apparently had a noticeable effect. However, the length of the period of soaking seems to exert considerably more influence on the rate of deterioration of the specimens than does the effect of intermediate cycles.

Effects of Specimen Drying

One part of the Phase I experiments was to examine the effects of a seven-day drying period prior to testing. The dilations in the fourth measured cycle for companion specimens, half of which were dried for seven days at 75 F and 50 percent relative humidity, are given in Table B-5. It is evident that the drying period had a profound effect on frost resistance.

Determination of Test End Point

A deterioration-function model leading to definition of the end point of the test was developed in the studies reported

PHASE I

AGGREGATE	REPLICA MIXTURE	CONDITIONING PROCEDURE[a]	SPECIMEN NUMBER PROCEDURE 1[b]			PROCEDURE 2[c]		
02SLs1	1	Dried	1	2	3	4	5	6
		Saturated	7	8	9	10	11	12
	2	Dried	1	2	3	4	5	6
		Saturated	7	8	9	10	11	12
05SSs1+2	1	Dried	1	2	3	4	5	6
		Saturated	7	8	9	10	11	12
	2	Dried	1	2	3	4	5	6
		Saturated	7	8	9	10	11	12
40SSs2	1	Saturated	1	2	3	4	5	6
		Dried	7	8	9	10	11	12
	2	Saturated	1	2	3	4	5	6
		Dried	7	8	9	10	11	12

[a]Dried = 1 week in air at 50% RH, 2 weeks in water at 35 F; saturated = 3 weeks in water at 35 F.
[b]One measured cycle and 9 intermediate cycles every 2 weeks.
[c]One measured cycle every two weeks.

PHASE II

AGGREGATE	SPECIMEN NUMBER[a]		
02SLs2	1	2	3
03SLs1	1	2	3
04SLs4	1	2	3
06SSs1+2	1	2	3
06SSs3+SCh	1	2	3
08SD12	1	2	3
10SLs1	1	2	3
14SSt1+2	1	2	3
14SSs3+SAk	1	2	3
16SSs1	1	2	3
16SSs2	1	2	3
18IS+IT	1	2	3
25IL1	1	2	3
25IP1	1	2	3
28IGr1	1	2	3
28MSh	1	2	3
34MAm1	1	2	3
34MAm2	1	2	3
38MGn2	1	2	3
42SLs2	1	2	3
44SLs3+4	1	2	3

[a]All conditioned 3 weeks in 35 F water and subjected to 1 measured and 9 intermediate cycles every 2 weeks.

PHASE III

AGGREGATE	REPLICA MIXTURE	SPECIMEN NUMBER[a]			
02SLs1	1	1	2	3	4
	2	1	2	3	4
	3	1	2	3	4
14SSt1+2	1	1	2	3	4
	2	1	2	3	4
	3	1	2	3	4
42SLs2	1	1	2	3	4
	2	1	2	3	4
	3	1	2	3	4
44SLs3+4	1	1	2	3	4
	2	1	2	3	4
	3	1	2	3	4

[a]All conditioned 3 weeks in 35 F water and subjected to 1 measured and 4 intermediate cycles per week for 4 weeks, then 3 months soaking in 35 F water and final measured cycle.

Figure B-1. Experimental designs to develop specification for slow-cooling test.

in *NCHRP Report 15*. The relationship between specimen dilation and cycle number (or length of soaking period) was shown to fit the proposed model quite well. However, insufficient data prohibited recommending the new concept as a practical technique for evaluating the period of frost immunity (test end point).

The deterioration-function model is based on two experimentally observed phenomena: (1) during the period of frost immunity, the dilation increases linearly with the soaking time; (2) after the period of frost immunity is exceeded, the dilation increases exponentially with the soaking time. The first of these conditions can be represented by the following equation:

$$D = Cn \tag{B-1}$$

in which

D = dilation;
C = constant; and
n = length of soaking period.

The second condition is mathematically equivalent to

$$D = BA^n \tag{B-2}$$

in which A and B are constants and D and n have the same connotation as in Eq. B-1. These points are shown in Figure B-3.

It is evident that at the critical point the slope of the

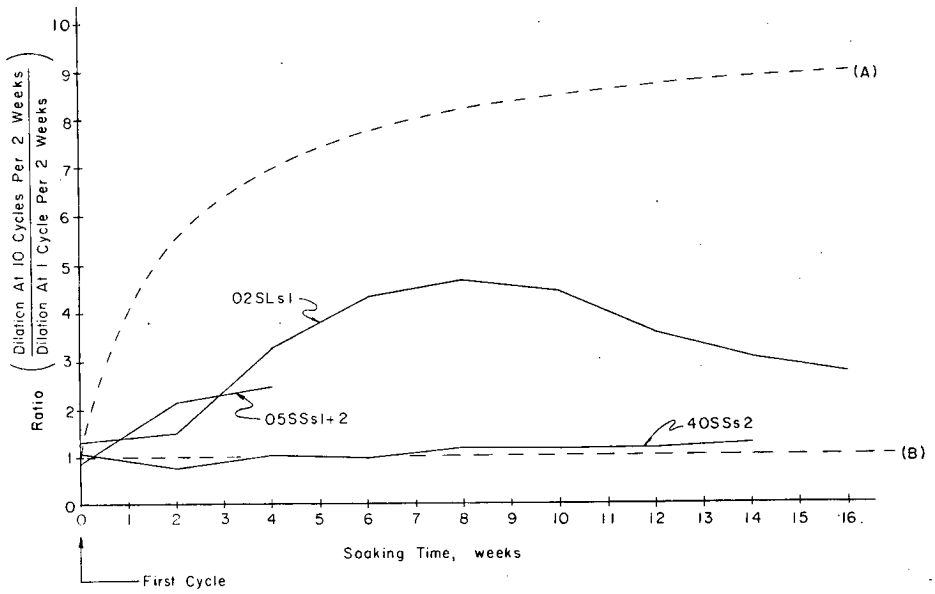

Figure B-2. Effect of number of freeze-thaw cycles per unit soaking period.

exponential curve is the same as the slope of the linear relation. Therefore, the following relationship must hold:

$$d(BA^n)/dn = d(Cn)/dn \qquad \text{(B-3)}$$

or

$$BA^n \ ln \ A = C \qquad \text{(B-4)}$$

But at the critical point, $n = n'$, where n' is the critical soaking time, and $D = D_c$, where D_c is the critical dilation. Therefore,

$$D_c = Cn' = (BA^{n'} \ ln \ A)n' \qquad \text{(B-5)}$$

Also,

$$D_c = BA^{n'} \qquad \text{(B-6)}$$

If Eqs. B-5 and B-6 are combined to eliminate D_c, then

$$BA^{n'} = (BA^{n'} \ ln \ A)n'$$

or

$$n' = 1/(ln \ A) \qquad \text{(B-7)}$$

The regression equation fitted to the data is of the form

$$\log_{10} D = Sn + I \qquad \text{(B-8)}$$

in which S is the slope and I is the intercept. Therefore,

$$D = (\text{antilog}_{10} S)^n \ (\text{antilog}_{10} I) \qquad \text{(B-9)}$$

From Eq. B-9 it is evident that

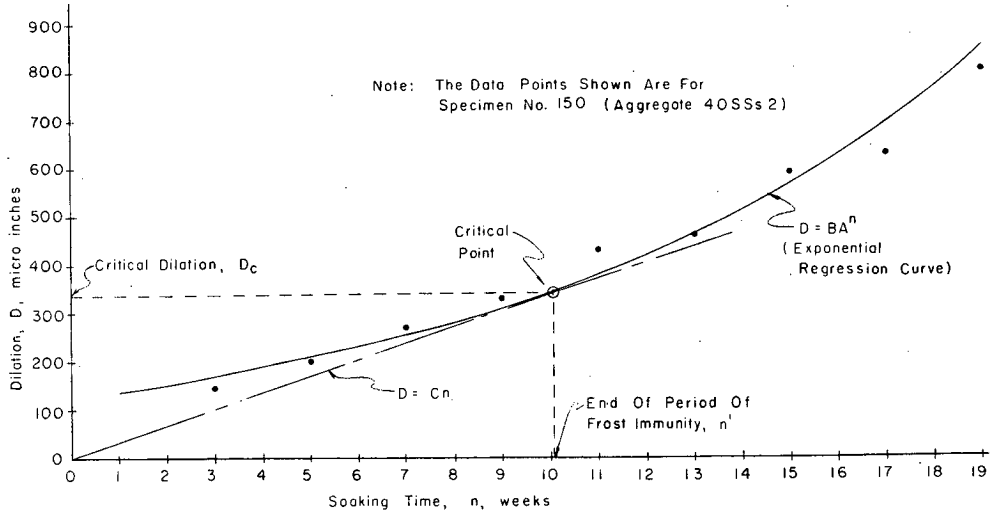

Figure B-3. Deterioration-function concept.

TABLE B-4

SOURCES OF VARIATION IN RELIABILITY OF TEST METHOD

SOURCE	F RATIO	SIGNIFICANCE LEVEL (%)
Aggregate type:		
Cycle 1	6.669	95 or higher,
2	2.028	each cycle
3	2.224	
4	2.074	
5	2.626	
6	3.043	
7	3.899	
8	4.502	
9	5.096	
Aggregate type + cycle:		
Aggregate type	9.397	95 or higher
Cycle	4.683	95 or higher
Interaction	1.613	
Aggregate type + mixture:		
Aggregate type	7.673	95 or higher
Mixture	1.506	
Interaction	0.796	

$$\text{antilog}_{10}\, S = A \qquad \text{antilog}_{10}\, I = B$$

Therefore,

$$n' = 1/[ln(\text{antilog}_{10}\, S)] = 1/2.30S \qquad \text{(B-10)}$$

TABLE B-5

EFFECT OF SEVEN-DAY DRYING PERIOD ON FROST RESISTANCE

AGGREGATE AND MIX	SPECIMEN NO.	TOTAL DILATION, 4TH CYCLE (μIN.) DRIED	NOT DRIED
O2SLs1			
Mix 1	1	70	770
	2	60	1,450
	3	60	1,180
Mix 2	1	60	1,180
	2	40	1,150
	3	60	1,810
40SSs2			
Mix 1	1	60	260
	2	30	330
	3	50	260
Mix 2	1	60	520
	2	50	360
	3	60	250
O5SSs1 + 2			
Mix 1	1	60	1,090
	2	70	4,140 [a]
	3	50	3,480
Mix 2	1	90	4,630
	2	60	3,970
	3	45	3,310

[a] Value for 3rd cycle; specimen removed from test.

Eq. B-10 translates the slope of the regression curve into the value of the critical cycle or soaking time. From Eq. B-8, the value of the critical dilation is

$$D_c = 10 \exp (Sn' + I) \qquad \text{(B-11)}$$

Combining Eqs. B-10 and B-11 gives the following relationship between critical dilation and intercept value:

$$D_c = 10 \exp (I + 0.435) \qquad \text{(B-12)}$$

If the cycle-dilation data for each specimen are fitted to a curve of the form represented by Eq. B-8, the values of the critical cycle (length of soaking period) and the critical dilation can be determined by Eqs. B-10 and B-12, respectively.

Since the critical dilation is the point beyond which the dilation per cycle (or per unit soaking time) progressively increase, it appears that the critical dilation is a measure of the elastic limit of the paste phase. Note also that dilation is equal to the longitudinal strain multiplied by the length of the specimen. According to the generalized Hooke's law,

$$\epsilon_z = (1/E)[\sigma_z - \mu(\sigma_x + \sigma_y)] \qquad \text{(B-13)}$$

in which

ϵ_z = unit longitudinal strain;
E = Young's modulus;
σ_z = longitudinal stress;
σ_x, σ_y = stress components in plane perpendicular to longitudinal direction; and
μ = Poisson's ratio

Since the stress developed by freezing is caused by hydraulic pressure, $\sigma_z = \sigma_x = \sigma_y$. Also, by the argument presented previously, σ_z equals the tensile strength, f_t, of the paste, at the critical point. Therefore,

$$D_c = L\epsilon_z = (L/E)[f_t - \mu(f_t + f_t)]$$

or

$$D_c = (L/E)(1 - 2\mu)f_t \qquad \text{(B-14)}$$

in which L is the specimen length. Hence, as long as the elastic properties of the paste are constant, the critical dilation is invariant. Assuming that the following rule-of-thumb relations are approximately correct,

$$E = 1{,}000f_c \quad f_t = 0.1f_c \quad \mu = 0.15$$

in which f_c is the compressive strength of the paste, it is found that

$$D_c \simeq 70L \qquad \text{(B-15)}$$

in which D_c is in microinches and L is expressed in inches.

The experimentally observed relation between dilation and soaking period (number of cooling cycles) and theoretical stress-strain relationships therefore indicate that (1) the critical dilation and the critical cycle (or period of frost immunity) can be readily calculated from the coefficients of the exponential regression of dilation on cycle number; (2) the critical dilation is constant for a cement paste with given elastic constants; and (3) the critical cycle is a function of the frost susceptibility of the coarse aggregate.

To investigate the validity of these points, the exponential regression equations and correlation coefficients were calculated for the dilation-cycle data from 284 concrete

specimens 3 in. in diameter and 6 in. long, tested by the slow-cooling method over a four-year period. The computations were performed on Penn State's electronic computer, with a program specially written for this purpose. Of the 284 specimen data sets, 173 yielded correlation coefficients significant at the 95 percent level. The remaining 111, which were eliminated from further consideration, generally failed to yield significant correlation coefficients because the scatter in the dilation values was great compared with the average dilation values. Obviously, these specimens displayed very small dilations throughout their test periods and failed to reach the critical point.

It was also necessary to eliminate those data for which a significant correlation existed but the critical point fell outside the range of the number of cooling cycles that was run. In these cases it is probable that the critical point occurred before the second measured cooling cycle, or that it lay beyond the last measured cycle. The criteria for eliminating data were, for the first case, dilations in excess of 500 μin. in the first measured cycle, and, for the second case, failure to attain dilations greater than 300 μin. in the last measured cycle.

After these eliminations, 124 data sets remained for analysis. Although the specimens were made and tested over a four-year period, the same cement and sand were used throughout and the mixture-proportioning and curing criteria were constant. Only the type of coarse aggregate and the conditioning and testing procedures were purposely varied. Therefore, the calculated critical dilations were expected to be relatively constant.

Figure B-4 is a histogram of the calculated values of the critical dilation for the 124 specimens. A strong central tendency is evident, indicating a relatively constant value. This tendency occurred in spite of possible variability due to the following factors: (1) the last-cycle dilations ranged between 310 and 4,970 μin.; (2) 15 of the specimens were subjected to a drying period and the rest were saturated; (3) 43 of the specimens received one cooling cycle per two weeks and the remaining 81 received ten cycles per two weeks; (4) the 124 specimens represented 52 individual concrete mixtures; and (5) 27 different coarse aggregate fractions were represented.

The mean value of the critical dilations of the 124 specimens was calculated to be 421.5 μin. This compares remarkably well with the approximate value calculated from Eq. B-15, which is 420 μin. for the 6-in. specimen length.

To further investigate the theorized invariance of the critical cycle (or period of frost immunity), correlation analyses were performed for a measure of frost damage (dilation in the last cycle) vs the dilation and cycle number at the critical point. The critical-point data used were those for the 124 specimens discussed previously. The correlations in Table B-6 show that the critical dilation bears no significant relationship to frost susceptibility, thus supporting the hypothesis regarding the invariant nature of the critical dilation. The critical cycle value, on the other hand, correlates at a very high level of significance with frost susceptibility. This result is in complete accord with the postulation that critical cycle (or period of frost immunity) is a function of the frost susceptibility of the aggregate.

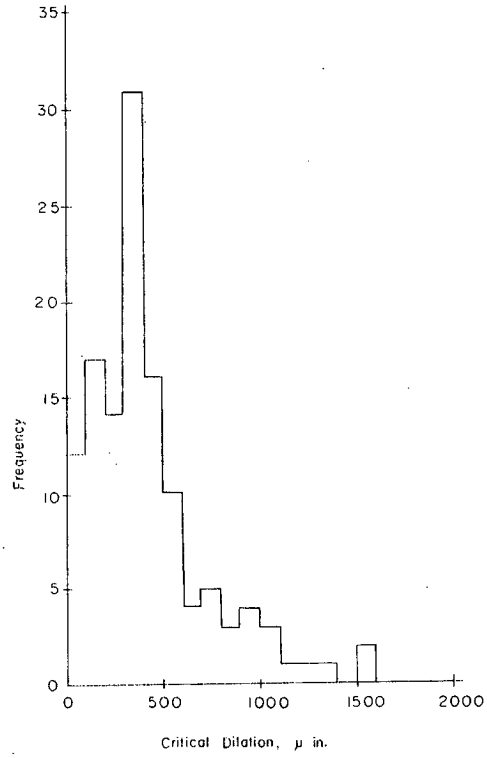

Figure B-4. Critical dilation values for 124 specimens.

Notice also that the correlation coefficient in the latter case is negative, revealing an inverse relationship (the greater the frost susceptibility, the shorter the period of frost immunity), which again is in accordance with the postulation.

Number of Test Specimens Needed

An estimate of the inherent variability in the deterioration-function method of analyzing freeze-thaw data was made (1) to provide confidence limits for the length of the period of frost immunity for given significance levels and sample sizes (number of specimens), and (2) to estimate the number of specimens required to obtain given confidence intervals at specified significance levels. The measure of variability used was the coefficient of variation, V, mathematically defined as

TABLE B-6

CORRELATION OF CRITICAL-POINT VALUES WITH DILATION IN LAST CYCLE

CORRELATION	COEFFICIENT [a]
Critical dilation vs last cycle dilation	0.087
Critical cycle vs last cycle dilation	—0.520

[a] Critical values: 95% significance, 0.174; 99% significance, 0.228.

$$V = 100\sigma/\overline{X} \qquad \text{(B-16)}$$

in which σ is the sample standard deviation and $\overline{X}$ is the sample mean. This statistic was employed in lieu of standard deviation or variance, both of which are also measures of variation, because it reduces the influence of the sample mean.

The expression relating variability, confidence interval, significance level, and sample size (*2*) is

$$n = (\sigma t_{a/2,n-1}/h)^2 \qquad \text{(B-17)}$$

in which

n = number of specimens;
σ = standard deviation;
$t_{a/2,n-1}$ = Student's t-value for significance level $100 - a$ and $n - 1$ degrees of freedom; and
h = one-half of confidence interval (confidence range $= \overline{X} \pm h$)

If the following substitutions are made in Eq. B-17,

$$\sigma = V\overline{X}/100 \qquad \text{(B-18)}$$

$$h = H\overline{X}/100 \qquad \text{(B-19)}$$

in which H is the confidence interval as a percent of the mean, then

$$n = (Vt_{a/2,n-1}/H)^2 \qquad \text{(B-20)}$$

The relationships expressed in Eq. B-20 are shown graphically in Figure B-5 for a significance level of 95 percent.

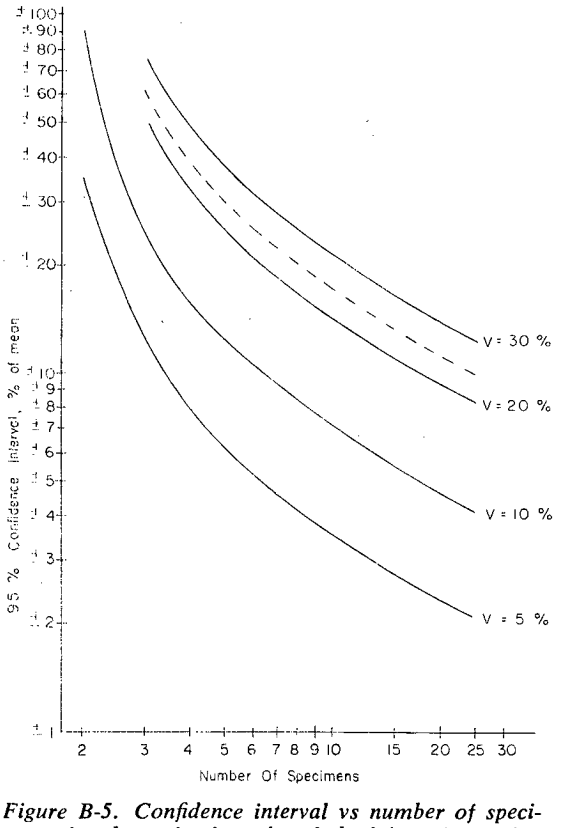

Figure B-5. Confidence interval vs number of specimens for determination of period of frost immunity.

The coefficient of variation was computed for each mixture-conditioning combination, and the mean value (24 percent) gives the dashed curve.

The practical utilization of Figure B-5 can best be explained by example. Suppose a batch of concrete consisting of 10 specimens is tested by the slow-cooling method. The mean value of the period of frost immunity is found to be 20 weeks, with a coefficient of variation of 20 percent. From Figure B-5, the 95 percent confidence interval is about ±14 percent of the mean, or $\pm 0.14 \times 20 = \pm 2.8$ weeks. It can therefore be stated, with only one chance in 20 of being wrong, that the period of frost immunity for this aggregate-conditioning combination is 20 weeks ±2.8 weeks, or at least 17.2 weeks.

The technique just described is the recommended use of Figure B-5, but the number of specimens required to produce a given confidence interval can also be calculated from this graph. Since the coefficient of variation will not be known in this case, the dashed line representing the average of the 54 mixture-conditioning combinations tested in this research project should be used. If a confidence interval of 20 percent is selected, Figure B-5 shows that eight specimens are required.

PROPOSED SPECIFICATION, SLOW-COOLING TEST FOR FROST RESISTANCE OF AGGREGATES IN AIR-ENTRAINED CONCRETE

The essence of this test method is simulation of field exposure conditions in the laboratory. Hence, the aggregate procurement and preparation procedures, the concrete mixture-proportioning criteria, the curing and conditioning of the test specimens, and the frequency of the testing cycles are left to the discretion of the testing agency. The degree of applicability of the test results to concrete in the field will be directly related to the care exercised in establishing these factors.

It is therefore of utmost importance that the user of this test method determine at the outset the anticipated field exposure conditions, including (1) the condition of the aggregate immediately before batching (stream-wet, saturated surface dry, air dry); (2) the curing procedures employed; (3) the length of the drying period, if any, and the hygrometric and thermal environment of the concrete before the start of the winter season; (4) the length of the period of potential frost damage and the frequency of freeze-thaw cycles for the location; (5) the accessibility of water to the concrete during the period of potential frost damage.

APPARATUS

Cooling Bath

A cooling bath is required, of sufficient size and depth to completely immerse the test specimens in water-saturated kerosene. The bath must be provided with controls to permit lowering the temperature from 35 F to 15 F at the rate of 5 ± 1 F per hour. Suitable temperature-recording facilities should be provided.

Constant-Temperature Water Bath

A water bath is required, with refrigeration and control facilities capable of maintaining the temperature at 35 ± 1 F. This bath must have sufficient capacity to contain, completely immersed, all of the specimens in a test program.

Strain-Measuring and Recording Facilities

Strain frames are needed to support the specimens in the cooling bath and to provide alignment for strain-measuring apparatus. Suitable recording strain-measuring facilities are required. Linear variable differential transformers (LVDT) appear to give the best results with respect to stability, sensitivity, and reliability. The strain-measuring apparatus should have a sensitivity of at least 10^{-5} in. Multichannel recording of up to six LVDT outputs has been found to be practical and efficient.

Environmental Conditioning Facilities

Facilities should be provided to allow conditioning of the specimens in relation to the field environment. Ideally, this would involve controlled temperature-humidity chambers or rooms. Simple environmental humidity control can be obtained with closed chambers or vessels containing various saturated salt solutions.

PROCEDURE

Coarse Aggregates

Secure samples of the processed coarse aggregate from the batch plant bins, taking care to preserve the plant moisture conditions by using airtight metal containers. For a virgin aggregate source, obtain pit-run or quarry-run samples and store them in airtight metal containers. Unless the aggregate is very homogeneous, it will have to be sorted into petrographic fractions by specific gravity fractionation and hand-picking techniques. This step requires the skills of a trained petrographer. The procedures followed in evaluating an aggregate source will be dictated largely by the testing philosophy of the responsible agency. A battery of tests, for which the fractionation procedure is only one step, is suggested in this report.

If specific fractions of a virgin aggregate are selected for testing, they should be conditioned in the most severe manner; that is, by vacuum saturation. In this conditioning process the aggregates are held under a vacuum of 2 mm Hg for 1 hr. Water is then admitted to the evacuated vessel and the aggregates are allowed to soak at least 24 hr before batching.

Concrete Mixture

Ingredients. The same cement, fine aggregate, and admixtures, if any, used in the job concrete should also be used in the test batches.

Proportioning Criteria. The mixture ingredients should be proportioned similarly to the job concrete.

Replication. Two identical mixtures should be made for each test aggregate.

Specimens

Size. The size of the test specimen is regulated by the maximum size of the coarse aggregate being tested. The specimens should be cylindrical and proportioned dimensionally so that the diameter is at least three times the maximum size of the coarse aggregate and the length is two times the diameter.

Number Required. If an estimate of the coefficient of variation of the critical soaking period, V, is available, the number, n, of specimens required for a given confidence interval, H (expressed as a percent of the mean), can be obtained from Figure B-5. In the absence of an estimate of the coefficient of variation, the dashed curve in Figure B-5 should be used. In no instance shall less than three specimens be molded for each mixture-conditioning combination.

Molding Procedure. Specimens 6 in. in diameter or larger shall be compacted in three layers by 25 blows with a standard tamping rod. Smaller specimens shall be compacted in two layers with 25 blows per layer.

Gauge Studs. The specimen molds shall be designed to permit axial centering of stainless-steel gauge studs (see ASTM C227 for gauge-stud specifications).

Conditioning Procedure. The conditioning procedure shall conform to the field environment as nearly as possible. In the absence of specific knowledge of the field environment, the specimens shall be allowed to soak in water at 35 ± 1 F for three weeks.

Testing

Testing shall begin immediately after completion of specimen conditioning.

Test Cycle. The test cycle shall consist of cooling the specimens in water-saturated kerosene from 35 F to 15 F at the rate of 5 ± 1 F per hour, followed by immediate return of the specimens to the 35 F water bath.

Frequency. The frequency of the test cycles shall be related to the frequency of natural freeze-thaw cycles at the job site. In the absence of data relative to this point, one test cycle shall be carried out every two weeks. In no case shall the frequency be less than biweekly.

Measured Variables. The measured variables are the specimen length changes during the cooling cycle and the cooling-bath temperature. It is not necessary to record specimen length changes for every test cycle. Two alternatives are available regarding the frequency of measured test cycles. The critical-point method requires periodic (biweekly recommended) measured test cycles, continued until the dilation of the specimen during cooling exceeds a predetermined critical value (see next subsection). The second technique, called the terminal-cycle method, involves the running of noninstrumented cooling cycles at a frequency determined as just described, for a time equal to the period of potential frost hazard for the given locale. The last cooling cycle is the only instrumented cycle in this case.

The critical-point method requires more work and more complete facilities because of the high frequency of measured cooling cycles, but it has the advantage of providing an estimate of the actual period of frost immunity for the

given test conditions. The terminal-cycle method is simpler in terms of work load and scheduling, but it reveals only whether or not an aggregate is suitable for a given locale under the test conditions employed. This method usually requires a greater amount of elapsed time for completion.

Duration of Test. If the critical-point method is employed, the test is continued until the critical dilation, as calculated from the following relationship, is exceeded:

$$D_c = (L/E)(1 - 2\mu)f_t$$

in which

D_c = critical dilation, in.;
L = specimen length, in.;
E = Young's modulus of paste, psi;
μ = Poisson's ratio; and
f_t = tensile strength of paste, psi.

If the values of the elastic constants are not known, the critical dilation may be approximated from the following relation:

$$D_c \simeq 70L$$

in which

D_c = critical dilation, μin.; and
L = specimen length, in.

It is advisable to make a mortar specimen by screening the coarse aggregate from the concrete mixture at the time the test specimens are made. The elastic constants for the mortar can then be determined from the mortar specimen.

The duration of the test under the terminal-cycle method is dictated by the length of the period of potential frost damage for the given locale.

TABLE B-7

CRITERIA FOR TERMINAL-CYCLE METHOD

NO. OF TEST SPECIMENS IN SET	MINIMUM REQUIRED TO PASS FOR SET TO PASS WITH 95 PERCENT CONFIDENCE
3	3
4	4
5	5
6	6
7	7
8	8
9	8
10	9
15	12
20	15
25	18

REPORTING OF RESULTS

Because the slow-cooling test method incorporates a high degree of flexibility with regard to test conditions, the report of the test results must include the following information:

1. Aggregate source.
2. Specific gravity fraction.
3. Mineralogical subgroup.
4. Moisture condition of the aggregate prior to batching.
5. Mix-proportioning criteria.
6. Entrained-air content.
7. Curing procedure.
8. Conditioning procedure.
9. Test method.

Critical-Point Method Results

The length of time from the start of soaking in the 35 F bath to the critical point—termed the period of frost immunity—is recorded for each specimen. The mean value, $\overline{X}$, and the coefficient of variation, V, for the period of frost immunity for each mixture-conditioning combination are computed. From these values, the 95 percent confidence interval of the mean, H, is obtained from Figure B-5. The period of frost immunity is then reported as $\overline{X} \pm H\overline{X}/100$. If the means of replica mixtures differ by more than the square root of the sums of the squares of the standard deviations of the mixtures, then an additional mixture must be tested. This procedure must be repeated until two replica mixtures meet the criterion.

Terminal-Cycle Method Results

The terminal-cycle dilation for each specimen is recorded, and the specimen is noted as having "failed" or "passed," depending upon whether or not the critical dilation was exceeded (see "Duration of Test," described previously). A mixture-conditioning specimen set will then be declared as having "passed" or "failed," depending upon the number of specimens in the set that pass according to the criteria in Table B-7.

For the aggregate to be declared as having passed, both replica mixtures must pass. If one passes and the other fails, a third set must be tested. The results of the third test will then decide passage or failure of the aggregate. The test results for each specimen and mixture are reported, as well as the over-all result.

APPENDIX C

AGGREGATE PORE SYSTEMS

The purpose of this part of the research was to investigate the possibility of developing a rapid, simple, economical method for selecting frost-resistant aggregates, based on their pore characteristics. To this end it was necessary to study the relationships between porosity, permeability, and frost susceptibility.

The work here reported is essentially an extension of studies described in *NCHRP Report 15* (*7*). The equipment was modified to surmount pressure limitations that were encountered in the earlier permeability tests. Additional investigations concerned specimen variability, effects of the nature of the permeating fluid, and possible destruction of pore walls by high pressures.

The major conclusions from the previous tests of aggregate permeability, porosity, and capillarity were as follows (*7*):

1. Significant correlations could not be found between porosity and the permeability coefficient, or between porosity and the average freeze-thaw durability factor.
2. The permeability coefficient correlated significantly (95 percent level) and directly with the freeze-thaw durability factor.
3. The logarithm of the ratio of porosity to the permeability coefficient correlated significantly (>99 percent) and inversely with the logarithm of the freeze-thaw durability factor.

On the basis of these findings, further experimental work was recommended, on a wider range of aggregates and with higher pressures in the permeability test. The need for the latter was apparent from the implausible results that were obtained with some of the highly impermeable aggregates. These were the negative permeability coefficients that were displayed when the data were extrapolated to infinite pressure.

EXPERIMENTS

Porosity

The porosity value used in *NCHRP Report 15* (*7*) was the true porosity based on true specific gravity, but true specific gravities are difficult and time-consuming to determine. In the study reported herein, apparent porosity and absorption were taken as measures of porosity. Apparent porosity is the ratio of the interconnected void volume to the total volume, and is numerically equivalent to the product of the bulk dry specific gravity and the absorption. Absorption is the ratio of the weight of water that is taken on when the sample is immersed to the oven-dry weight. Apparent porosity and absorption were determined for two absorption conditions: 24 hours of soaking, and vacuum saturation plus 23 hours of soaking.

Two additional pore parameters were developed and investigated in this research. "Effective absorption" is defined as the difference between the vacuum absorption and the 24-hr absorption. "Effective apparent porosity" is the difference between the vacuum apparent porosity and the 24-hr apparent porosity.

The porosity values for the aggregate fractions examined appear in Table C-1. They represent averages of 4 to 15 individual aggregate particles for each fraction.

Permeability

The technique for obtaining permeability data on the test aggregates was essentially the same as that described in *NCHRP Report 15*. The apparatus used in this study is shown in Figures C-1 and C-2. Some modifications were made to permit the use of higher pressures and to facilitate specimen preparation and testing. Bottled compressed gas instead of laboratory-line air was used as the permeating fluid. The pressure was controlled at any given level up to 180 psi by means of a gas regulator. A loop of brass tubing between the gas bottle and the drying column warmed the expanded gas to room temperature. Brass tubing and connectors were used for all tubing upstream from the specimen holder.

The specimen holder (Fig. C-3) was modified so that the specimens could be mounted more quickly. In the original apparatus the specimens were centered by placing them in a recess machined in one end of the specimen holder. A raised ring machined on the other end of the specimen holder was brought to bear against a polyethylene sleeve, forming an airtight seal. Because cutting the polyethylene sleeve and gluing it to the specimens was complicated and time-consuming, the sleeve was replaced with a rubber ring about 1/16 in. thick and 1/8 in. long. The recess was machined deeper to make room for the rubber ring, and the specimens were inserted in the ring. The raised ring on the other end of the specimen holder compressed the rubber ring, thus applying lateral pressure on the specimen and forming an airtight seal. To test the tightness of this sealing system an impermeable Plexiglas core was mounted in the specimen holder in the same manner as a rock core specimen. No leakage was observed after 1 hr at 180 psi.

A thermistor probe was inserted immediately downstream from the specimen holder to indicate the temperature of the permeating gas. Gas volumes were measured with a wet-test meter (high flow rates) or by volumetric water displacement (low flow rates), as in *NCHRP Report 15*.

The rock core specimens were prepared in the manner described in *NCHRP Report 15*, except that the polyethylene sleeve was omitted.

TABLE C-1

AGGREGATE POROSITY VALUES

AGGREGATE	VACUUM ABSORPTION (%)	24-HR ABSORPTION (%)	VACUUM APPARENT POROSITY (%)	24-HR APPARENT POROSITY (%)	EFFECTIVE ABSORPTION (%)	EFFECTIVE APPARENT POROSITY (%)	VACUUM BULK DRY SP GR	24-HR BULK DRY SP GR
02SLs1	2.502	1.815	6.425	4.620	0.687	1.805	2.618	2.608
02SLs2	2.249	1.388	5.883	3.626	0.861	2.256	2.635	2.633
03SLs1	5.234	4.413	12.381	10.466	0.821	1.914	2.366	2.372
04SLs4	2.627	1.998	6.680	5.068	0.629	1.612	2.567	2.558
05SSs1+2	5.294	2.215	12.256	5.112	3.079	7.144	2.332	2.333
06SSs1+2	1.751	0.877	4.427	2.221	0.874	2.206	2.545	2.540
06SSs3+SCh	0.320	0.238	0.827	0.618	0.082	0.082	2.651	2.608
08SD12	2.015	1.843	5.299	4.840	0.172	0.459	2.650	2.648
10SLs1	1.869	1.545	4.978	3.979	0.324	0.999	2.676	2.586
14SSt1+2	1.586	1.161	4.117	3.013	0.425	1.104	2.608	2.603
14SSs3+5Ak	1.204	0.774	3.101	1.989	0.430	1.112	2.583	2.576
16SSs1	1.391	1.009	3.543	2.578	2.578	0.381	0.974	2.580
16SSs2	2.460	1.988	6.190	5.009	0.472	1.181	2.537	2.539
18IS+IT	1.995	1.373	4.947	3.472	0.583	1.475	2.541	2.539
25IL1	5.314	3.297	12.372	7.572	2.051	4.800	2.336	2.299
25IP1	28.836	21.364	43.441	30.875	7.742	12.566	1.530	1.468
28IGr1	0.556	0.497	1.556	1.394	0.059	0.162	2.816	2.814
28MSh	0.593	0.524	1.594	1.409	0.069	0.186	2.703	2.701
34MAm1	0.221	0.161	0.676	0.492	0.061	0.184	3.071	3.061
34MAm2	0.323	0.284	0.987	0.866	0.040	0.121	3.064	3.065
38MGn2	1.712	1.403	4.393	3.605	0.309	0.789	2.596	2.593
40SSs2	2.028	1.581	5.153	4.017	0.497	1.136	2.572	2.567
42SLs2	2.548	1.593	6.603	4.109	0.955	3.494	2.593	2.581
44SLs3+4	2.619	2.176	6.922	5.519	0.443	1.403	2.648	2.544

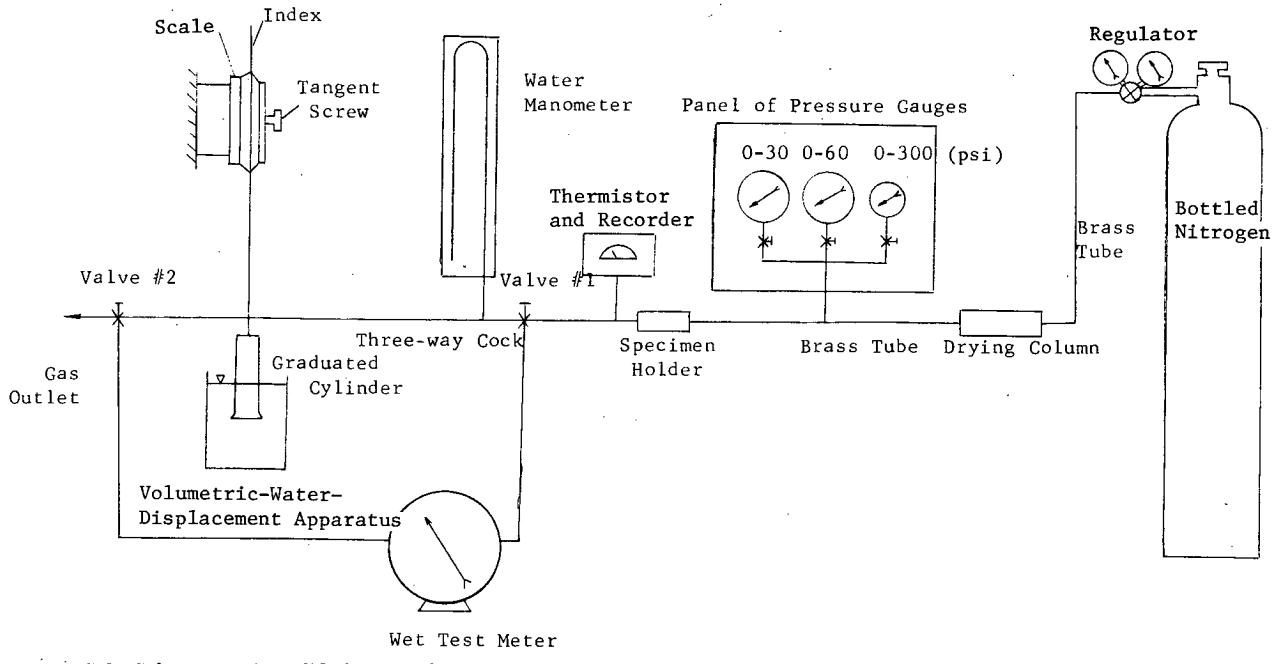

Figure C-1. Schematic of modified permeability measuring apparatus.

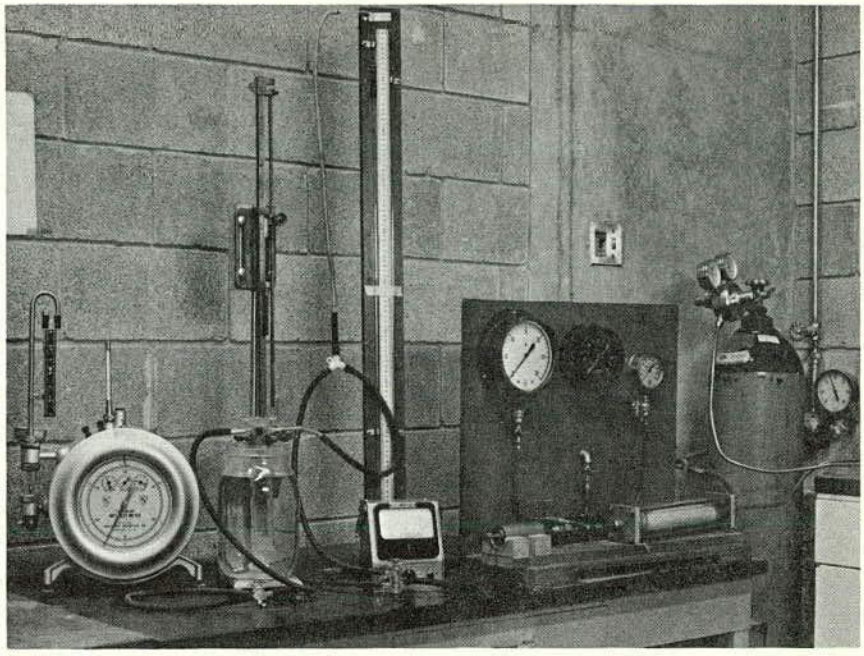

Figure C-2. Permeability measuring apparatus.

Correction of Negative Permeability Coefficients

In *NCHRP Report 15* some highly impermeable aggregates absurdly displayed negative permeability coefficients. Eight of the specimens that gave negative permeability coefficients were rerun at higher pressures. Positive coefficients were obtained for six of the eight specimens, and no gas permeated the other two, even at 180 psi. The results are given in Table C-2.

Nitrogen vs Air

Possible effects on permeability due to the nature of the permeating fluid were examined by conducting tests on a set of eight specimens, using first air and then nitrogen. The results are given in Table C-3. Comparison of the two data sets by means of Student's *t*-test revealed no significant difference at the 95 percent significance level (calculated *t*-value = 0.1649). Because air is more convenient to use, it was chosen as the permeating fluid for this study.

These results led also to another conclusion. As all of the specimens had been oven-dried and cooled to room temperature in a desiccator between the two runs, oven-drying did not significantly influence the test results.

Air Permeability vs Water Permeability

Six specimens obtained from the Portland Cement Association (PCA) were tested twice by the air-permeability method. The results are given in Table C-4, along with water-permeability data from PCA. In general, the air permeabilities were of the same order of magnitude as the water permeabilities. The greatest difference was for specimen No. 3, the air permeability coefficient for which was found to be greater than the PCA value by a factor of 10^3. No reasonable explanation for this can be offered.

Effect of Percolation Period

To investigate the possibility that high pressures might destroy pore structures and thus influence permeability test results, a supplemental study was undertaken. Eight specimens of structurally weak aggregates were first tested by the ordinary permeability procedure. Air was then percolated through the specimens at 150 psi for 1 hr, and their permeability coefficients were again determined. The results are

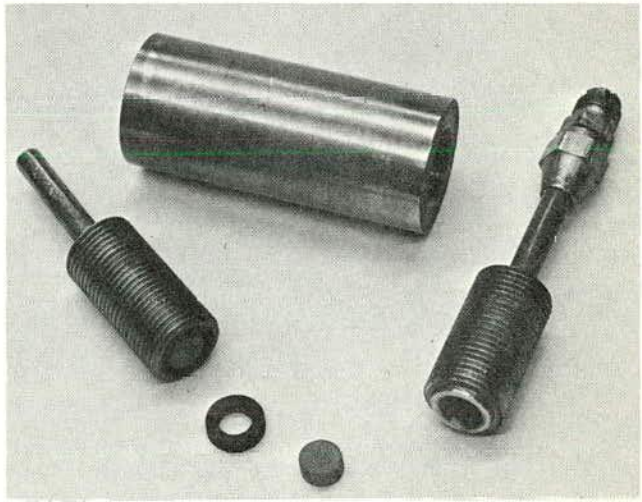

Figure C-3. Specimen holder for permeability measurements.

TABLE C-2

CORRECTION OF NEGATIVE PERMEABILITY COEFFICIENTS

AGGREGATE, SPECIMEN NO., AND SP GR	DATA FROM NCHRP REPORT 15		DATA FROM CURRENT STUDY	
	LEAST SQUARES PERMEABILITY (DARCYS)	PRESSURE RANGE (PSI)	LEAST SQUARES PERMEABILITY (DARCYS)	PRESSURE RANGE (PSI)
Maynes Creek and Eagle City limestone				
No. 6, <2.50	-5.659×10^{-7}	54-86	5.364×10^{-8}	100-180
Paducah river gravel				
No. 1, >2.50	-2.586×10^{-7}	58-87	—[a]	0-180
No. 3, >2.50	-1.038×10^{-7}	50-86	—[a]	0-180
White Marsh gravel				
No. 1, >2.50	-4.673×10^{-8}	25-85	1.200×10^{-8}	120-180
Meramec gravel				
No. 1, <2.50	-4.728×10^{-8}	11-86	2.922×10^{-7}	30-180
No. 9, <2.50	-9.637×10^{-8}	55-76	2.125×10^{-8}	30-180
No. 4, >2.50	-1.931×10^{-7}	41-85	1.653×10^{-7}	125-185
No. 5, >2.50	-3.120×10^{-7}	51-86	3.084×10^{-8}	120-180

[a] No air collected.

TABLE C-3

NITROGEN VS AIR AS A PERMEATING FLUID

AGGREGATE AND SPECIMEN NO.	LEAST SQUARES PERMEABILITY (DARCYS)	
	NITROGEN	AIR
02SLs1		
1	5.158×10^{-4}	5.004×10^{-4}
2	6.051×10^{-4}	6.043×10^{-4}
3	3.000×10^{-5}	2.523×10^{-5}
4	9.617×10^{-5}	9.592×10^{-5}
5	4.073×10^{-4}	3.801×10^{-4}
05SSs1		
1	2.917×10^{-3}	3.665×10^{-3}
2	4.788×10^{-3}	5.033×10^{-3}
3	5.380×10^{-4}	4.897×10^{-4}

given in Table C-5. Comparison of the permeability coefficient data by Student's *t*-test before and after the high-pressure percolation period revealed no significant difference at the 95 percent significance level (calculated *t*-value = 1.567). This indicated that neither the percolation period nor pressures up to 150 psi would cause significant error in the results.

Permeability Test Results

Permeability tests were run on 3 to 15 specimens of each aggregate fraction tested. The average permeability coefficient and the range of the coefficients for each aggregate are given in Table C-6.

Number of Permeability Specimens Needed

Although the aggregate particles tested were selected by a petrographer and were supposed to be homogeneous, the

TABLE C-4

AIR PERMEABILITY VS WATER PERMEABILITY

SPECIMEN NO.	PSU TEST DATA, PERMEABILITY TO AIR, 95% CONFIDENCE RANGE, (DARCYS)		PCA DATA, PERMEABILITY TO WATER (DARCYS)	
	1ST RUN	2ND RUN	1ST RUN	2ND RUN
1	2.616×10^{-1} to 2.472×10^{-1}	1.984×10^{-1} to 1.212×10^{-1}	0.430×10^{-1}	0.160×10^{-1}
2	1.049×10^{-2} to 6.361×10^{-3}	1.286×10^{-2} to 6.020×10^{-3}	1.500×10^{-3}	1.500×10^{-3}
3	5.784×10^{-4} to 0.000[a]	5.406×10^{-4} to 4.288×10^{-5}	3.500×10^{-7}	3.500×10^{-7}
4	4.027×10^{-3} to 1.839×10^{-3}	2.480×10^{-3} to 1.279×10^{-3}	1.200×10^{-3}	1.200×10^{-3}
5	4.675×10^{-3} to 2.344×10^{-3}	2.565×10^{-3} to 2.002×10^{-3}	1.160×10^{-3}	—
6	2.714×10^{-3} to 0.000[a]	1.233×10^{-3} to 5.373×10^{-4}	1.380×10^{-3}	9.200×10^{-4}

[a] Negative lower limit replaced by zero.

results indicated that the range of permeability coefficients for the aggregates was still very wide. Causes for the spread of the data may include the presence or absence of bedding planes or varying angles of coring relative to bedding planes, as well as subtle mineralogical and structural differences.

The number of specimens required to give an average permeability value for an aggregate fraction depends upon the confidence range for the average that one is willing to accept at a preselected significance level, and the variability of the test results. These parameters are related by Eq. B-17 in Appendix B:

$$n = (\sigma t_{\alpha/2,n-1}/h)^2$$

If it is assumed that a confidence interval of one order-of-magnitude is acceptable for the mean at the 95 percent significance level, then $h = 0.818\bar{X}$. Since the standard deviation, σ, is related to the coefficient of variation, V, and the mean, $\bar{X}$, by $\sigma = V\bar{X}/100$, substitution will result in

TABLE C-5

EFFECT OF HIGH PRESSURE AIR PERCOLATION ON PERMEABILITY OF AGGREGATES

AGGREGATE	SPECIMEN	LEAST SQUARES PERMEABILITY (DARCYS) BEFORE PERCOLATION	AFTER PERCOLATION
14SSs3+SAk	5	2.293×10^{-4}	2.413×10^{-4}
05SSs1+2	5	4.852×10^{-3}	4.509×10^{-3}
14SSt1+2	1	4.467×10^{-4}	4.597×10^{-4}
06SSs1+2	2	2.818×10^{-5}	2.298×10^{-5}
02SSs1	3	2.350×10^{-4}	2.372×10^{-4}
03SLs1	5	1.413×10^{-4}	1.444×10^{-4}
03SLs1	4	5.760×10^{-4}	5.627×10^{-4}
Sandstone		7.182×10^{-5}	6.657×10^{-5}

TABLE C-6

PERMEABILITY DATA AND FROST-SUSCEPTIBILITY FACTORS FOR TEST AGGREGATES

AGGREGATE	PERMEABILITY TESTS: NO. SPECIMENS TESTED	RANGE OF PERMEABILITY COEFFICIENT (DARCYS)	AVERAGE PERMEABILITY COEF. (DARCYS)	COEF. OF VARIATION (%)	NO. SPECIMENS REQUIRED[a]	DILATION PER F-T CYCLE[b] (μIN.)
02SLs1	5	2.595×10^{-7} to 1.034×10^{-3}	3.353×10^{-4}	141	14	48.66
02SLs2	11	1.204×10^{-7} to 1.796×10^{-5}	9.531×10^{-6}	68	6	76.38
03SLs1	15	1.069×10^{-4} to 6.741×10^{-4}	2.832×10^{-4}	60	5	61.89
04SLs4	15	8.152×10^{-6} to 8.407×10^{-4}	2.227×10^{-4}	113	10	71.17
05SSs1+2	15	4.260×10^{-5} to 5.900×10^{-3}	1.658×10^{-3}	119	11	119.54
06SSs1+2	15	3.915×10^{-6} to 1.115×10^{-4}	2.182×10^{-5}	127	12	8.08
06SSs3+SCh	5	0 to 2.347×10^{-4}	7.718×10^{-5}	142	15	3.66
08SD12	13	3.119×10^{-7} to 2.875×10^{-4}	3.981×10^{-5}	206	27	3.22
10SLs1	5	3.029×10^{-7} to 5.744×10^{-5}	1.847×10^{-5}	129	12	5.84
14SSt1+2	15	8.783×10^{-8} to 4.467×10^{-4}	3.764×10^{-5}	304	55	11.64
14SSs3+SAk	10	1.470×10^{-6} to 2.293×10^{-4}	4.110×10^{-5}	172	20	7.71
16SSs1	14	2.358×10^{-7} to 1.221×10^{-4}	2.053×10^{-5}	174	20	10.00
16SSs2	15	2.260×10^{-7} to 3.128×10^{-5}	4.688×10^{-6}	169	19	16.53
18IS+IT	14	1.370×10^{-7} to 4.722×10^{-5}	7.732×10^{-6}	186	23	6.09
25IL1	4	1.329×10^{-4} to 3.077×10^{-4}	2.166×10^{-4}	40	4	205.66
25IP1	4	0 to 2.575×10^{-2}	7.476×10^{-3}	164	18	1067.88
28IGr1	15	8.679×10^{-7} to 1.073×10^{-4}	1.750×10^{-5}	173	20	1.95
28MSh	14	9.566×10^{-7} to 9.884×10^{-5}	1.315×10^{-5}	192	24	1.41
34MAm1	14	3.711×10^{-8} to 1.643×10^{-6}	5.663×10^{-7}	92	8	0.87
34MAm2	15	3.871×10^{-8} to 1.048×10^{-5}	1.837×10^{-6}	145	15	3.21
38MGn2	5	8.090×10^{-7} to 9.457×10^{-6}	2.941×10^{-6}	126	12	3.08
40SSs2	4	2.883×10^{-8} to 3.223×10^{-6}	1.644×10^{-6}	99	9	10.96
42SLs2	3	4.310×10^{-5} to 1.443×10^{-4}	1.028×10^{-4}	52	4	21.65
44SLs3+4	5	3.468×10^{-7} to 3.540×10^{-5}	1.005×10^{-5}	143	15	28.93
	10 AVG.			139 AVG.	14 AVG.	

[a] For confidence interval of one order of magnitude of mean value at 95% significance level.

[b] Based on five cycles per week.

$$n = (Vt_{a/2,n-1}/81.8)^2$$

The number of specimens required, according to this expression, is plotted in Figure C-4. A statistical summary of the permeability tests is given in Table C-6.

For the statistical criterion chosen, too few specimens were tested in two-thirds of the cases. This points to the wide variability, even with hand-picked specimens, and the need for testing large numbers of specimens to arrive at a meaningful average permeability value. Table C-6 also indicates that at least 14 specimens are usually required.

CORRELATION OF POROSITY, PERMEABILITY, AND FROST SUSCEPTIBILITY

Frost Susceptibility

To examine the potential use of aggregate pore data to identify aggregate particles that undergo destructive volume change when frozen, the pore parameters were compared with a measure of frost susceptibility. The indicator selected was the average dilation per cooling cycle (based on five cooling cycles per week) from the slow-cooling tests. Since those aggregates were tested in concrete under conditions approaching a natural environment, the chosen indicator was believed to offer the best measure of frost susceptibility. Susceptibility factors for the 24 test fractions are given in Table C-6.

Frost Susceptibility vs Pore Parameters

Correlation analyses of the frost-susceptibility factor vs the various pore measures (Tables C-1 and C-6), including the data in *NCHRP Report 15* (Table C-7), are summarized in Table C-8. All of the pore parameters correlated with frost susceptibility above the 99.9 percent significance level, but vacuum saturated absorption and 24-hr absorption (the easiest pore parameters to obtain) gave considerably better correlations than did permeability.

Evaluation of Intermediate Frost-Susceptibility Range

To test the sensitivity of relationships between the pore parameters and the intermediate range of frost susceptibility, the correlation analyses were repeated after eliminating the very poor and the very good aggregates. The elimination criteria, chosen arbitrarily on the basis of the frost-susceptibility factor, were as follows: (1) very sound aggregate, dilation less than 5 μin. per cycle; (2) very susceptible aggregate, dilation more than 100 μin. per cycle. Of the 30 aggregate fractions involved, 18 fell in the intermediate range (5 to 100 μin. per cycle).

With the extremes thus eliminated, none of the correlations was significant at the 99 percent level and only vacuum saturated absorption was significant at the 95 percent level (correlation coefficient 0.470 vs 0.463 critical value). Evidently none of the pore parameters is an excellent indicator of frost susceptibility in the intermediate range. This point is well illustrated in Figure C-5, which is a plot of frost susceptibility vs vacuum saturated absorption. Figure C-5 also indicates that aggregates with absorption values below 1 percent always had very good frost resistance, and (with one exception) values above 5 percent identified very poor frost resistance. In the range between, absorption values tell little about frost resistance.

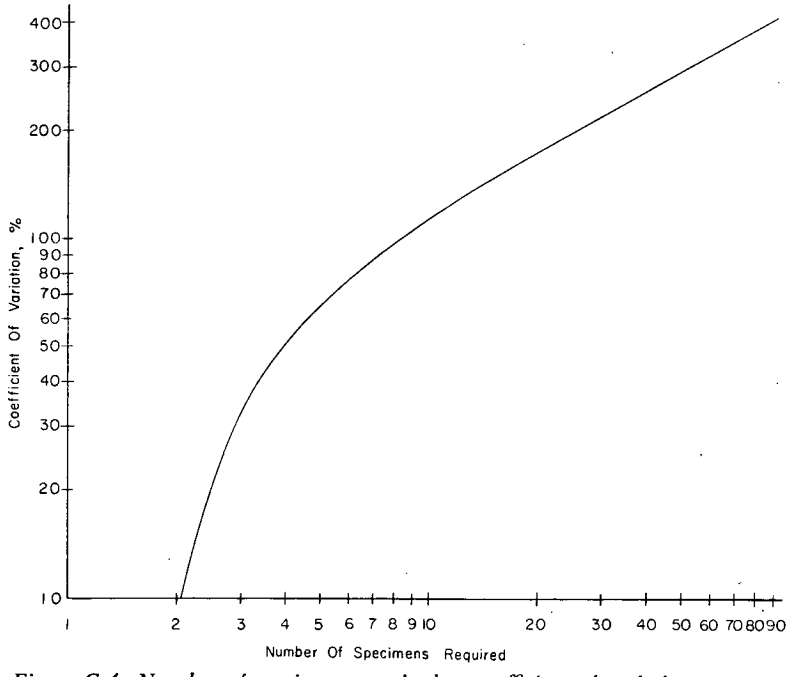

Figure C-4. Number of specimens required vs coefficient of variation.

TABLE C-7

SUMMARY OF AGGREGATE DATA FROM NCHRP REPORT 15

AGGREGATE AND SP GR	ABSORP. (%) VAC. SAT.	ABSORP. (%) 24-HR	APPARENT POROSITY (%) VAC. SAT.	APPARENT POROSITY (%) 24-HR	EFF. ABS. (%)	EFF. APP. POR. (%)	BULK DRY SP GR VAC. SAT.	BULK DRY SP GR 24-HR	FROST SUSCEPT. FACTOR[a] (μIN./CYC.)	LEAST SQUARES PERMEABILITY (DARCYS)
Maynes Creek and Eagle City limestone, > 2.50	3.22	2.20	8.275	5.665	1.02	2.610	2.570	2.575	13.96	1.134×10^{-3}
Paducah river gravel, < 2.50	7.71	5.25	16.869	11.503	2.46	5.366	2.188	2.191	753.8	7.58×10^{-6}
Benner and Snyder limestone, > 2.50	0.25	0.25	0.676	0.676	0.00	0.000	2.705	2.703	4.10	Negative, assumed zero
Meramec gravel < 2.50	4.86	3.19	11.368	7.465	1.67	3.903	2.339	2.340	55.38	1.819×10^{-4}
> 2.50	1.68	1.30	4.240	3.277	0.38	0.963	2.524	2.521	16.66	4.385×10^{-5}
Rapid and Coralville limestone, > 2.50	4.57	3.97	11.411	9.906	0.60	1.505	2.497	2.497	11.79	3.633×10^{-5}

[a]Based on five cycles per week.

Combinations of Pore Parameters vs Frost Susceptibility

In an attempt to find an improved relationship between the pore parameters and frost susceptibility in the intermediate range, various combinations of the pore parameters were investigated. According to Verbeck and Landgren's critical-size concept (*14*), hydraulic pressure that is developed in saturated pores during freezing varies directly with the amount of freezable water and inversely with permeability. If that is true, then frost susceptibility should vary directly with absorption or porosity and inversely with the permeability coefficient. This rationale was the basis for the *T*-factor (porosity vs permeability coefficient) found to correlate with the freeze-thaw durability factor in the work described in *NCHRP Report 15*.

An attempt to correlate the *T*-factor with frost susceptibility in the study reported herein failed to show the existence of a significant relationship. The reason for this is that the previous work encompassed only ten aggregate fractions, half of which were highly durable. Four of the five frost-susceptible aggregates were cherts, which characteristically display high porosity and low permeability. The concrete-distention process with such aggregates results directly from expansion of the aggregate. In aggregates that

TABLE C-8

CORRELATION OF PORE DATA WITH FROST SUSCEPTIBILITY, ALL TEST AGGREGATES

PORE PARAMETER	CORRELATION COEFFICIENT [a]
Vacuum saturated absorption	0.898
24-hr absorption	0.883
Vacuum saturated apparent porosity	0.891
24-hr apparent porosity	0.869
Effective absorption	0.888
Effective apparent porosity	0.851
Vacuum saturated bulk dry sp gr	−0.808
24-hr bulk dry sp gr	−0.812
Least squares permeability	0.781

[a] All significant at 99.9% level. Critical correlation coefficient = 0.568.

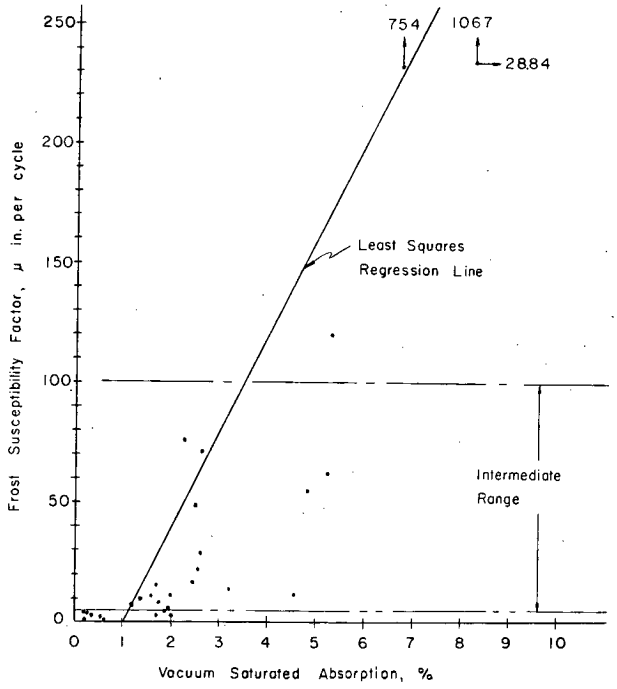

Figure C-5. Frost susceptibility vs vacuum saturated absorption.

TABLE C-9

CORRELATION OF PORE DATA WITH FROST SUSCEPTIBILITY, AGGREGATES IN INTERMEDIATE RANGE

PORE PARAMETER	CORRELATION COEFFICIENT
Vacuum saturated absorption	0.470 [a]
24-hr absorption	0.397
Vacuum saturated apparent porosity	0.466
24-hr apparent porosity	0.378
Effective absorption	0.466
Effective apparent porosity	0.467
Vacuum saturated bulk dry sp gr	−0.277
24-hr bulk dry sp gr	−0.265
Least squares permeability	0.126
Log_{10} (permeability $\times 10^6$)	
$\times$ vac. sat. absorption	0.555 [a]
$\times$ vac. sat. apparent porosity	0.555 [a]
$\times$ effective absorption	0.505 [a]
$\times$ effective apparent porosity	0.503 [a]

[a] Significant at 95% level. Critical correlation coefficient = 0.468.

are not cherty, permeability generally increases with porosity. Concrete destruction where aggregates have high permeability and porosity is caused by the expulsion of water from the aggregate into the highly impermeable paste phase. Because cherts with high porosity are invariably highly frost susceptible, aggregates in the intermediate range of frost susceptibility should, in general, fall into the expulsion-type failure category. For these aggregates, then, frost susceptibility should correlate with a direct combination of permeability and the various measures of porosity.

To test this hypothesis, correlation analyses of frost susceptibility vs several combinations of pore parameters were performed for test aggregates in the intermediate range. The results are given in Table C-9. The combination of permeability with various measures of porosity resulted in considerable improvement in the correlation coefficient. The most significant correlations were obtained from the combinations of permeability with absorption and apparent porosity. A plot of frost susceptibility vs $\log_{10}$ (permeability $\times 10^6$) $\times$ vacuum saturated apparent porosity is shown in Figure C-6. Although the data scattered considerably, a definite trend is evident.

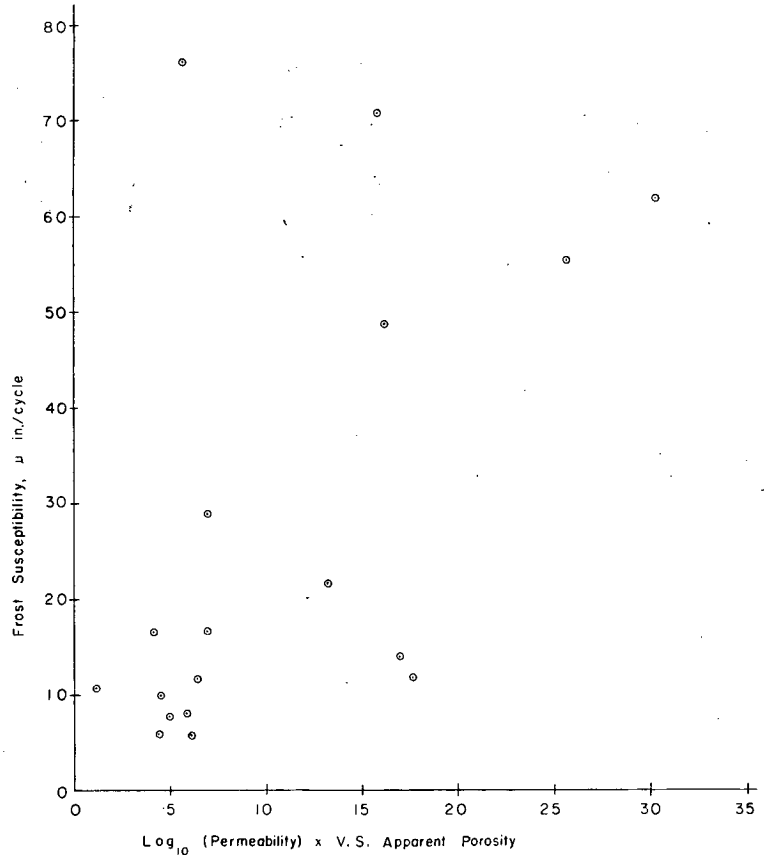

Figure C-6. Effect of permeability and vacuum saturated apparent porosity on frost susceptibility.

APPENDIX D

LINEAR EXPANSION OF INDIVIDUAL AGGREGATE PARTICLES

Previous work on linear expansion of saturated aggregate particles, reported in *NCHRP Report 15* (7), indicated that permanent length change induced by freezing correlated well with frost resistance of concrete made with the aggregates. It also indicated that permanent length change could be determined at sufficient accuracy with a simple dial-gauge comparator. This technique seemed to offer much promise because of its simplicity, speed, apparent reliability, and low cost. Because of the limited scope of the experiments, additional work was recommended.

EXPERIMENTAL PROCEDURE

The experimental work carried out in the research reported herein was intended to provide further evaluation of the test method over a broad range of aggregate types. Twenty-two of the 24 aggregate fractions used in the slow-cooling tests were employed to this end.

The eight particles of each aggregate type that were selected for testing passed the 1½-in. sieve and were retained on the 1-in. sieve. To determine the effect of the direction of measurement, those particles exhibiting fissility, bedding planes, fracture planes, or other structural features that would tend to force dilation to occur in a preferred direction, were divided into two groups. Relative length changes for particles of the first group were recorded along the expected axis of maximum dilation. Changes in length for the second group were measured along a perpendicular axis. If there was no discernible direction of maximum dilation, the direction of measurement was randomly selected—in most cases the longest axis of the particle.

Stainless-steel gauge studs were attached along the appropriate axis with epoxy cement, using the technique described in *NCHRP Report 15*. The specimens were tested in the vacuum saturated condition.

The specimens were cooled in a kerosene bath from 35 F to 15 F at the rate of 5 F per hour. Immediately upon reaching 15 F, the bath was heated to 35 F by means of an electric immersion heater. Each specimen was subjected to two freeze-thaw cycles, with an intermediate three-week soaking period.

The lengths of the specimens were continuously monitored with linear variable differential transducers (LVDT) during the freeze-thaw cycles. The necessary strain frames and electronic equipment are described in *NCHRP Report 15*. The determinations from these measurements were dilation (expansion during freezing) and permanent length change (difference in length change at 35 F between beginning and end of test cycle). The specimen lengths were also measured at room temperature with a dial-gauge comparator before and after the test cycles, providing a second measure of permanent length change.

For the particles measured in the direction of maximum dilation, the three test variables were compared with the frost susceptibility of the aggregates by means of correlation analyses. Frost susceptibility was defined as the average dilation per cycle of concrete specimens containing the aggregates in the slow-cooling tests.

RESULTS AND EVALUATION

Table D-1 gives the frost-susceptibility factors and the average values of the test variables for the aggregate fractions. The results of the correlation analyses are given in Table D-2. All three of the measured variables correlated significantly at the 99.9 percent significance level, but the permanent length change determined from the transducer output appears to be the best indicator of frost susceptibility.

Sensitivity of Variables in Intermediate Range of Frost Susceptibility

Table D-1 shows that two aggregate fractions, 25IL1 and 25IP1, are exceptionally susceptible to frost action. Because of the magnitude of the difference in their behavior, they could significantly affect the results of the correlation analyses. The correlations were therefore rerun with 25IL1 and 25IP1 eliminated. The results are given in Table D-2. In this case none of the measured variables correlated significantly at the 99 percent level, and only the permanent length change as determined from the transducer output correlated significantly at the 95 percent level.

Effect of Aggregate Permeability

The permeability of an aggregate particle should significantly influence its behavior in the individual-particle test. If two frost-susceptible particles with the same porosity but widely different permeability are frozen while in the saturated condition, the one with lower permeability should dilate more. This follows from Powers' hydraulic pressure theory, which states that internal pressure due to freezing varies inversely with permeability. Hence, in the individual-particle test, an aggregate with low permeability would appear to be more frost susceptible than one with high permeability. But an aggregate particle with high permeability will attempt to expel water during freezing. In concrete, since the permeability of cement paste is much less than that of most aggregates, hydraulic pressure and consequent distention occur in the vicinity of the particle. A highly permeable aggregate could therefore be more detrimental than one with low permeability, even though the individual-particle test would indicate the opposite. Neglecting the effect of permeability is a major weakness of any individual-particle test.

In an attempt to improve the correlations between frost

TABLE D-1

AGGREGATE TEST DATA AND FROST-SUSCEPTIBILITY FACTORS

AGGREGATE	AVERAGE DILATION (μIN./IN.)	PERMANENT LENGTH CHANGE (μIN./IN.)		FROST SUSCEPTIBILITY (μIN./CYCLE)
		TRANSDUCER	DIAL GAUGE	
02SLs1	225.0	34.33	1360	48.66
02SLs2	100.3	12.83	99	76.38
03SLs1	423.5	139.50	356	61.89
04SLs4	341.8	74.67	−156	71.47
05SSs1+2	241.2	64.00	293	119.54
06SSs1+2	412.5	52.00	−97	8.08
06SSs3+SCh	18.7	0.00	224	3.66
08SD12	110.3	23.80	−24	3.22
14SSt1+2	137.5	42.70	199	11.64
14SSs3+SAk	184.5	21.00	110	7.71
16SSs1	169.5	20.00	−214	10.00
16SSs2	266.0	20.50	−140	16.53
18IS+IT	176.8	26.70	330	6.09
25IL1	792.5	111.80	—	205.66
25IP1	2437.3	2296.00	2425	1067.88
28IGr1	166.7	18.00	−105	1.41
28MSh	189.7	26.00	−140	1.45
34MAm1	23.8	−8.30	27	0.87
34MAm2	74.2	10.16	−62	3.21
38MGn2	246.8	37.00	157	3.08
40SSs2	327.8	87.00	−10	10.96
42SLs2	140.0	2.75	—	21.65

susceptibility and the linear measures of distention in the individual-particle test, three parameters incorporating the effect of permeability were computed for each aggregate except 25IP1 and 25IL1. The results are also given in Table D-2. Both dilation and transducer-measured permanent length change became significant at the 99.9 percent level; but length change as measured by the dial gauge still failed to yield a significant correlation, probably because of the relatively narrow range of frost susceptibility of the aggregates and the low sensitivity of dial gauges. The relationship between $\log_{10}$ (permeability $\times 10^6$) $\times$ permanent length change (transducers) is shown in Figure D-1.

TABLE D-2

CORRELATION OF TEST VARIABLES AND FROST SUSCEPTIBILITY: WITH AND WITHOUT FRACTIONS 25IL1 AND 25IP1 AND IN COMBINATION WITH $\log_{10}$ (PERMEABILITY $\times 10^6$)

VARIABLE	CORRELATION COEFFICIENT		
		FRACTIONS OUT	
	FRACTIONS IN	VARIABLE ALONE	VARIABLE × PERMEABILITY
Dilation	0.972[a]	0.323	0.747[a]
Permanent length change:			
Transducer	0.983[a]	0.466[b]	0.765[a]
Dial gauge	0.852[a]	0.346	0.388

[a] Significant at 99.9% level.
[b] Significant at 95% level.

Effect of Direction of Measurement

Comparison of the dilations measured along the predicted axis of maximum dilation with those measured along an orthogonal axis revealed (1) that the petrographer had been able to predict quite accurately the performance and the direction of maximum expansion of an aggregate particle, and (2) that the amount of expansion of a saturated aggregate particle during freezing differs significantly along different axes. These results point out the advantages of petrographic examination and the absolute necessity of careful selection and testing of the aggregate particles if meaningful results are to be obtained with this test.

Number of Specimens Needed

The number of specimens needed to provide a specified range for the mean value of permanent length change or dilation at a given significance level can be calculated by the method outlined in Appendix C.

For some fractions no more than six particles may be needed, but for fractions with more internal variation 50 or more particles may have to be tested to satisfy the same statistical criteria. It is the responsibility of the testing agency to select statistical criteria suitable to its needs and to pursue the tests until the criteria are satisfied.

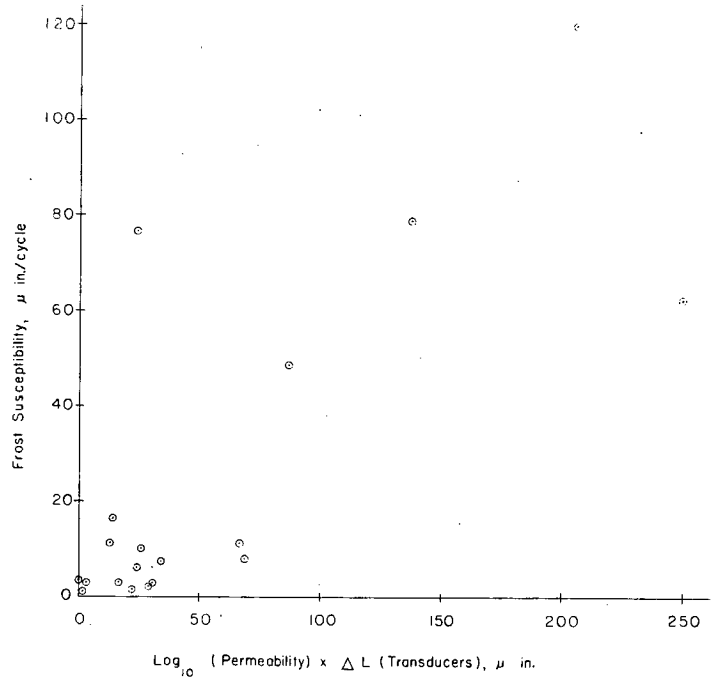

Figure D-1. Effect of permeability factor on correlation of permanent length change as measured by transducers.

APPENDIX E

VOLUMETRIC PARTICLE EXPANSION TESTS

The purpose of this research phase was to evaluate the hypothesis that the freezing of saturated aggregate particles can produce volumetric expansions that will relate to the frost susceptibility of concrete. Like the linear particle expansion and pore studies, this technique is simple, fast and economic compared to the slow-cooling method. The work included development of suitable apparatus to measure volumetric particle expansion during freezing, and evaluation of the method with a wide range of aggregate types.

The fact that aggregate particles can dilate during freezing is well established. In 1930, Scholer (*12*) observed that certain aggregates ". . . appear to expand and break when frozen in concrete saturated with water, and the expansive forces are sufficient to disrupt large masses of concrete." This concept has since been accepted and explored by various agencies and investigators. Cordon (*1*) noted in 1966:

> The aggregate particle itself need not fail in order for the concrete in which it is used to suffer damage from freezing and thawing. Aggregates may have enough strength and elasticity to withstand the stresses without failure, but the surrounding mortar may be damaged by the expansion of the aggregate particle.

TEST METHOD AND EQUIPMENT

Test Method

The volumetric expansion of saturated aggregate particles during freezing was determined with a simple mercury-displacement dilatometer. Single aggregate particles were enclosed in mercury-filled dilatometers at room temperature. The dilatometers were then placed in a constant-temperature bath at 15.0 ± 0.5 F for 25 min. Figure E-1 shows the temperature in the dilatometer as a function of time in the cooling bath. Changes in the volume of the dilatometer and its contents during this period were indicated by the level of mercury in a capillary glass tube connected to the top of the dilatometer. Comparison of a plot of mercury level vs cooling time with a calibration curve for the dilatometer indicated the amount of dilation of the test particle. The technique employed is similar to that used by Valore (*13*) to study the volume changes in small concrete cylinders during freezing and thawing.

Equipment

The equipment developed in this study consisted of a constant-temperature bath and two mercury-displacement

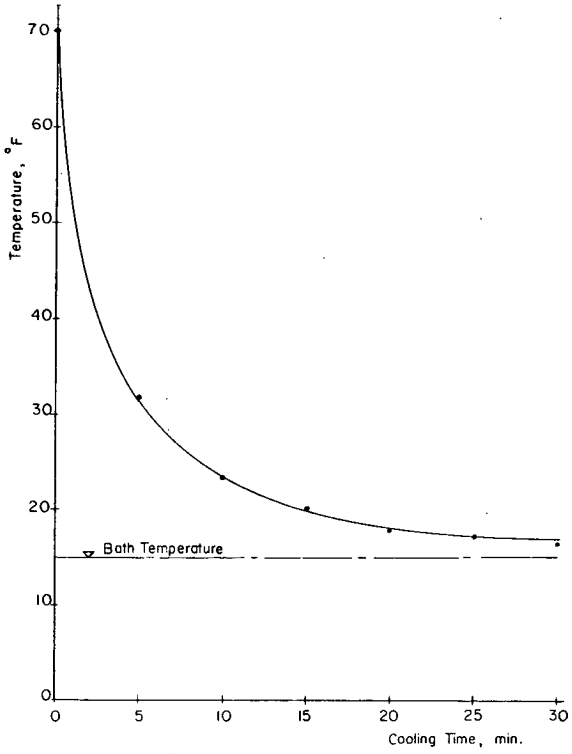

Figure E-1. Dilatometer temperature as a function of immersion time in cooling bath.

dilatometers. The kerosene bath (Fig. E-2), was made of galvanized sheet metal. Foam insulation 2½ in. thick was placed around the sides and bottom of the tank, and the whole assembly was enclosed in a plywood container. Two ½-in. copper tubing coils on the inside walls of the tank furnished the cooling, with Freon 12 as the refrigerant. The coolant was circulated through the coils continuously throughout the test. Temperature control was maintained by an electric-resistance immersion heater actuated by a temperature controller. This system permitted maintenance of the temperature within ±0.5 F of the set point. A propeller-type electric stirrer maintained temperature uniformity in the bath.

The mercury-displacement dilatometer is shown schematically in Figure E-3. The body was made of Invar 36 nickel steel, which has a very low coefficient of thermal expansion. This material was chosen to minimize the thermal volume change of the vessel. Mercury was used as the displacement medium because of its many advantages in the temperature range of 70 F to 15 F, which include a uniform and relatively low coefficient of thermal expansion, a relatively high coefficient of thermal conductivity, low specific heat, and immiscibility with water.

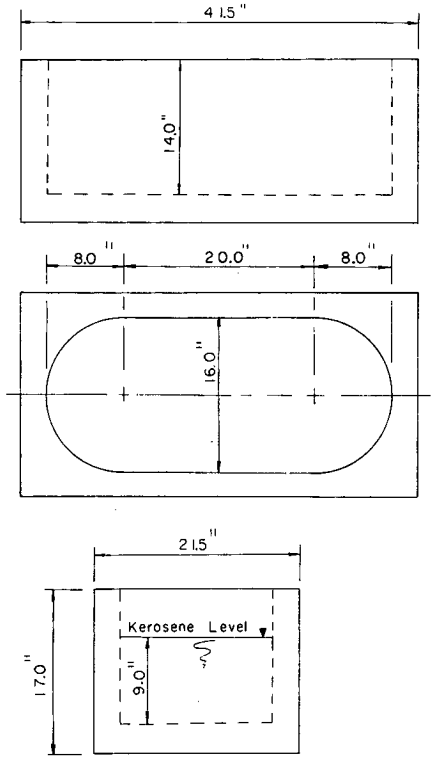

Figure E-2. Constant-temperature bath.

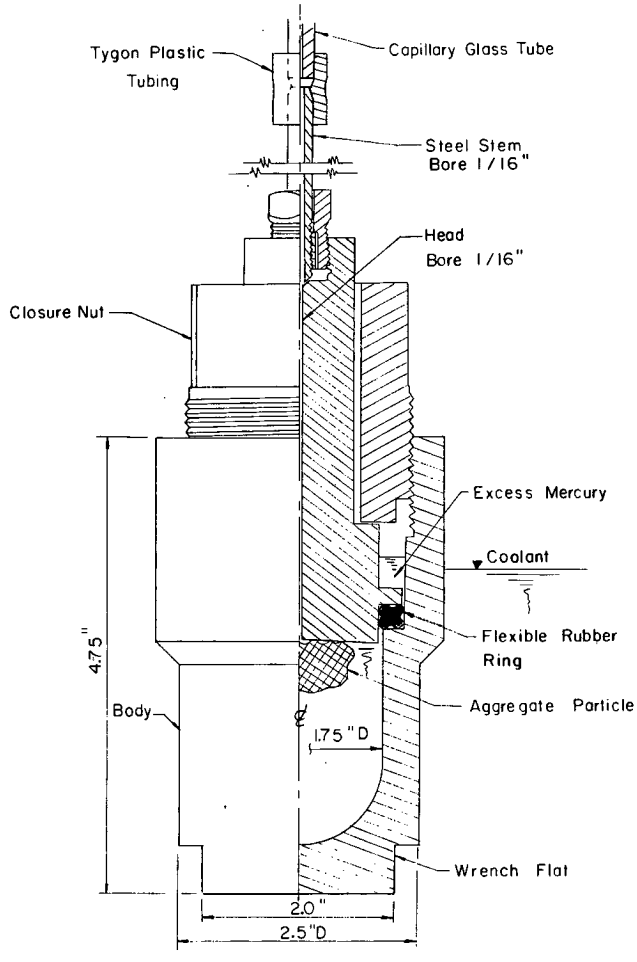

Figure E-3. Mercury-displacement dilatometer.

The dilatometer was filled with mercury to a level just below the chamber lip, leaving enough space to accommodate the test specimen. The chamber was sealed, and mercury was forced into the capillary tube by tightening the closure nut. The disassembled components of the dilatometer are shown in Figure E-4.

The capillary glass tubes in the dilatometers were selected to optimize three conditions: (1) minimum bore size to facilitate measurement of small changes in volume, (2) bore size large enough to permit upward displacement of entrapped air and water, and (3) bore size large enough to accommodate volume changes due to thermal contraction as the chamber was cooled from 70 F to 15 F, within a reasonable tube length. A 1¼-mm to 1¾-mm tube satisfied these requirements. The mean diameter of the capillary tube was accurately determined by weighing the quantity of mercury required to fill a given length of tube. The average bore size was 1.51 mm. Because the lowest reading of the height of the mercury column was 1 mm, the volume sensitivity of the apparatus was 0.0018 cc. A general view of the test apparatus appears in Figure E-5.

Calibration of Dilatometers

Changes in the height of the mercury column owing to thermal contraction of the mercury and the dilatometer during cooling were determined in order to provide a base from which volume changes of aggregate particles could be read. This was accomplished by replacing the aggregate particle with an approximately equal volume of Invar 36 nickel steel during a test run. If the volume change of the Invar specimen was negligible, the relationship between the time of immersion and the height of the mercury column would provide a base line for the experiments with aggregate particles. This relationship was found to be represented by curve IDALF in Figure E-6. Actual tests with aggregate particles produced curves similar to curve ID′A′BC in Figure E-6. The datum from which dilations were measured was then taken to be A′L′F, drawn parallel to the calibration base line ALF. The upward shift of the base line for the test aggregate is attributed to the difference in heat capacity between the aggregate and the Invar calibration specimen.

THE EXPERIMENT

Five particles of each of the 22 aggregate test fractions were carefully hand-picked by the petrographer. The aggregate particles were vacuum saturated at 0.4 cm Hg for 1 hr and soaked an additional 24 hr before testing. The volumes of the particles were determined from the difference in vacuum saturated, surface-dry (VSSD) weights in air and water. Each particle was submitted to one cooling cycle. The maximum dilation during cooling was defined as the percentage volume change at 25 min cooling time. The method for computing the maximum dilation is shown in Figure E-7.

TEST RESULTS

The average dilations for the five specimens of each aggregate type are given in Table E-1. These values correlated at the 99.9 percent significance level with the measure of frost susceptibility (correlation coefficient 0.960). The linear dilation per cycle of concrete specimens in the slow-cooling method containing the aggregates was used as the measure of frost susceptibility. The relationship between volumetric particle dilation and frost susceptibility is shown in Figure E-8.

Sensitivity, Moderate Frost-Susceptibility Range

The primary measure of the value of any technique for frost susceptibility is its ability to rate accurately the aggregates that fall into the moderate range of frost susceptibility. Therefore, the correlation between frost susceptibility and volume percent dilation was rerun without the two aggregates that show very high frost susceptibility (25IL1 and 25IP1). The correlation coefficient decreased considerably (0.685), but was still significant at the 99.9 percent level.

Effect of Permeability

The major drawback of unconfined aggregate-particle tests is that they tend to underrate frost susceptibility for aggregates of high porosity and permeability. Such aggregates usually do not show expansions in single-particle tests com-

Figure E-4. Dilatometer assembly.

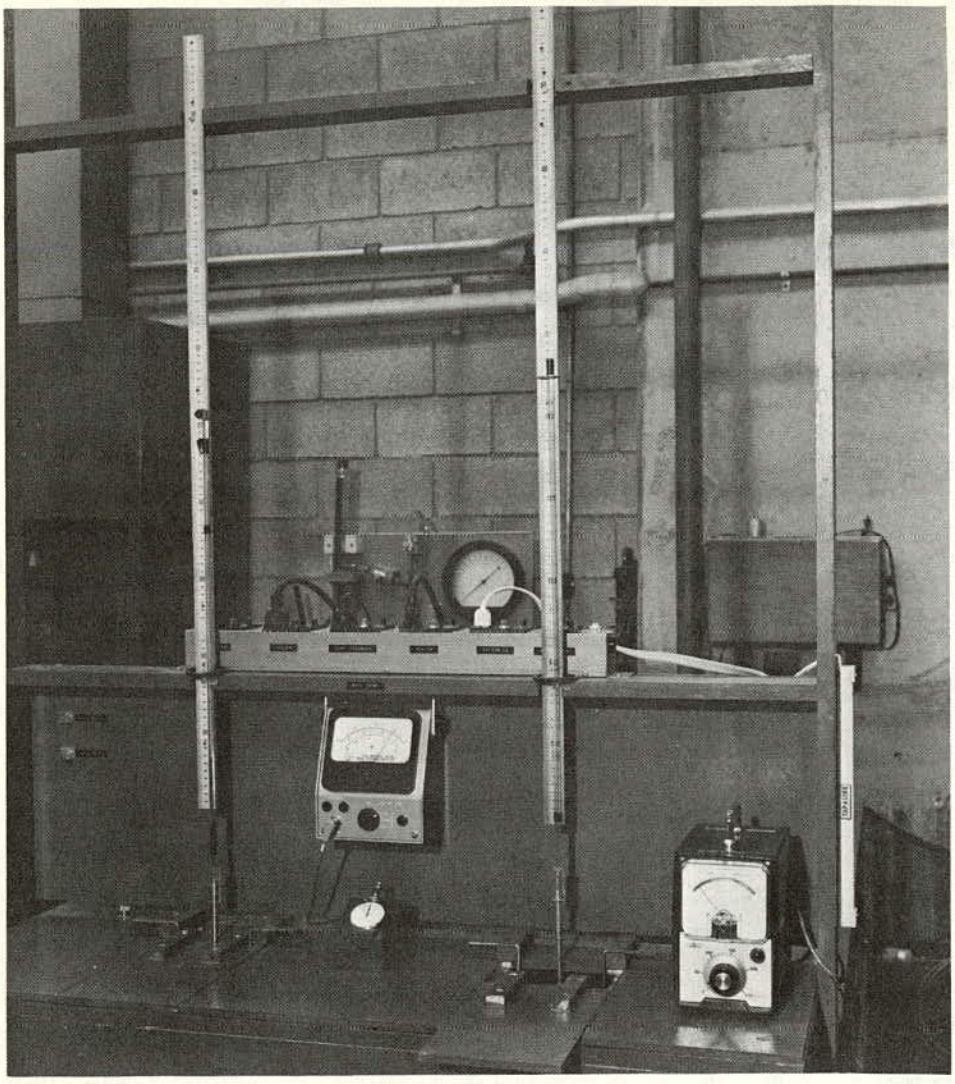

Figure E-5. Apparatus for volumetric particle expansion tests.

AGGREGATE PARTICLE:	02SLs2, specimen No. 3					
DILATOMETER:	No. 2					
BATH TEMPERATURE:	15 F ± 0.5 F					
PARTICLE VOLUME:	7.8839 cc					
Time, Min	0	5	10	15	20	25
Dilatometer reading, cm	30.0	14.7	11.3	14.4	13.4	12.8
Calibration datum, cm	30.0	14.7	11.0	9.5	8.7	8.1
Differential reading, cm	0.0	0.0	0.3	4.9	4.7	4.7
Dilation Volume, cc	0.000	0.000	0.005	0.088	0.084	0.084
Volume percent	0.00	0.00	0.06	1.11	1.06	1.06

Figure E-7. Example of dilation calculation.

TABLE E-1

AVERAGE VOLUMETRIC DILATION OF AGGREGATE PARTICLES

INDEX NO.[a]	AGGREGATE	DILATION (%)
1	02SLs1	0.33
2	02SLs2	0.68
3	03SLs1	0.54
4	04SLs4	0.43
5	05SSs1	0.90
6	06SCh	0.27
7	06SSs1	0.41
8	06SSs3	0.31
9	08SD12	0.48
10	10SLs1	0.44
11	16SSs1	0.30
12	16SSs2	0.50
13	25IL1	1.35
14	25IP1	3.33
15	28IGr1	0.13
16	28MSh	0.11
17	34MAm1	0.08
18	34MAm2	0.20
19	38MGn2	0.17
20	40SSs2	0.53
21	42SLs2	0.66
22	44SLs4	0.76

[a] See Figure E-8.

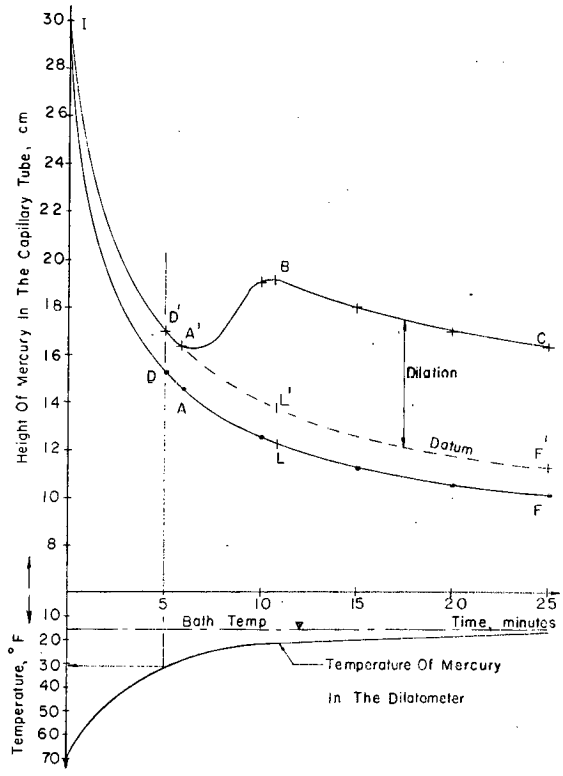

Figure E-6. Height of mercury column and temperature vs time.

mensurate with their destructive potential, because they tend to expel water during freezing. In concrete, the expelled water can produce high external pressures in the surrounding mortar.

The following combined effect of volume percent expansion and permeability was computed for all of the aggregate test fractions except 25IL1 and 25IP1:

$$\text{Volume percent dilation} \times \log_{10} (\text{permeability} \times 10^6)$$

Correlation of this factor with frost susceptibility produced

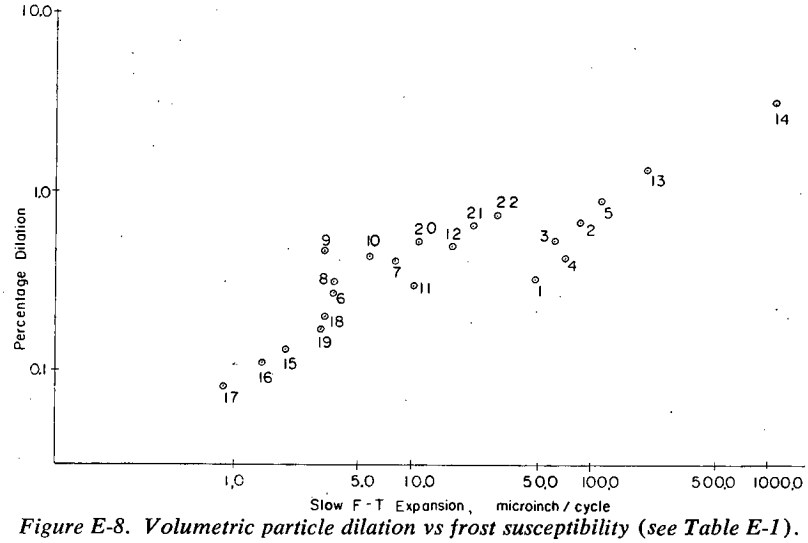

Figure E-8. Volumetric particle dilation vs frost susceptibility (see Table E-1).

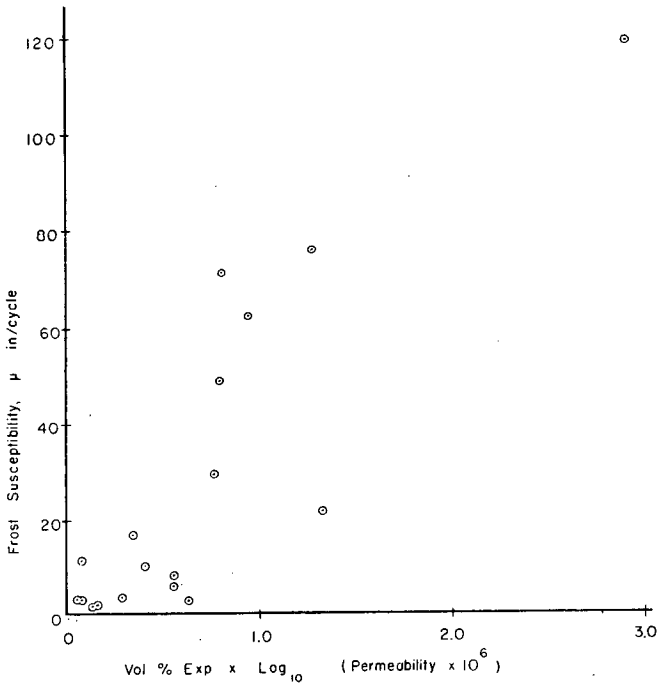

Figure E-9. Combined dilation-permeability factor vs frost susceptibility.

a coefficient of 0.864, significant at the 99.9 percent level. This is a meaningful improvement over the correlation coefficient obtained without the effect of permeability (0.685). The relationship between this combined factor and frost susceptibility is shown in Figure E-9.

Number of Specimens Needed

The number of specimens needed to provide a specified confidence range for the mean value of the volume percent dilation at a given significance level can be calculated by the method outlined in Appendix C. For this test the variability of the data is much less than for the linear particle expansion and permeability tests, because the effect of particle orientation is eliminated. On the average, therefore, fewer replications are required to produce results at the same level of significance.

APPENDIX F

RESEARCH ON THE MECHANISMS OF FROST ACTION

All of the existing test methods for frost susceptibility of concrete aggregates have a degree of empiricism. For this reason they are qualitative rather than quantitative indicators of frost susceptibility. They can show the relative frost susceptibilities of several aggregates, but they cannot predict the performance of an aggregate under specific field conditions.

Two factors are largely responsible for the empirical nature of the test methods: (1) the difficulty of simulating field conditions in the laboratory, and (2) inadequate understanding of the basic mechanisms of frost action. Better knowledge of the mechanisms of frost action would aid in establishing model-prototype relationships that would permit extrapolation from laboratory test results to anticipated field conditions. Any quantitative test for frost susceptibility must be based on a rational rather than an empirical approach, and a clear understanding of the basic mechanisms involved is prerequisite to the rational approach.

BACKGROUND

Powers' Hydraulic Pressure Theory

In 1955, Powers (*9*) proposed a theory of frost action. His hypothesis attributes frost destruction mainly to the generation of hydraulic pressure by an advancing ice front in critically saturated pores. When water freezes, a 9-percent volume change occurs. If the interconnected void system of an aggregate is more than 91.7 percent filled, the volume change associated with freezing will cause excess water to be forced through the voids, with resulting hydraulic pressure against the confining pore walls. The hydraulic pressure theory agrees well with phenomena observed in laboratory freeze-thaw tests, as indicated in *NCHRP Report 15* (*7*).

Dunn and Hudec's Ordered-Water Theory

In 1965, Dunn and Hudec (*3*) proposed a mechanism of frost destruction derived from research conducted at Rensselaer Polytechnic Institute. By differential thermal

analysis (DTA) techniques, they determined the quantities of water that froze in clay-bearing dolomitic limestones of widely varying frost susceptibility. Their studies indicated that smaller percentages of the contained water froze in unsound rocks than in sound rocks. In several instances, no freezing at all was detected in unsound rocks, and when freezing did occur in those rocks it was very gradual. Sound rocks, on the other hand, invariably displayed some freezing, and it usually occurred as a single pulse. These rather surprising results are in direct contradiction to Powers' hydraulic pressure concept.

In the light of their experimental findings, Dunn and Hudec hypothesized that the major mechanism in the frost destruction of rock is a temperature-dependent volume change of adsorbed or "ordered" water contained in intergranular "force spaces." Absorbed water is an orderly arrangement of tightly packed water molecules on a solid surface. It results from surface forms of attraction, known collectively as Van der Waals forces, and electrostatic attraction of the water molecule dipole by ionic surface changes. Since the Van der Waals forces are operative over extremely short ranges (varying inversely with the sixth power of the surface-molecule separation), the ordered-water concept is effective only in very fine pores, perhaps five molecular diameters (about 15 A).

To explore their hypothesis further, Dunn and Hudec carried out adsorption experiments on the rocks that had been subjected to DTA tests. In these experiments, they exposed the specimens to various relative humidities at constant temperature, and determined the amount of moisture adsorbed in each humidity environment as compared to the amount of water absorbed by the rock under vacuum saturation conditions. From these data and the DTA tests, they came to the following conclusions:

1. Water adsorbed at 100 percent relative humidity is not freezable.
2. Sound rocks tend to have more than 30 percent air space after 24-hr absorption, and unsound rocks less than 30 percent.
3. Unsound rocks tend to have large quantities of adsorbed water (water taken on at relative humidities less than 45 percent) and large quantities of small capillary water (water taken on by capillary condensation at relative humidities between 45 and 100 percent).

Inconsistencies of the Two Theories

The contradictions between Powers' and Dunn and Hudec's hypotheses are given in Table F-1. The two hypotheses appear to be in direct opposition regarding the role of water in the destructive process.

TABLE F-1

CONTRADICTIONS BETWEEN POWERS' AND DUNN AND HUDEC'S HYPOTHESES

RELATIONSHIP	POWERS	DUNN AND HUDEC
Frost susceptibility		
vs amount of water frozen	Direct	None
vs percent of water frozen	Direct	Inverse
vs percent absorption	Direct	None
vs percent adsorption	Inverse [a]	Direct
Occurrence of freezing relative to dilation (saturated condition)	Coincidental	No relation

[a] Assuming that adsorbed water does not freeze.

COMPARATIVE EXPERIMENTS

The purpose of this part of the research was to examine the comparative validity of the frost-action theories proposed by Powers and by Dunn and Hudec. This examination seemed necessary because (1) the two hypotheses are in total disagreement about the role of water; (2) Dunn and Hudec experimented with a single mineralogical type, and extrapolation of their results to other aggregates might not be warranted; and (3) their hypothesis, derived from research on rock cores only, needed to be evaluated in terms of coarse aggregates in concrete.

Adsorption Experiments

Experiments similar to those of Dunn and Hudec were performed with 32 aggregate subfractions from the slow-cooling tests described in Appendix B, using six relative humidities and two temperatures, 35 F and 75 F. Duplicate specimens of each aggregate were run, yielding a total of 124 isotherms (31 aggregates $\times$ 2 specimens $\times$ 2 temperatures). The six humidity environments were produced with saturated salt solutions and distilled water (Table F-2).

The adsorption test environment was evacuated to the boiling point of the solution or 2 mm Hg, whichever occurred first, and the specimen and the environment were allowed 72 hr to reach equilibrium and to complete the adsorption process (the length of time reported by Dunn and Hudec to be sufficient). The specimens were then removed and weighed to the nearest 0.1 mg, and the weight of water adsorbed was obtained from the difference between the specimen weight after removal from the adsorption environment and the oven-dry weight. This cycle—72 hr drying, 72 hr over a saturated solution, and weighing—was repeated for each solution at the two test temperatures. To provide the ordinate values for the adsorption isotherms,

TABLE F-2

ADSORPTION SOLUTIONS

SOLUTIONS	RELATIVE HUMIDITY (%)
Zinc chloride, $ZnCl_2$	6.8
Chromic acid, CrO_3	32.0
Potassium thiocyanate, KCNS	45.6
Magnesium acetate, $Mg(C_2H_3O_2)_2$	63.0
Potassium bromide, KBr	83.0
Distilled water, H_2O	100.0

the weight of water adsorbed by each specimen in each cycle was divided by the weight of water absorbed by the specimen.

The adsorption experiments were carried out in two vacuum desiccators. One was placed in a refrigerator at 35 F and the other was kept in the laboratory environment at 75 F, to provide the two test-temperature conditions. Each specimen was contained in a 1-oz. wide-mouth sample bottle. A rack of 16 bottles per run was handled by each desiccator. The test arrangement is shown in Figure F-1. At the completion of the adsorption period, the rack was removed from the desiccator and the bottles were quickly capped. During the weighing process, the specimens were removed from the bottles. They were handled with disposable plastic gloves to prevent surface contamination and absorption of skin moisture.

Some difficulty was encountered on removing the specimens from the desiccator after the adsorption cycles at 35 F. At this temperature both the specimens and the bottles tended to condense moisture from the atmosphere. To alleviate this problem, a sheet of thin plastic wrap was placed over the mouths of the bottles immediately upon opening the desiccator, and the bottle caps were then screwed on over the plastic covering.

The complete adsorption test data are given in Table F-3. The 75-F adsorption isotherms for the nine aggregate fractions used in the DTA tests are shown in Figure F-2. These represent averages of the duplicate adsorption-test specimens, and of the aggregate subfractions when subfractions are present. The discontinuity in the isotherms due to capillary condensation, noted by Dunn and Hudec, is clearly shown in Figure F-2. The abscissa values are shown, in the conventional manner, as relative vapor pressure (relative humidity ÷ 100).

Adsorption vs Frost Susceptibility

Four adsorption parameters and a sorption criterion proposed by Dunn and Hudec were compared with the frost susceptibility of the test aggregates as determined in the slow-cooling tests. Dilation per cycle (based on 10 cycles per 2 weeks) was used as the measure of frost susceptibility. The four adsorption parameters were (1) adsorption at 35 F and 1.000 relative vapor pressure, (2) adsorption at 75 F and 1.000 relative vapor pressure, (3) difference in adsorption at 35 F between relative vapor pressures 0.630 and 0.456, and (4) difference in adsorption at 75 F between relative vapor pressures 0.630 and 0.456.

The dilation per cycle, the four adsorption parameters, and the correlation of each of the adsorption parameters with frost susceptibility are given in Table F-4. As indicated in Table F-1, Powers' theory predicts an inverse relationship between frost susceptibility and adsorption, whereas Dunn and Hudec predict a direct correlation. Although none of the parameters in Table F-4 correlates significantly at the 95 percent level, an inverse relationship exists in every case at a lower significance level (negative correlation coefficients), favoring Powers' hypothesis.

Dunn and Hudec (*4*) proposed as measures of frost susceptibility certain measures of pore characteristics, based on sorption properties. They presented these criteria in the

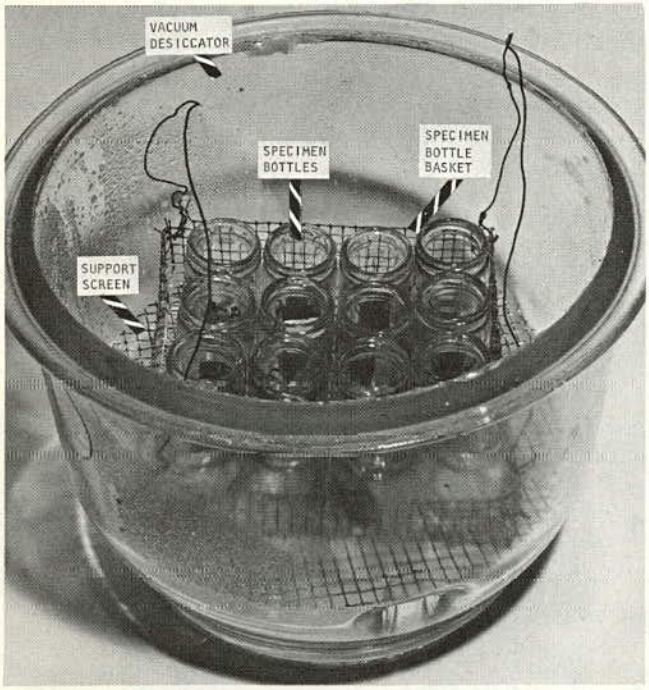

Figure F-1. Adsorption test setup.

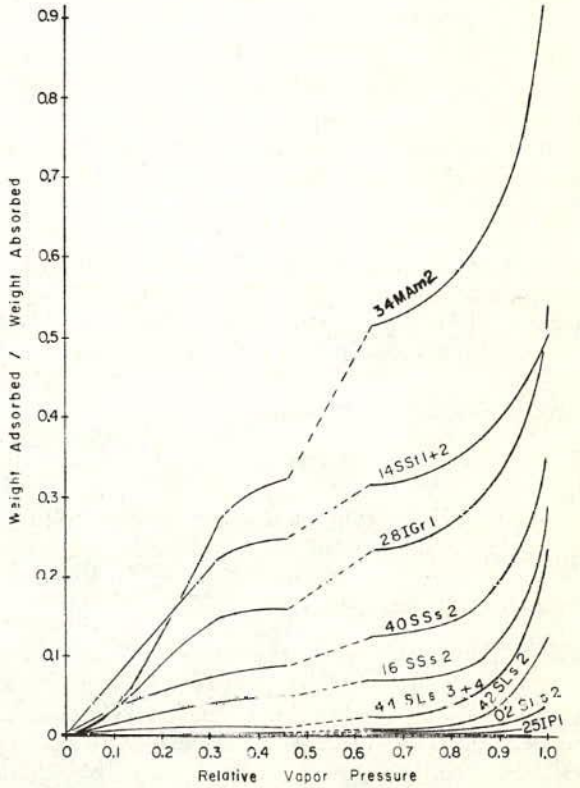

Figure F-2. Adsorption isotherms at 75 F for aggregate fractions in DTA tests.

form of a trilinear diagram, in which the three axes have the following connotation:

1. Void spaces $= 100 - \dfrac{\text{24-hr absorption}}{\text{vac. sat. absorption}} \times 100$
2. Adsorbed water = relative adsorption $\times$ 100
3. Bulk water $= 100 \times \left[\dfrac{\text{24-hr absorption}}{\text{vac. sat. absorption}} - \text{rel. adsorption} \right]$

The values obtained are expressed as percentages. Dunn and Hudec subdivided the area bounded by the trilinear axes into three zones: sound, sorption sensitive, and frost sensitive. Figure F-3 shows their trilinear diagram, but the points represent the 24 aggregates tested in the research reported herein. Notice that the three most frost-susceptible aggregates appear in the "sound" region and the five least-susceptible aggregates fall in the "sensitive" areas. Dunn and Hudec's plot evidently does not apply to the wide mineralogical range of the aggregates used in this study.

DIFFERENTIAL THERMAL ANALYSIS OF FREEZING

To investigate the amount of water frozen and the instant when freezing occurs, concrete specimens were submitted to differential thermal analysis (DTA) tests. The DTA technique is a means of examining chemical or physicochemical reactions involved in the evolution or absorption of heat. The heat effect, measured by the difference in temperature between the reacting substance and the test-chamber environment, is recorded as a function of time or temperature while the reacting substance is heated or cooled at a uniform rate. Experimentally this is accomplished by opposing two temperature-sensing elements (thermocouples, thermistors, or resistance thermometers), one located in the reacting substance and one in a dummy specimen (nonreacting substance with thermal properties similar to the reactive substance). The net output of the two temperature-sensing elements represents a temperature differential between the reacting substance and the test environment.

The advantages of the DTA technique over simple temperature measurements of the reactive substance are

No.	Aggregate	Frost * Susceptibility
1	25IPI	1067.88
2	25ILI	205.66
3	05SSsI+2	119.54
4	02SLs2	76.38
5	04SLs4	71.17
6	03SLsI	61.89
7	02SLsI	48.66
8	44SLs3+4	28.93
9	42SLs2	21.65
10	16SSs2	16.53
11	14SStI+2	11.64
12	40SSs2	10.96
13	16SSsI	10.00
14	06SSsI+2	8.08
15	14SSs3+SAk	7.71
16	18IS+IT	6.09
17	10SLsI	5.84
18	06SSs3+SCh	3.66
19	08SDI2	3.22
20	34MAm2	3.21
21	38MGn2	3.08
22	28IGrI	1.95
23	28MSh	1.41
24	34MAmI	0.87

Increasing Susceptibility To Frost Action

*Dilation Per Cycle, Based On 10 Cycles Per 2 Weeks

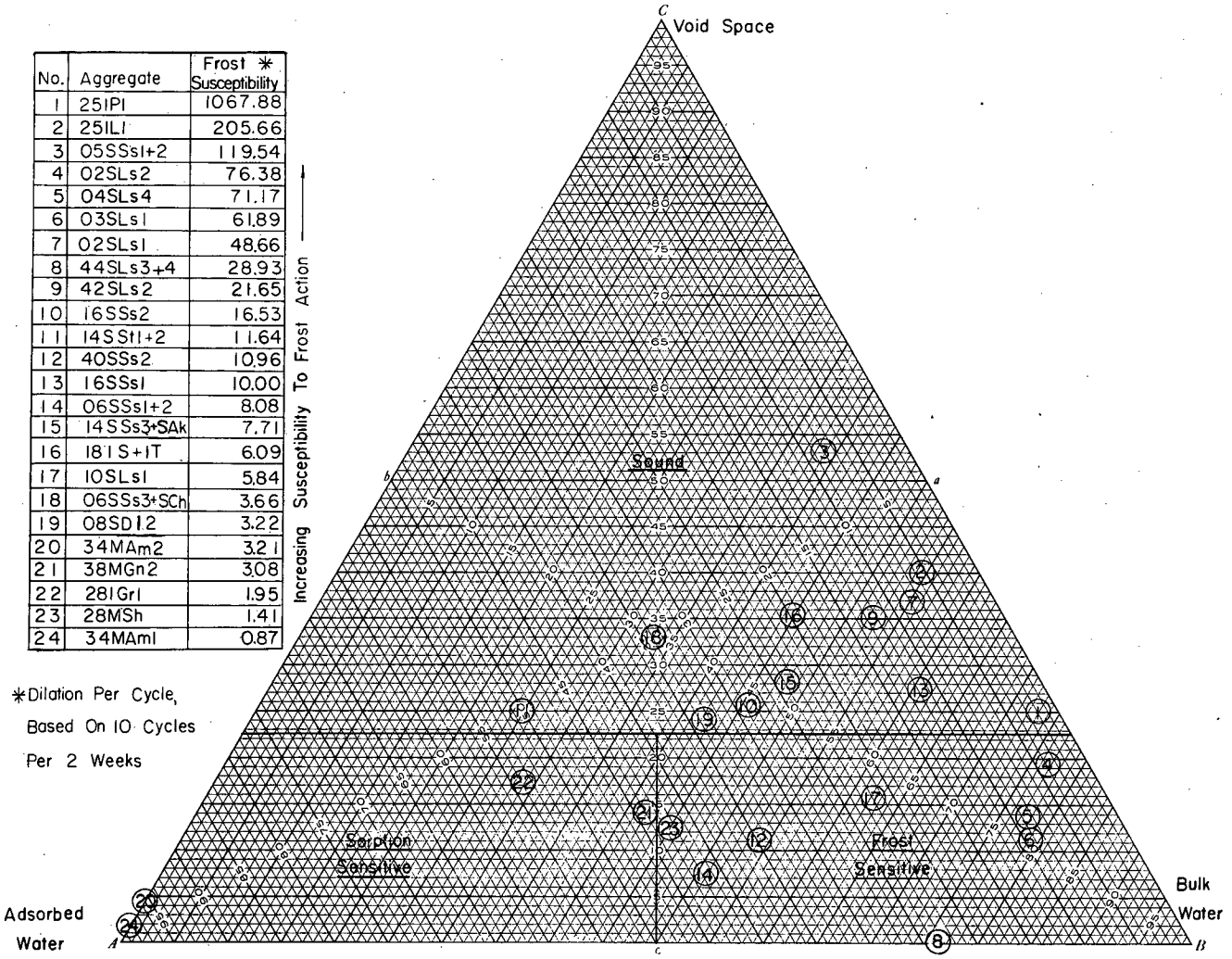

Figure F-3. Frost susceptibility vs sorption criteria, after Dunn and Hudec.

(1) that it produces a much sharper thermal peak, and (2) that for a given recorder chart width, it permits greater amplification of the output signal and consequently improves the precision of test measurements.

The conversion of water to ice is an exothermic phase transition process, resulting in the release of approximately 80 cal of heat per gram of ice formed (latent heat of fusion). Hence, DTA analysis is a logical choice for

TABLE F-3

ADSORPTION TEST DATA

AGGREGATE	SPECIMEN NO.	RELATIVE VAPOR PRESSURE AT 35 F						RELATIVE VAPOR PRESSURE AT 75 F					
		0.068	0.320	0.456	0.630	0.830	1.000	0.068	0.320	0.456	0.630	0.830	1.000
02SLs1	1	0.004	0.009	0.013	0.023	0.038	0.079	0.000	0.007	0.007	0.015	0.018	0.104
	2	.000	.010	.008	.015	.038	.132	.001	.002	.006	.010	.016	.055
02SLs2	1	.002	.006	.009	.013	.023	.052	.000	.005	.005	.009	.011	.071
	2	.000	.005	.004	.006	.022	.069	.000	.002	.003	.005	.006	.021
03SLs1	1	.004	.009	.010	.012	.025	.091	.000	.004	.005	.008	.011	.165
	2	.001	.013	.008	.017	.049	.238	.000	.006	.008	.013	.014	.068
04SLs4	1	.006	.015	.015	.020	.036	.110	.000	.010	.010	.011	.018	.140
	2	.001	.007	.004	.010	.025	.111	.000	.005	.005	.007	.008	.031
05SSs1	1	.003	.009	.010	.015	.020	.033	.000	.007	.007	.010	.014	.038
	2	.002	.026	.022	.044	.079	.163	.003	.019	.021	.033	.044	.109
05SSs2	1	.007	.028	.040	.047	.061	.087	.002	.023	.026	.039	.046	.103
	2	.013	.048	.049	.079	.136	.302	.007	.007	.045	.044	.078	.264
06SSs1	1	.016	.061	.071	.083	.113	.149	.004	.049	.055	.075	.086	.182
	2	.018	.064	.071	.125	.187	.344	.008	.056	.063	.095	.122	.247
06SSs2	1	.081	.234	.301	.368	.569	.780	.000	.172	.220	.325	.397	.952
	2	.014	.076	.045	.114	.190	.569	.007	.062	.067	.095	.102	.301
06SSs3	1	.027	.079	.109	.147	.204	.312	.008	.095	.116	.181	.210	.451
	2	.003	.049	.036	.059	.112	.215	.001	.043	.046	.068	.080	.145
06SCh	1	.022	.060	.064	.082	.118	.145	.004	.052	.059	.089	.107	.195
	2	.035	.384	.093	.186	.326	.779	.012	.209	.209	.233	.279	.558
08SD12	1	.012	.045	.066	.118	.198	.383	.006	.041	.047	.090	.123	.442
	2	.005	.027	.031	.069	.140	.361	.002	.026	.026	.049	.068	.223
10SLs1	1	.008	.023	.033	.059	.100	.219	.004	.017	.023	.045	.062	.285
	2	.003	.021	.017	.038	.075	.345	.002	.019	.017	.025	.036	.158
14SSt1	1	.070	.272	.358	.481	.561	.683	.060	.282	.324	.437	.500	.705
	2	.080	.268	.316	.414	.501	.692	.063	.284	.306	.374	.433	.601
14SSt2	1	.025	.057	.084	.086	.104	.128	.018	.063	.067	.089	.097	.142
	2	.070	.250	.299	.398	.455	.691	.045	.271	.287	.355	.398	.558
14SSs3	1	.016	.045	.052	.072	.113	.193	.007	.039	.040	.064	.076	.223
	2	.005	.016	.013	.034	.071	.279	.000	.019	.015	.022	.034	.139
14SAk	1	.079	.196	.226	.245	.269	.289	.065	.193	.203	.244	.253	.320
	2	.009	.037	.027	.062	.160	.531	.004	.038	.035	.049	.063	.274
16SSs1	1	.003	.014	.016	.030	.051	.121	.003	.016	.015	.052	.032	.141
	2	.002	.015	.012	.020	.034	.204	.000	.006	.002	.010	.017	.104
16SSs2	1	.014	.050	.056	.092	.133	.305	.008	.044	.054	.077	.091	.284
	2	.013	.049	.052	.083	.117	.421	.010	.041	.041	.064	.077	.291
18IS	1	.005	.032	.037	.058	.079	.144	.007	.040	.048	.075	.091	.133
	2	.033	.086	.101	.126	.154	1.000	.027	.082	.082	.108	.121	.249
18IT	1	.014	.075	.085	.112	.151	.339	.024	.065	.072	.107	.126	.226
	2	.017	.041	.040	.060	.081	.223	.003	.032	.020	.046	.053	.182
25IL1	1	.000	.003	.001	.006	.013	.056	.000	.002	.002	.002	.004	.066
	2	.000	.004	.003	.007	.009	.110	.000	.001	.001	.001	.004	.041
25IP1	1	.000	.002	.002	.004	.007	.032	.000	.002	.002	.003	.004	.024
	2	.000	.002	.001	.003	.004	.024	.000	.001	.000	.001	.002	.010
28IGr1	1	.031	.146	.172	.242	.328	.657	.040	.165	.186	.250	.291	.504
	2	.035	.204	.219	.296	.373	1.000	.000	.135	.127	.211	.269	.573
28MSh	1	.022	.088	.114	.176	.265	.875	.026	.099	.110	.136	.180	.415
	2	.033	.146	.183	.219	.274	.580	.026	.133	.107	.177	.207	.440
34MAm1	1	.025	.220	.309	.483	.614	.829	.023	.286	.356	.540	.623	.972
	2	.033	.325	.455	.756	.891	1.000	.015	.358	.443	.819	.928	1.000
34MAm2	1	.021	.199	.301	.489	.649	1.000	.016	.255	.338	.513	.609	.960
	2	.036	.250	.342	.525	.625	1.000	.014	.289	.307	.511	.568	.914
38MGn2	1	.032	.138	.174	.221	.276	.437	.027	.124	.143	.192	.228	.382
	2	.029	.111	.170	.219	.285	.601	.025	.111	.120	.192	.233	.496
40SSs2	1	.023	.086	.113	.169	.223	.456	.027	.084	.097	.132	.168	.335
	2	.025	.083	.101	.143	.183	.366	.022	.067	.077	.115	.137	.358
42SLs2	1	.000	.003	.005	.015	.023	.104	.000	.000	.000	.003	.012	.159
	2	.002	.011	.011	.025	.034	.182	.001	.006	.005	.012	.021	.091
44SLs3	1	.001	.008	.012	.022	.036	.118	.001	.006	.008	.013	.019	.121
	2	.003	.011	.015	.040	.183	.183	.001	.007	.006	.016	.025	.102
44SLs4	1	.000	.020	.032	.084	.143	.792	.005	.020	.020	.038	.077	.502
	2	.006	.022	.028	.054	.075	.304	.001	.014	.012	.031	.047	.213

TABLE F-4

CORRELATION OF ADSORPTION PARAMETERS WITH FROST SUSCEPTIBILITY

AGGREGATE	FROST SUSC. (DIL./CYCLE)	ADSORPTION PARAMETERS P/P_o = 1.000 AT 35 F	P/P_o = 1.000 AT 75 F	P/P_o = 0.630 - 0.456 AT 35 F	P/P_o = 0.630 - 0.456 AT 75 F
02SLs1	48.66	0.106	0.080	0.008	0.006
02SLs2	76.38	.037	.039	.003	.003
03SLs1	61.89	.165	.090	.006	.004
04SLs4	71.17	.111	.086	.005	.001
05SSs1+2	119.54	.147	.083	.028	.007
06SSs1+2	8.08	.461	.421	.050	.046
06SSs3+SCh	3.66	.363	.338	.043	.036
08SD12	3.22	.372	.333	.045	.033
10SLs1	5.84	.282	.222	.024	.015
14SSt1+2	11.64	.549	.502	.081	.068
14SSs3+SAk	7.71	.323	.239	.024	.022
16SSs1	10.00	.163	.123	.011	.022
16SSs2	16.53	.363	.288	.034	.023
18IS+IT	6.09	.427	.198	.023	.029
25IL1	205.66	.083	.054	.005	.000
25IP1	1067.88	.028	.017	.002	.001
28IGr1	1.95	.829	.539	.073	.074
28MSh	1.41	.728	.428	.049	.048
34MAm1	0.87	.915	.986	.238	.280
34MAm2	3.21	.980	.957	.185	.189
38MGn2	3.08	.519	.439	.048	.060
40SSs2	10.96	.411	.347	.049	.037
42SLs2	21.65	.143	.125	.012	.005
44SLs3+4	28.93	.350	.235	.025	.014
Correlation coefficient[a]		-0.381	-0.339	-0.238	-0.216

[a]Critical value for 95% confidence level = 0.404.

studying the behavior of water in concrete at subfreezing temperatures.

DTA Theory and Adaptation

According to Wendlandt (*16*), the area enclosed by the differential temperature curve is given by

$$\frac{M(\Delta H)}{gk} = \int_a^c \Delta T\, dt \qquad \text{(F-1)}$$

in which

M = mass of reactive material;
ΔH = heat of reaction;
g = geometrical shape factor;
k = thermal conductivity of sample;
ΔT = differential temperature;
dt = time differential; and
a,c = integration limits of differential curve.

The right side of the equation represents the area under the differential temperature vs time curve. Since ΔH, g, and k are constant for any given apparatus and reactant, the area under the DTA curve is proportional to the amount of reacting substance. Thus, by empirical calibration techniques the DTA method can be elevated from a qualitative to a quantitative tool.

The DTA technique developed for the work described here differs significantly from that used by Dunn and Hudec. Instead of examining a reacting specimen vs a dummy specimen, the differential heat evolution between two reacting specimens was used. The need for this technique stems from one of the shortcomings of Dunn and Hudec's work. If an examination is to be made of the mechanisms of destruction of concrete by saturated frost-susceptible aggregates, the aggregates should be encased in concrete. If saturated concrete specimens were subjected to conventional DTA analysis, it would not be possible to separate the effect of reacting (freezing) water in the paste phase from that in the aggregate. The saturated dummy specimen contained a volume of relatively nonabsorptive aggregate equal to the volume of aggregate in the test specimen, and the effects of the reactive water in the paste phase of the test specimen and the dummy therefore canceled out. Hence, the net area under the DTA curve does indicate the amount of water frozen in the test aggregate.

Specimen Preparation

Nine aggregates and one blank (mortar) were tested in duplicate. The mortar specimens were included to determine whether the water contained in the paste phase of the sample and dummy specimens actually did cancel in the DTA test.

The concrete mixtures were prepared in accordance with

American Concrete Institute method ACI 613-54, with the following proportioning criteria: cement factor, 5½ sacks per cubic yard; slump, 3± ½ in.; and air content 6 percent. Neutralized Vinsol resin was used as an air-entraining agent, and air contents were determined by the Chase meter method during mixing.

The coarse aggregate in the test specimens was evenly divided into four size fractions: ¼ to ⅜ in., ⅜ to ½ in., ½ to ¾ in., and ¾ to 1 in. The test aggregate comprised the latter two size fractions. The smaller sizes were either a quartz river gravel or a dense limestone of very low absorption (0.38 and 0.25 percent, respectively). The quartz aggregate was used with gravel-type test aggregates and the limestone with crushed aggregates. The coarse aggregate in the dummy specimens was entirely one of the low-absorption fillers, quartz being used in dummies paired with test specimens containing a gravel aggregate and limestone with those containing crushed aggregates. The dummies were proportioned to have the same volume of coarse aggregate as their companion test specimens.

The amount of cement, fine aggregate, water, and air-entraining agent was the same for the companion mixtures. The fine aggregate used throughout was a quartz river sand of low absorption (0.12 percent). The cement was a blend of three low-alkali type I cements. The physical and chemical properties of the fine aggregate and the cement are given in *NCHRP Report 15* (*7*).

A rigid procedure was followed to permit an accurate material balance during the production of the test and dummy specimens. The purpose was to determine the weight of coarse aggregate contained in the specimens and, by virtue of known absorption values, the amount of water contained in the coarse aggregates in each specimen. The procedure for the self-checking material balance is outlined in Exhibit F-1. The essential data regarding the quantity of coarse aggregate and aggregate water content for each specimen appear in Table F-5. Exhibit F-2 is an example of the calculations involved in compiling these data.

The concrete mixtures were cast in steel molds 3 in. in diameter and 6 in. long, in two equal layers, each layer compacted with 25 blows from a standard tamping rod. Stainless-steel gauge points and a centered copper-constantan thermocouple were installed in each specimen. The specimens were removed from the molds one day after casting, soaked in limewater at 77 F for 13 days, and conditioned in 35 F water for three weeks prior to testing.

Tests

The DTA tests consisted of obtaining differential temperature recordings for each specimen pair while cooling them from 35 F until the differential trace returned to its null position. This usually occurred between 15 F and 20 F. The cooling rate was maintained as close to 7 F per hr as possible. As is demonstrated in this Appendix F, however, the cooling rate can be varied considerably with negligible effect on the DTA test results.

The specimen length changes were also monitored continuously during the DTA tests. Each specimen pair received one instrumented cooling cycle and four intermediate (noninstrumented) cycles per week. The specimens were

EXHIBIT F-1

SAMPLE MIX DESIGN SHEET

MIX NO.: 11 AGGREGATE: 34MAm2 with Pa. filler DATE MIXED: 10/3/66

Fine aggregate free moisture

	Grams
Weight of pan + wet F.A.	1234.9
Weight of pan	235.0
Weight of wet F.A.	999.9 (A)
Weight of pan + dry F.A.	1233.6
Weight of pan	235.0
Weight of dry F.A.	998.6 (B)

Percent moisture: 100(A - B)/B = 100(999.9 - 998.6)/998.6 = 0.13 (C)

Percent free moisture: C - 0.12 = 0.13 - 0.12 = 0.01 (D)

Correction: (D/100) x wt F.A. in mix = 0.01/100 x 2.34 = 0.000234 (E)

Corrected F.A.: Wt F.A. in mix + E = 2.34 + 0.00 = 2.34 lb

Corrected water: Wt H_2O in mix - 454E = 241 - 0 = 241 ml

Mix quantities

	Basic Quant.	*Adjustment*	*Adj. Quant.*
Cement	0.96 lb	0	0.96 lb
F.A.	2.34 lb	0	2.34 lb
C.A.	3.50 lb	0	3.50 lb
Water	241 ml	0	241 ml
AEA	1.0 ml	0	1.0 ml

Batching

Weight of pan No. 2	1.43
Weight of cement	0.96
Subtotal	2.39
Weight of F.A.	2.34
Subtotal	4.73
Weight of C.A.	3.50
Subtotal	8.23
Weight of H_2O + AEA	0.53
Subtotal	8.76 (F)

Weight of assembled clean mold, empty	7.69 (G)
Weight of filled mold	11.30 (H)
Weight of waste material on paper	0.30 (I)
Weight of mix pan + remainder of mix	5.11 (J)

Weight of fresh concrete in specimen: H - G = 11.30 - 7.69 = 3.61 lb

Check: F - I - J = 8.76 - 0.03 - 5.11 = 3.62 lb

Percent air (Chase meter): 6%

DUMMY

Moisture corrections

Correction for F.A. moisture:
(D/100) x wt F.A. in mix = 0.01/100 x 2.34 = 0.000234 (K)

Corrected F.A.: Wt F.A. in Mix + K = 2.34 + 0.00 = 2.34 lb

Corrected water: Wt H_2O in mix - 454K = 245 - 0 = 245 ml

Mix quantities

	Basic Quant.	*Adj. Quant.*
Cement	0.96 lb	0.96 lb
F.A.	2.34 lb	2.34 lb
C.A.	3.13 lb	3.13 lb
Water	245 ml	245 ml
AEA	1.0 ml	1.0 ml

Batching

Weight of pan No. 2	1.43
Weight of cement	0.96
Subtotal	2.39
Weight of F.A.	2.34
Subtotal	4.73
Weight of C.A.	3.13
Subtotal	7.85
Weight of H_2O + AEA	0.53
Subtotal	8.39 (L)

Weight of assembled clean mold, empty	7.68 (M)
Weight of filled mold	11.11 (N)
Weight of waste material on paper	0.01 (O)
Weight of mix pan + remainder of mix	4.94 (P)

Weight of fresh concrete in dummy: N - M = 11.11 - 7.68 = 3.43 lb

Check: L - O - P = 8.39 - 0.01 - 4.94 = 3.44 lb

Percent air (Chase meter): 7%

WEIGHT OF SSD AGGREGATES IN TEST SPECIMEN AND DUMMY

Weight of remaining SSD aggregates, washed on No. 4 sieve:	
From test specimen, total	1.70 lb (Q)
From test specimen, test aggregate	0.76 lb (R)
From dummy, total	1.47 lb (S)
Original weight SSD test aggregate	1.99 lb (T)
Original weight SSD filler aggregate	1.99 lb (U)
Weight SSD test aggregate remaining after batching	0.18 lb (V)
Weight SSD filler aggregate remaining after batching	0.30 lb (W)

Weight of SSD test aggregate in test specimen:
T - R - V = 1.99 - 0.76 - 0.18 = 1.05 lb

Weight of SSD filler aggregate in test specimen:
U - Q + R - W = 1.99 - 1.70 + 0.76 - 0.30 = 0.75 lb

Weight SSD filler aggregate in dummy:
SSD wt C.A. in batch - S = 3.13 - 1.47 = 1.66 lb

EXHIBIT F-2

SAMPLE CALCULATIONS FOR AGGREGATE VOLUME AND QUANTITY OF WATER IN COARSE AGGREGATES OF TEST SPECIMENS

TEST SPECIMEN SET NO. 12

Test aggregate: 42SLs2
Absorption (V.S.SSD) 3.198 (A_t)
Specific gravity (V.S.SSD) 2.664 (S_t)

Filler aggregate: Pa.
Absorption (V.S.SSD) 0.250 (A_f)
Specific gravity (V.S.SSD) 2.708 (S_f)

Weight of test aggregate in specimen: 0.88 lb (W_t)
Weight of filler aggregate in specimen: 0.77 lb (W'_f)
Weight of filler aggregate in dummy: 1.66 lb (W_f)

Volume of coarse aggregate:
In specimen $454(W_t/S_t + W'_f/S_f) = 454(0.88/2.664 + 0.77/2.708) = 279$ cc
In dummy $454(W_f/S_f) = 454(1.66/2.704) = 278$ cc

Water in coarse aggregate:
Test aggregate $454(W_t \times A_t/100) = 454(0.88 \times 3.198/100) = 12.8$ g
Filler aggregate $454(W'_f \times A_f/100) = 454(0.77 \times 0.250/100) = 0.9$ g
Total $12.8 + 0.9 = 13.7$ g
Dummy $454(W_f \times A_f/100) = 454(1.66 \times 0.250/100) = 1.9$ g

Difference in C.A. water content between test specimen and dummy:
$\Delta = 13.7 - 1.9 = 11.8$ g

run for seven weeks, or until a dilation (an increase in specimen length during cooling) exceeding 4,000 μin. was observed.

Equipment Design and Calibration

A description of the length-change measuring apparatus, the constant-temperature bath, and the cooling bath, and a discussion of the calibration of the length-change measuring equipment are given in *NCHRP Report 15* (*7*).

The DTA and length-change measuring apparatus is shown in Figure F-4. The differential thermocouples were made from one spool of 24 AWG copper-constantan (type T) thermocouple wire to minimize manufacturing variability. The hot junctions were soldered with rosin-core electronic solder. The plastic-insulated differential temperature lead wires (constantan-constantan) were wrapped with a continuous sheet of aluminum foil, to which was soldered a copper wire connected to ground. This shielding procedure was used to relieve interference due to induction of electronic "noise." The cable was wrapped with plastic electrical tape to prevent mechanical damage to the shielding.

The d-c amplifier boosted the microvolt range output from the differential thermocouple leads to recordable levels. With the maximum gain set on the amplifier (10^5), the DTA apparatus shown was capable of detecting a temperature difference between the test and dummy specimens of 0.0079 F. This is approximately equivalent to the freezing of about 0.03 g of water in a 3-in. by 6-in. concrete specimen over a period of 1 min.

The amplifier gain was set at approximately 10,000 after trial and error procedures to find a setting compatible with

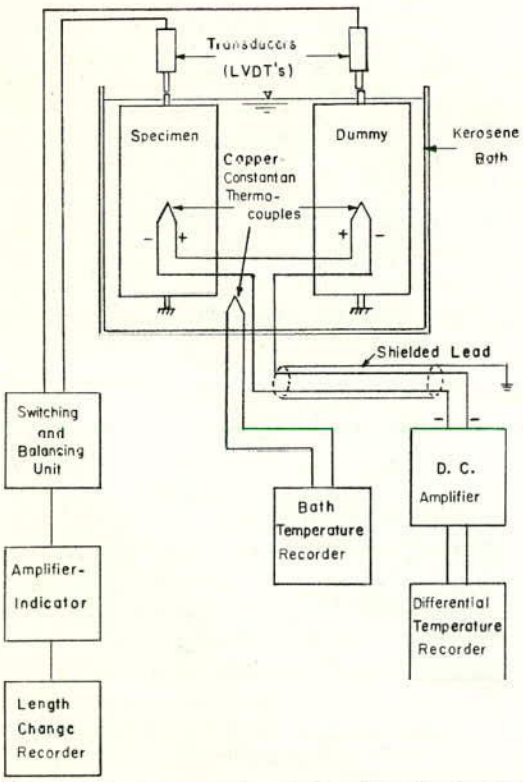

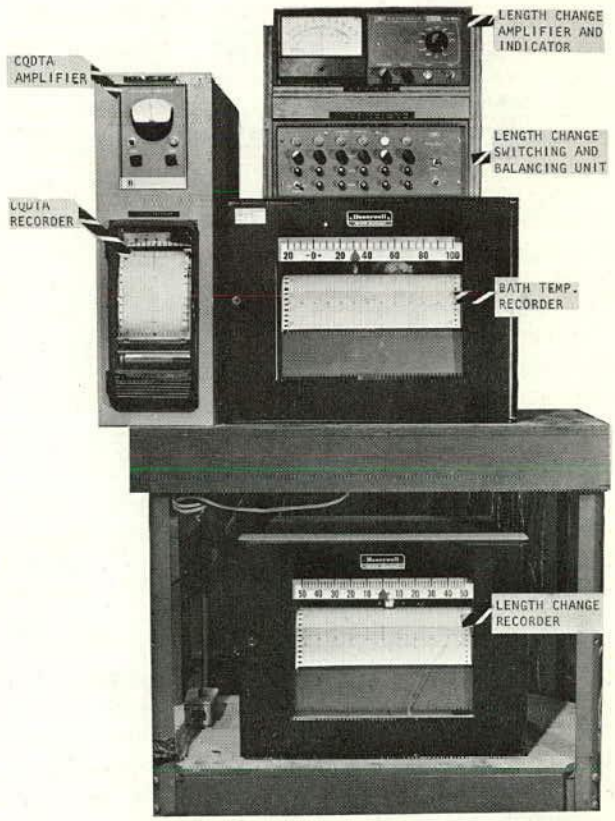

Figure F-4. Apparatus for DTA and length-change measurements.

TABLE F-5

DTA TEST SPECIMEN DATA

SPECIMEN NO.[a]	AGGREGATE[b]	SSD AGGREGATE (LB) TEST	SSD AGGREGATE (LB) FILLER	TEST AGGREGATE VAC. SAT. ABS. (%)	TEST AGGREGATE VAC. SAT. SP. GR.	AIR (%)	COARSE AGGR. (CC)	WATER IN AGGREGATE (G) TEST	WATER IN AGGREGATE (G) FILLER	WATER IN AGGREGATE (G) TOTAL	Δ[c]
1S	16SSs2/Md.	1.17	0.86	3.356	2.578	6 1/2	356	17.8	1.5	19.3	16.5
1D	Md.	--	1.60	--	--	7 1/2	278	--	2.8	2.8	
2S	25IP1/Md.	0.97	0.46	18.890	2.090	5 1/2	291	83.2	0.8	84.0	81.2
2D	Md.	--	1.60	--	--	5	278	--	2.8	2.8	
3S	40SSs2/Md.	0.94	0.75	3.016	2.582	6	296	12.9	1.3	14.2	11.2
3D	Md.	--	1.72	--	--	6 1/2	282	--	3.0	3.0	
4S	14SSt1+2/Md.	1.03	0.79	2.099	2.650	5 1/2	314	9.8	1.4	11.2	8.2
4D	Md.	--	1.72	--	--	6	300	--	3.0	3.0	
5S	34MAm2/Pa.	0.99	0.57	0.977	3.028	4 1/2	244	4.4	0.6	5.0	3.1
5D	Pa.	--	1.64	--	--	6	275	--	1.9	1.9	
6S	44SLs3+4/Pa.	0.81	0.84	2.343	2.765	5	274	8.6	1.0	9.6	7.8
6D	Pa.	--	1.55	--	--	5	260	--	1.8	1.8	
7S	28IGr1/Pa.	0.94	0.69	0.930	2.730	5	272	4.0	0.8	4.8	2.9
7D	Pa.	--	1.66	--	--	5	278	--	1.9	1.9	
8S	16SSs2/Md.	1.06	0.71	3.356	2.578	5	310	16.2	1.2	17.4	14.4
8D	Md.	--	1.73	--	--	6	301	--	3.0	3.0	
9S					MORTAR	8 1/2					
9D					MORTAR	8 1/2					
10S	42SLs2/Pa.	0.98	0.67	3.198	2.664	6	279	14.2	0.8	15.0	13.1
10D	Pa.	--	1.69	--	--	6	283	--	1.9	1.9	
11S	34MAm2/Pa.	1.05	0.75	0.977	3.028	6	283	4.7	0.9	5.6	3.7
11D	Pa.	--	1.66	--	--	7	278	--	1.9	1.9	
12S	42SLs2/Pa.	0.88	0.77	3.198	2.664	7	279	12.8	0.9	13.7	11.8
12D	Pa.	--	1.66	--	--	10	278	--	1.9	1.9	
13S	44SLs3+4/Pa.	0.89	0.73	2.343	2.765	7	269	9.5	0.8	10.3	8.5
13D	Pa.	--	1.61	--	--	7	270	--	1.8	1.8	
14S					MORTAR	7					
14D					MORTAR	7					
15S	02SLs2/Pa.	0.81	0.82	5.078	2.564	6	281	18.7	0.9	19.6	17.9
15D	Pa.	--	1.50	--	--	9	252	--	1.7	1.7	
16S	02SLs2/Pa.	1.03	0.69	5.078	2.564	8	298	23.7	0.8	24.5	22.6
16D	Pa.	--	1.66	--	--	11	278	--	1.9	1.9	
17S	25IP1/Md.	0.95	0.47	18.890	2.090	8	288	81.5	0.8	82.3	79.5
17D	Md.	--	1.64	--	--	6	286	--	2.8	2.8	
18S	14SSt1+2/Md.	1.06	0.75	2.099	2.650	7	312	10.1	1.3	11.4	8.3
18D	Md.	--	1.78	--	--	5	310	--	3.1	3.1	
19S	28IGr1/Pa.	0.97	0.73	0.930	2.730	7	284	4.1	0.8	4.9	3.1
19D	Pa.	--	1.62	--	--	7	271	--	1.8	1.8	
20S	40SSs2/Md.	0.94	0.82	3.016	2.582	8	308	12.9	1.4	14.3	11.4
20D	Md.	--	1.68	--	--	10	292	--	2.9	2.9	

[a] S = sample specimen; D = dummy specimen.

[b] Md. = quartz gravel filler (dummy) aggregate: vacuum saturated absorption, 0.380%; bulk SSD vacuum saturated specific gravity, 2.608.
Pa. = crushed limestone filler (dummy) aggregate: vacuum saturated absorption, 0.250%; bulk SSD vacuum saturated specific gravity, 2.708.

[c] Δ = difference between weight of water in coarse aggregate of sample specimen and dummy specimen.

the range of the recording instrument. The value of the gain did not have to be accurately known, because the entire system was calibrated by comparing the recorder output with a known differential heat input. Figure F-5 shows a test specimen and dummy specimen pair secured in strain frames and ready for testing.

The net areas under the DTA curves were determined by tracing the recorder charts on high-quality vellum paper, cutting out the areas under the curves, and weighing them to the nearest 0.1 mg on an analytical balance. This technique was used by Dunn and Hudec; it was employed in lieu of planimetering because of its greater sensitivity.

To permit quantitative evaluation of the DTA data, it was necessary to perform calibration tests on the equipment. This involved obtaining areas under the DTA curves for known heat input values. In practice, it was accomplished by making calibration specimens of the same dimensions as the test and dummy specimens. The calibration sample specimen contained a helical heating element consisting of soft iron wire wound around a fiber glass support and concentric with the axis of revolution of the cylindrical specimen. The heating element, which extended to within ½ in. of the ends of the specimen, was dimensioned in cross section so that half of the specimen volume was contained inside it and half outside. Air-entrained mortar was used in the calibration specimens, which were compacted on a

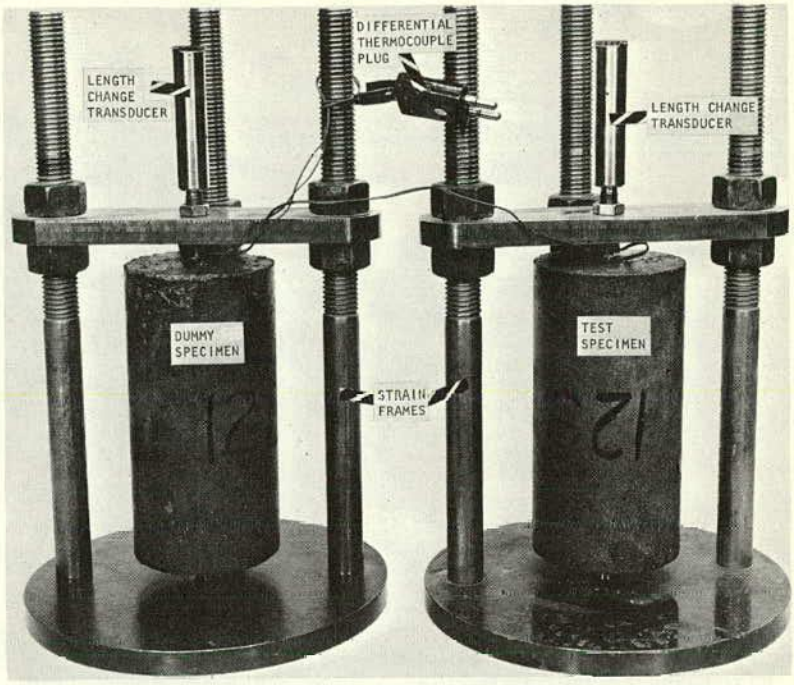

Figure F-5. Setup of test and dummy specimens for DTA tests.

vibrating table to ensure coverage of the heating-element wires without damage. Both specimens were cured in lime-water for two weeks, oven-dried at 250 F for one week, allowed to cool in a desiccator for 3 hr, and coated with epoxy to retain the internal oven-dry condition.

The heat input to the calibration specimen was determined as follows: From basic electrical theory, the relationship between power, P, in watts, and heat per unit time, Q/t, in calories per minute, is

$$P = (Q/t)/14.34 \qquad \text{(F-2)}$$

Power is related to electrical potential, E, in volts, and current, I, in amperes, by

$$P = EI \qquad \text{(F-3)}$$

Combining Eqs. F-2 and F-3 to eliminate P results in the following equation relating heat evolved Q, in calories, to electrical potential, current, and time:

$$Q - 14.34EIt \qquad \text{(F-4)}$$

in which t is in minutes. Hence the quantity of heat released in the calibration specimen by applying an electrical potential across the heating element for a period of time could be calculated by measuring the voltage, the current, and the time. The value of Q thus obtained was divided by the area under the DTA curve generated by the heat released in the sample specimen, to give the calibration factor Q/A, in calories per milligram, for the DTA apparatus.

Theoretically, the calibration factor should remain constant within the anticipated range of temperature rise of the sample specimen and the variability of the bath cooling rate, because changes in the heat capacity and conductivity of the specimen are negligible in these ranges. To verify this point and to check for instrumentation effects, calibration factors were calculated for different values of (1) total heat evolved, (2) rate of heat evolution, (3) environmental temperature at the start of heat evolution, (4) zero offset (shifting the null position of the DTA recorder to permit optimum utilization of chart space), (5) length of the period of heat evolution, (6) rate of temperature decrease of the cooling bath, and (7) varying heating rate in a single run.

A diagram of the calibration equipment is shown in Figure F-6. The rate of heat evolution was varied by means of the rheostat. The calibration experiment variables and results are summarized in Table F-6. If the calibration factor Q/A is independent of the test variables within the ranges explored and independent of instrumentation effects, a plot of A vs Q for the calibration test results should be a straight line passing through the origin. Such a plot is shown in Figure F-7. The graph is set to logarithmic scales to facilitate plotting, but because the line passing through the test points makes a 45-degree angle with the axes, on a rectangular coordinate plot it would be a straight line passing through the origin. The close fit of the test points to the line emphasizes the constancy of the calibration factor.

The curve in Figure F-7 is represented by the equation

$$Q = 12.50A \qquad \text{(F-5)}$$

in which

Q = heat released, cal
A = DTA area, mg of vellum paper

However, since the latent heat of fusion of ice is 79.71 cal per gram, the amount of water converted to ice, X, in grams, is

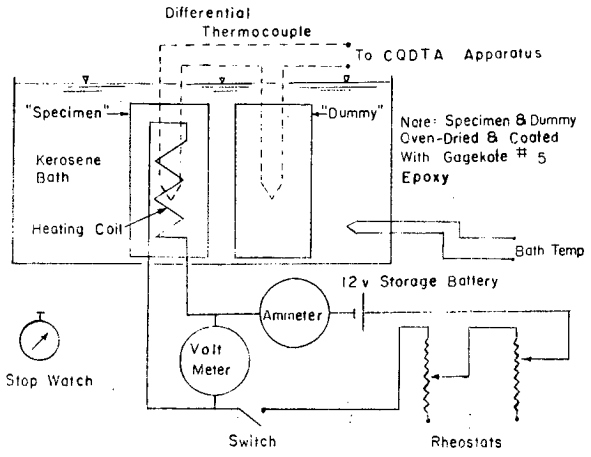

Figure F-6. Diagram of DTA calibration apparatus.

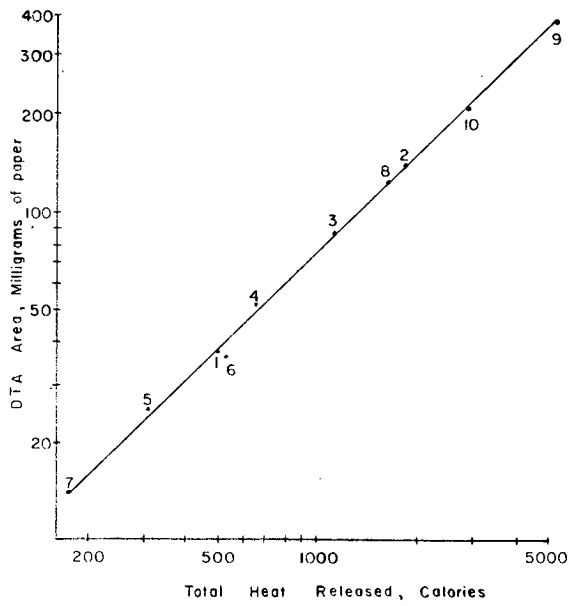

Figure F-7. DTA calibration, area vs heat (see Table F-6).

$$X = Q/79.71 \qquad \text{(F-6)}$$

Substituting the right side of Eq. F-5 for Q in Eq. F-6 and reducing the constants results in

$$X = 0.157A \qquad \text{(F-7)}$$

which is the calibration factor for the DTA apparatus in terms of grams of water converted to ice.

It is necessary to recognize that this calibration factor is applicable only within the limits of the ranges of the test variables covered, and only for the DTA amplifier gain at which the calibration tests were run. All of the DTA tests subsequently carried out met these criteria.

DTA Test Results

The measured variables in the DTA test consisted of the sample specimen dilation, the temperature at which the dilation started, the area under the DTA curve, the temperature at which the peak of the DTA curve was reached, the elapsed time from the beginning of the cooling cycle until dilation was completed, the elapsed time until freezing within the specimen ceased, and the dilation at the time freezing was completed. The manner in which these variables were obtained from the recorder charts is shown in Figure F-8, an assemblage of the recorder charts from a typical test run (the second measured cycle for specimen No. 16).

The results of the DTA tests are summarized in Table F-7. The column headed "Specimen Water Differential" is the difference in evaporable water content between the test specimens and the dummy specimen. This was obtained by determining the saturated surface dry and oven-dry weights

TABLE F-6

DTA CALIBRATION EXPERIMENTS, CONDITIONS AND AREA MEASUREMENTS

EXPT. NO.	ZERO OFFSET	POTENTIAL, E (V)	CURRENT, I (AMP)	TIME, t (MIN)	COOLING RATE (°F/HR)	START TEMP. (°F)	HEAT RELEASED, Q (CAL)	Q/t (CAL/MIN)	DTA AREA (MG)
1	0	2.34	1.40	10.0	7.8	28.0	469.8	47.0	37.1
2	0	1.86	1.12	60.0	7.7	28.0	1792.4	29.9	143.4
3	0	1.86	1.12	35.0	7.5	28.1	1045.6	29.9	86.2
4	0	1.86	1.12	20.0	8.4	27.8	597.5	29.9	50.6
5	0	1.86	1.12	10.0	7.2	27.7	298.7	29.9	25.6
6	0	1.00	0.60	60.0	7.2	28.1	516.2	8.6	36.2
7	0	1.00	0.60	20.0	6.9	28.1	172.1	8.6	13.9
8[a]	0	1.53[b]	0.92[b]	69.0[c]	7.7	28.2	1515.9[c]	22.0[b]	123.3[c]
9	−23.0	3.10	1.84	60.0	7.3	28.1	4907.7	81.8	385.4
10	−10.0	2.24	1.34	60.0	4.1	25.0	2582.6	43.0	205.5

[a] Rate of heat released varied purposely in this run.
[b] Average value.
[c] Total.

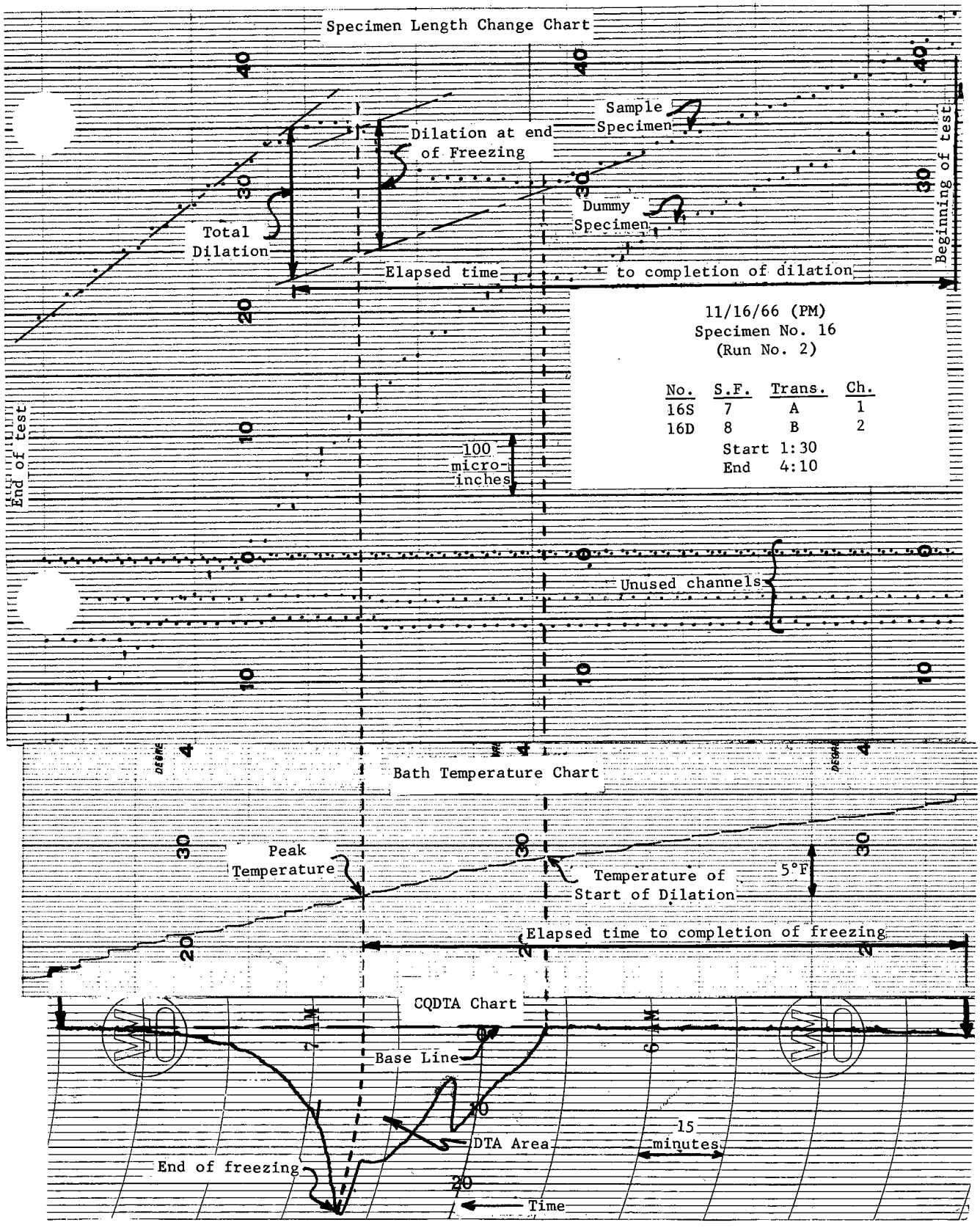

Figure F-8. Recorder charts from a typical DTA test run.

TABLE F-7

SUMMARY OF DTA RESULTS

AGGREGATE AND SPECIMEN NO.	NO. OF COOLING CYCLES	DILATION PER CYCLE (μIN.)	LAST CYCLE DTA TESTS				SPECIMEN WATER DIFFERENTIAL (G)	WATER FROZEN (%)
			AREA (MG)	ICE EQUIV. (G)	TIME, DIL./DTA	DIL. AT DTA PEAK, % TOT. DIL.		
02SLs2								
1	31	86.13	85.2	13.38	1.30	76	25.1	53
2	31	120.00	107.7	16.91	1.27	87	27.0	63
14SStl+2								
1	31	19.35	48.4	7.60	1.13	77	8.1	94
2	31	11.94	34.6	5.43	1.03	95	6.6	82
16SSs2								
1	16	11.88	51.6	8.10	1.04	84	11.8	75
2	31	19.68	42.8	6.72	1.18	82	12.1	56
25IP1								
1	6	770.00	239.0	37.52	1.44	52	65.4	57
2	6	1145.00	245.0	38.51	1.52	65	69.2	56
28IGr1								
1	31	4.19	26.9	4.22	1.13	69	5.3	80
2	31	5.16	23.9	3.75	0.99	100	3.0	100
34MAm2								
1	31	5.16	15.0	2.36	1.05	69	1.1	100
2	31	3.23	11.6	1.82	0.93	100	1.8	100
40SSs2								
1	31	12.90	20.8	3.27	1.34	35	11.9	28
2	31	40.65	32.7	5.13	1.33	60	12.3	42
42SLs2								
1	31	14.19	52.6	8.26	1.11	95	15.5	53
2	31	9.35	57.7	9.06	1.09	74	12.1	75
44SLs3+4								
1	31	7.10	27.9	4.38	0.86	100	4.0	100
2	31	8.06	40.0	6.28	1.06	84	6.7	94
Mortar								
1	31	2.58	-7.3	-1.15	--	--	-0.4	
2	6	3.33	-5.5	-0.86	--	--	-0.4	

of the specimens after the last test cycle. The "Water Frozen" column is the ratio of the ice equivalent of the DTA area to the specimen water differential, expressed as a percentage.

Analysis of DTA Tests

Correlation analyses were performed between frost susceptibility, expressed as dilation per cycle (based on five cycles per week), and the DTA test variables. The results are given in Table F-8.

In every one of the 127 DTA tests conducted, the initiation of freezing, as indicated by the deviation of the DTA trace from its null position, occurred at the same time as the start of the dilation of the specimen.

Comparison of the correlations from the DTA and adsorption tests, and the occurrence of freezing relative to dilation, with the inconsistencies given in Table F-1 reveals that Powers' hypothesis is generally supported by the test data (Table F-9).

Variability of the DTA Test Method

The DTA tests conducted on the mortar specimens gave an average net DTA area of 2.7 mg of paper, which is equivalent to 0.42 g of ice. Since the choice of designation of the test specimen and the dummy in this case was arbitrary, the value can be positive or negative. This figure, then, is the average error in the DTA tests due to variability in the paste phases of the test and dummy specimens. It readily explains the variability of the calculated percent of water frozen in aggregates with small amounts of freezable water (Table F-10).

Post-Freezing Dilations

An examination of the recorder charts from the DTA tests showed that dilation usually continued after the freezing had ceased. Cessation of freezing corresponds to the point on the DTA curve where the trace starts to return to its null position, according to an exponential decay function in accordance with the heat-loss relation.

To determine the tendency and extent of this phenomenon it was necessary to compute the ratio of the time from the beginning of the test until the end of dilation to the time for completion of freezing (T ratio), and the ratio of the dilation at the completion of freezing to the total dilation (D ratio). The results of this computation are given in Table F-10. Obviously, if total correspondence existed between dilation and the DTA curves, both of the ratios would be unity—as they were not.

TABLE F-8

CORRELATION OF DTA TEST VARIABLES WITH FROST SUSCEPTIBILITY

VARIABLE	CORRELATION COEFFICIENT [a]
Ice equivalent of DTA area (amount of water frozen)	0.965
Water in test aggregate	0.962
Percent water frozen	−0.313
Vacuum saturated absorption	0.987

[a] Critical values: 90% significance, 0.582; 95% significance, 0.666; 99.9% significance, 0.898.

TABLE F-9

CORRELATION OF TEST DATA WITH POWERS' AND DUNN AND HUDEC'S HYPOTHESES

RELATIONSHIP	CORRELATION [a]	THEORY FAVORED
Frost susceptibility		
vs amount of water frozen	Direct	Powers
vs percent of water frozen	None	Neither
vs percent absorption	Direct	Powers
vs percent adsorption	None	Neither
Occurrence of freezing relative to dilation (saturated condition)	Simultaneous	Powers

[a] Significance level 95% or higher.

THE DUAL-MECHANISM THEORY

The occurrence of post-freezing dilations is difficult to reconcile with Powers' hydraulic pressure theory. However, suppose, for the moment, that after the completion of freezing a portion or all of the remaining unfrozen bulk water becomes "ordered" by adsorption on the ice and pore surfaces. This possibility is enhanced by the fact that the adsorption tendency increases with decreasing temperatures. It can be further supposed that the "ordering" process entails a volume increase. The net result would be an increase in the hydraulic pressure and continued dilation until ordering ceased. For the sake of simplicity it was assumed that the ordering process began with the cessation of freezing, but the argument is equally valid for the more logical possibility that it starts at a much higher temperature, although probably not until freezing is initiated.

One bit of evidence in favor of this hypothesis is that the nearer the quantity of water frozen is to 100 percent, the closer the values of the D and T ratios are to unity. This is shown in Table F-10. Obviously, if all of the water freezes, none is available to be adsorbed. Furthermore, if the suggested hypothesis is valid, the T ratio should correlate inversely (negative correlation coefficient) and the D ratio should correlate directly with the percentage of water frozen. Additional correlation analyses revealed that both of the ratios correlated significantly at the 99 percent level, in the manner suggested.

In the light of this argument, it appears that in most cases two mechanisms of destruction were at work—the hydraulic pressure proposed by Powers, and the adsorption proposed by Dunn and Hudec. In eight of the nine cases hydraulic pressure apparently was the dominant factor—"apparently" because the contribution of adsorption during freezing is not known. In one case (aggregate 40SSs2) adsorption was definitely the dominant mechanism, as indicated by the fact that more than half of the total dilation took place after freezing had ceased.

There is a distinct difference between the adsorption mechanism proposed here and that proposed by Dunn and Hudec. To explain the mechanism of destruction, they depended upon the difference between the thermal coefficients of adsorbed water and minerals, and direct action of the adsorbed water on the pore walls. It is suggested here that some portion of the unfrozen water is adsorbed, resulting in an increase in volume that produces hydraulic pressure in much the same manner as in the freezing process.

TABLE F-10

WATER FROZEN VS D AND T RATIOS

AGGREGATE	WATER FROZEN (%)	RATIO T	RATIO D
34MAm2	100	0.99	0.85
44SLs3+4	97	0.96	0.92
28IGr1	90	1.06	0.85
14SSt1+2	88	1.08	0.86
16SSs2	66	1.11	0.83
42SLs2	64	1.10	0.85
02SLs2	58	1.29	0.82
25IP1	57	1.48	0.59
40SSs2	35	1.34	0.48

FREE-ENERGY DIFFERENCES AS AN ALTERNATIVE EXPLANATION

Various literature sources indicate the possibility that the post-freezing dilations could be caused by pressure gradients that are generated by differences in free-energy levels within the concrete specimens. In 1953, Powers and Helmuth (*11*) set down a descriptive model for the generation of internal stresses by free-energy differences, as an adjunct to Powers' hydraulic pressure theory. The nature of the pore system in concrete plays a major role in this model. According to Dunn and Hudec (*3*), three classes of void systems are found in mineral aggregates: voids, capillaries, and force spaces. The same is true of hydrated-cement paste, except that the smallest pores, called gel pores, are usually about an order of magnitude smaller than the force spaces in mineral aggregates. The gel pores are so small that water cannot freeze in them, at least down to −88 F.

Basically, the chain of events visualized by Powers and Helmuth proceeds as follows. The temperature of a saturated concrete specimen is reduced until ice starts to form

in the larger capillaries. The gel water will be in thermodynamic equilibrium with the capillary ice under these conditions only (1) if freezing occurs at 32 F, (2) if the gel water has the same free energy as bulk water, (3) if the capillaries are large enough to have negligible surface energy, and (4) if the ice and the gel water are both under a pressure of 1 atm. If the temperature is reduced below the point at which the water in the capillaries freezes, the system will no longer be in equilibrium. This is a consequence of the thermodynamic definition of entropy under constant pressure conditions, expressed as

$$(\partial G/\partial T)_p = -S \qquad \text{(F-8)}$$

in which G, T, and S are Gibbs' free energy, absolute temperature, and entropy, respectively. Statistical mechanics defines entropy as a measure of the degree of randomness of a state. From this definition, water must have higher entropy than ice because ice is a considerably more ordered state than water, as evidenced by its crystalline nature. Reflection on these points and Eq. F-8 reveals that a temperature decrease will produce a *gain* in free energy by both the ice and the gel water, but the gel water will gain more free energy than the ice because of its higher entropy. Thus, a difference in free energy between capillary ice and gel water ensues. Because the gel water has the higher free energy, it will tend to flow to the capillary ice in accordance with Le Chatelier's principle.

The Powers and Helmuth model is detailed here to point out weaknesses that are not clearly evident in the original text. At least three of the four conditions given for thermodynamic equilibrium are definitely not valid. The freezing temperature of the water in capillaries is always depressed in inverse proportion to the diameter of the capillary. Supercooling is invariably encountered in various degrees, as indicated by the observed initial freezing pulse. This factor alone precludes the accurate definition of a free-energy model, because of the enthalpic change produced.

Moreover, gel water cannot be supposed to be thermodynamically synonymous with bulk water. The entropy of gel water is less than the entropy of bulk water because of the orienting effect of the surface force field of the gel pores and the dipole nature of the water molecule. Since the average size of the gel pores is about five water molecule diameters, most, if not all, of the gel water must be in a highly ordered state. Hence the entropy of the gel water is probably not greatly different from the entropy of the capillary ice. In any case, it is evident that the free-energy difference between the gel water and the capillary ice is considerably diminished when the ordered nature of the gel water is taken into consideration.

Finally, it is difficult to imagine that the capillary ice and the gel water could remain at atmospheric pressure once ice starts to form in the capillaries. In the first place, the initial freeze pulse generates hydraulic pressure, as indicated by the inevitable increase in specimen length that accompanies freezing. Indeed, the very basis for Powers' theory of frost destruction of concrete is the generation of hydraulic pressure. Furthermore, this is a dynamic and not a hydrostatic pressure condition.

These points raise serious doubts regarding the application of Eq. F-8 to the problem at hand. One further digression will bring them into even sharper focus.

In 1961, Helmuth (*6*) discussed volume changes caused by temperature changes in cement pastes. He proposed a thermodynamic model based on the same relationships as those of the model that he and Powers had proposed earlier, but with somewhat different assumptions and drastically different results. Consider a saturated concrete specimen at a temperature above the freezing point. Eq. F-8 may be rewritten as

$$\Delta G = -\int_{T_1}^{T_2} S\,dT \qquad \text{(F-9)}$$

For a small temperature change like $\Delta T = T_2 - T_1$, Eq. F-9 may be written as

$$\Delta G \simeq -S\,\Delta T \qquad \text{(F-10)}$$

Therefore, for the capillary water,

$$\Delta G_c \simeq -S_c\,\Delta T \qquad \text{(F-11)}$$

Likewise, for the gel-water system,

$$\Delta G_g \simeq -S_g\,\Delta T \qquad \text{(F-12)}$$

Subtracting Eq. F-12 from Eq. F-11 gives

$$\Delta G_c - \Delta G_g \simeq -(S_c - S_g)\,\Delta T \qquad \text{(F-13)}$$

The entropy of the gel water must be less than the entropy of the capillary water because of the orienting effect of the surface force field and the larger surface-to-volume ratio of the gel water. With a decrease in temperature, then, the right side of Eq. F-13 will be positive. Notice that according to Eq. F-10 a decrease in temperature produces an increase in free energy. Hence, for this model a decrease in temperature will cause the capillary water to gain more free energy than the gel water, and that will promote the flow of capillary water to the gel pores. Note that this result is exactly the opposite of that for the earlier model.

It may be argued that Helmuth's model was developed for conditions above the freezing range (although he proceeded to apply it to pastes subject to freezing). Not all of the freezable water in concrete is frozen instantaneously. Rather, freezing occurs over a considerable range, as shown by the DTA tests, and bulk water is therefore in contact with gel water for extended periods of time in the presence of ice. In view of the two thermodynamic models discussed, what is the direction of the chemical potential (free-energy difference) in this case?

Obviously, the problem is more complicated than either of the two models would indicate. The basic thermodynamic relationships are correct, of course. The absurd result obtained by applying the two models to the same problem is the consequence of the simplifying assumptions made in each case.

The purpose of this lengthy digression is to show that there is no sound mathematical basis for attributing the post-freezing dilation to free-energy differences. Furthermore, the experimental observations also failed to support the free-energy theory. Consider the case of the 25IP1 aggregate. The DTA tests on two specimen sets gave practically identical values for the amount of water frozen—56 and 57 percent. This means that about 43 percent of the

water contained in the aggregate was not frozen at temperatures down to 20 F. According to Helmuth (*5*), the smallest pore size in which freezing can occur at this temperature, based on Thomson's equation, is 83A (0.83×10^{-2} microns). To discourage arguments relative to supercooling, electrolyte concentration, and pressure effects on freezing, it can be assumed that the water contained in all voids ten times this size (0.083 microns) is frozen at 20 F. Powers and Brownyard (*10*) present data showing that the radius of curvature of the meniscus corresponding to a pore of radius of 0.042 microns can be attained at a relative vapor pressure of 0.76. This means that at a relative vapor pressure of 0.76 or higher, all of the pores smaller in diameter than 0.083 microns should be filled by capillary condensation. Table F-3 shows that even at a relative vapor pressure of 1.000 only about 2 percent of the total sorption is achieved. Clearly, at least 95 percent of the water that did not freeze—$100 \times (43 - 2)/43$—could not have existed as bulk water at 20 F. If it did not freeze and it could not have existed as bulk water, the only alternative is to assume that it became ordered (adsorbed).

Another reason for rejecting free-energy differences as the cause of the post-freezing dilation is based on examination of length vs temperature data for aggregate particles during thermal cycles through the freezing-and-thawing range. These tests are described in Appendix D. It is obvious that during a thawing cycle (as the temperature is increased) the same free-energy-difference phenomenon would occur, but in the reverse direction. However, the generation of hydraulic pressure is not dependent on the direction in which the water tends to flow, but rather on the hydraulic properties of the intervening medium. In other words, if the free-energy difference can produce dilations during cooling, it should also be able to produce them during warming. Since warming cycles were not investigated for the DTA specimens, it was necessary to resort to the aggregate data mentioned here. Careful examination of approximately 15 test runs on each of the aggregates used in the DTA tests revealed the absence of a single clear-cut case of dilation during the thawing portion of the cycle. However, the dilations during freezing were usually measurable and appeared to be proportional to the dilations of the concrete specimens containing the respective aggregates.

SHAPE OF THE DTA CURVE

Dunn and Hudec (*3*) illustrated four basic DTA trace profiles that were observed in their experiments. These same general types were observed in the experiments carried out for this project, and they are shown in Figure F-9. The shape of the curve is a function of the rate of freezing, the heat capacities of the specimens and the environment, and the rate of temperature change of the environment. Since all of these factors except the first one were constant throughout the experiments, the shapes of the curves represent changes in the rate of freezing of the water in the test aggregate contained in the test specimen. This assumes, of course, that the water in the paste phase of the test and the dummy specimens exactly cancels.

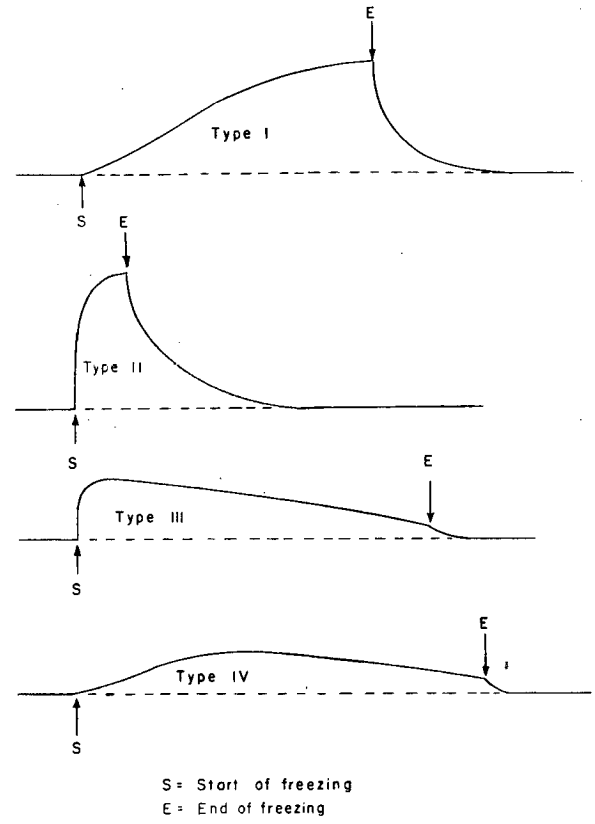

Figure F-9. Types of DTA curves observed in experiment.

A curve of type I represents a moderately high constant rate of freezing over a long period of time. Type II curve indicates virtually instantaneous freezing of all of the freezable water. Type III curve shows instantaneous freezing of a portion of the freezable water, followed by gradual freezing at a decreasing rate. A curve of type IV represents gradual freezing at an increasing, then decreasing, rate.

In comparing the shapes of the DTA curves with the frost resistance of their rock specimens, Dunn and Hudec observed that unsound rocks, when they displayed any freezing at all, showed gradual freezing over a long period of time (types I and IV). Sound rocks usually displayed pulse-type freezing profiles (types II and III). A similar comparison for the data collected in this research (Table F-11) leads to the same general conclusions, but a much closer relationship appears to exist between the type of curve and the amount of water frozen (ice equivalent of the DTA area).

The data in Table F-11 show that the type I curve was observed for specimens having 38.02 and 15.15 g of water frozen; the type II curve for specimens having 8.66, 7.41, and 6.52 g; the type IV curve for specimens having 5.33 g; and the type III curve for specimens having 4.20, 3.99, and 2.09 g. Although this grouping effect is striking, its basis and significance are not readily apparent. The gradual freezing would seem to indicate the presence of a broad and uniform distribution of void sizes in the aggregate, whereas sudden freezing would indicate a narrow size range.

The basis for that conclusion is as follows. The normal

TABLE F-11

FROST DAMAGE, ICE EQUIVALENT, AND CORRESPONDING DTA CURVE

AGGREGATE	DILATION PER CYCLE (μIN.)	ICE EQUIVALENT, DTA AREA (G)	DTA CURVE TYPE
25IP1	957.5	38.02	I
02SLs2	103.1	15.15	II
40SSs2	26.8	4.20	III
16SSs2	15.8	7.41	II
14SSt1+2	15.6	6.52	II
42SLs2	11.8	8.66	II
44SLs3+4	7.6	5.33	IV
28IGr1	4.7	3.99	III
34MAm2	4.2	2.09	III

fusion temperature of water in capillaries is depressed in relation to the smallness of the capillary. A certain degree of supercooling is always required to initiate the fusion reaction, the extent of which is dependent upon the vapor pressure (capillary size) and the presence of "motes" or nucleation points. In bulk water the degree of supercooling required is usually so small as to go undetected. Once freezing has started, it will continue until all of the supercooled water has frozen or until the latent heat of fusion has raised the temperature to the fusion point. With a constant cooling rate, the freezing of water in a rock with a uniform distribution of pore sizes will occur in small discrete steps, starting with the largest capillaries and proceeding until the freezable water in the smallest capillaries has frozen. In a rock with essentially one pore size, freezing will occur as a single discrete step, a pulse.

Interpretation of the types of DTA curves in this light indicates that type I might represent an aggregate with a wide distribution of pore sizes, increasing in frequency with decreasing sizes. Type II has essentially one pore size. Type III would appear to have the highest relative frequency of pores in the largest pore size and a rather uniform distribution of the smaller pore sizes. Type IV apparently has a relatively uniform distribution of pore sizes, the frequency of occurrence approaching that of a normal statistical distribution.

Unfortunately, few test data are available to support this hypothesis. Pore size distributions were determined with a high-pressure mercury porosimeter on specimens of three of the nine aggregates used in the DTA tests: 16SSs2, 02SLs2, and 14SSt1 + 2. The number of specimens tested in each case was two, three, and eight, respectively. The samples tested for the first two aggregates were too few to permit drawing a meaningful composite pore size distribution, because of the variability of the data. For the 14SSt1 + 2 aggregate the data were sufficient to construct a pore size distribution curve, and it compared favorably with the hypothesis; that is, a large percentage of the voids was found to be contained in a narrow size range at the larger void size end of the distribution curve. This one case does not prove the theory, but the fact that it lends support is worthy of note.

APPENDIX G

ANNOTATED BIBLIOGRAPHY

One of the first tasks completed on NCHRP Project 4-3 was a literature search and the compilation of an annotated bibliography on frost action in concrete, published in 1964 as part of *HRB Special Report 80* (*8*). Since that time a considerable quantity of related literature has come into being. The classification system in this bibliography supplement is the same as that employed in *Special Report 80* and the numbering is consecutive with the entries therein:

- A Original Research and Development
- B Reviews or Compilations of Data
- C Descriptive Articles
- D Books
- E Unpublished Theses

- 101-199 Soundness Tests
- 201-299 Petrographic Analysis
- 301-399 Pore System Studies
- 401-499 Physicochemical Properties Studies
- 501-599 Unconfined Freezing-and-Thawing Tests
- 601-699 Freezing-and-Thawing Tests
- 701-799 Test Method Proposed by T. C. Powers
- 801-899 Miscellaneous Possible Approaches

SOUNDNESS TESTS

B119. BUTTERWORTH, B., "Frost Resistance of Bricks and Tiles." *Jour. Brit Ceramic Soc.*, No. 2, 1:203-223 (June 1964).

Reviews existing and proposed test methods for determining frost resistance of bricks and tiles, and suggests probable lines of future test work. Butterworth concludes that a single mechanism does not explain all instances of frost damage to porous materials.

C120. HVEEM, F. N., and SMITH, T. W., "A Durability Test for Aggregates." *Hwy. Res. Record No. 62* (1964) pp. 119-136.

Describes a test developed by the California Di-

vision of Highways for classifying aggregates according to a durability rating, using equipment developed for other routine tests. Primarily a measure of mechanical breakdown that might be related to weathering, the test effectively discriminates various aggregate types.

PETROGRAPHIC ANALYSIS

A212. DUNN, J. R., "Characteristics of Various Aggregate Producing Bedrock Formations in New York State." Physical Res. Proj. No. 4, Phase 3, New York State Dept. of Pub. Works (Nov. 1963) 258 pp.

Discusses results of physical tests on a number of aggregate materials in New York State, and suggests other testing procedures. Water content of an aggregate was shown to be the principal factor affecting the advance of an ice front in unindirectional freezing. Dunn questions the validity of the "critical size" concept because of the existence in nature of saturated outcroppings larger than critical size, and also because he thinks it unreasonable that getting excess water out of a piece of aggregate at a relatively slow rate during freezing should require a force greater than the capillary pressure that drew the water into the rock.

B213. MCLAUGHLIN, J. F., "Chert and Shale in Concrete." *Conc. Prod.*, No. 9, 67:27, 62 (Sept. 1964).

Considers the problem of deleterious constituents in concrete aggregates, particularly chert and shale. Chert and shale are defined, and their effects on concrete are reviewed.

A214. WOO, C. C., "Heavy Media Column Separation: A New Technique for Petrographic Analysis." *Am. Mineralogist,* Nos. 1 and 2, 49:116-126 (Jan.-Feb. 1964).

A heavy-media column is used to separate the mineral fractions of a sample, and the percentage composition of the sample is directly weighed. The technique may be applied to determine the concentration of a particular species, even in trace amounts, for mineralogical studies or for commercial metallurgical beneficiation.

PORE SYSTEM STUDIES

E356. FRANZEN, M. H., "Aggregate Pore System Studies." M.S. Thesis, The Pennsylvania State Univ. (1964) 153 pp.

Discusses aggregate and mortar pore systems in terms of porosity, permeability, and capillarity. Describes equipment developed for measuring air permeability of aggregates and mortars, specimen preparation, and test procedures. A porosity-permeability index was devised and correlated with rapid freeze-thaw tests of concrete made with the test aggregates. The reported probability of correlation is 99.8 percent or better. A sharp distinction was found between aggregate porosity values for two different specific gravity fractions of the same geologic category, but no such differentiation could be determined on the basis of permeability.

B357. MANGER, G. E., "Porosity and Bulk Density of Sedimentary Rocks." *U.S. Geological Survey Bull. 1144-E* (1963) 55 pp.

A tabulation of the porosity and bulk density of over 900 sedimentary rocks according to general mineralogical type and era, obtained from the more accessible American, British, German, and Swiss literature.

A358. OROVEANU, T., "Some Considerations on the Flow of Compressible Fluids Through Nonhomogeneous Porous Media" (in German). *Revue de Mecanique Appliquee,* No. 5, 8:769-778 (1963).

Flow of compressible fluids through nonhomogeneous porous media is considered in the case in which the nonstationary character of the phenomenon is predominant. Differential equations for the flow of compressible liquids and the flow of gases are deduced.

C359. ROBSON, R. A., "Mobility of Water in Porous Media of High Surface Area." *RILEM Bull. 27* (June 1965) pp. 65-72.

Structure and connectivity of the porous medium is analyzed in the light of a partially confirmed hypothesis postulating that flow in certain porous media considered statistically uniform is confined to channels.

A360. SCHLOESSER, J., "The Correlation Among Pore Size Distribution, Permeability, and Diffusion in Graphite." *Nuclear Science and Engineering,* No. 2, 24:123-132 (Feb. 1966).

A model of parallel capillaries with different diameters has been developed to explain back-diffusion experiments on four different graphites, both impregnated and unimpregnated.

C361. TALASH, A. W., and CRAWFORD, P. B., "Rock Properties Computed from Random Pore Size Distribution." *Jour. of Sedimentary Petrology,* No. 4, 35:917-921 (Dec. 1965).

Describes a mathematical procedure for calculating the porosity and permeability of a porous matrix. The tecnnique involves a solution of Poisseville's and Darcy's equations across each pore and opening. The method employs a digital computer, a random number generator, and an approximate range of pore diameters. The effect of small samples is also discussed.

A362. U.S. Naval Engineering Laboratory, "Water Vapor Transmission of Concrete and Aggregate." *Tech. Report R244* (1963) 70 pp.

The water-vapor transmission of concrete was investigated in terms of the effects of water-cement ratio, types of reinforcing steel, aggregate size, relative humidity, concrete slice position, and two admixtures (sodium chloride and oleic acid). Collateral investigations explored the water-vapor transmission of aggregates and the growth of sodium chloride whisker crystals on concrete. Water-vapor transmission rates decrease with increased strength of concrete (decreased water-cement ratio), and with increased aggregate size and the presence of sodium chloride. Rates appear to decrease with increased relative humidity, but the data were inconclusive. Rates are independent of type of reinforcing steel and oleic acid.

A363. WEIRIG, H. J., "A Simple Method for Measuring the Water-Vapor Permeability of Mortars and Concrete." *Zement-Kalk-Gips,* 16:125-30 (1963).

Method involves the use of a jar containing conc. H_2SO_4 with the test piece clamped on to serve as a cover. The increase in weight after a seven-day storage period in a chamber with controlled temperature and humidity is a measure of the amount of water that has diffused through the specimen. Plotted data of diffusion rate as a function of humidity gradient are presented.

E364. WOO, S. C., "Permeability, Porosity, and Frost Susceptibility of Concrete Aggregates." M.E. thesis, The Pennsylvania State Univ. (1966) 104 pp.

Air-permeability and porosity tests were carried out on 16 aggregate types to determine the relation of aggregate pore characteristics to frost susceptibility. Very high correlations with frost susceptibility were found for the permeability coefficient and for effective absorption. Porosity also correlated highly. Evaluation of the permeability apparatus revealed that test results are unaffected by the type of gas used, oven-drying of specimens, and percolation pressures up to 150 psi.

A365. YOUNG, A., LOW, P. F., and MCLATCHIC, A. S., "Permeability Studies of Argillaceous Rocks." *Jour. Geophys. Res.*, No. 20, 69:4237-4245 (Oct. 15, 1964).

Permeability of argillaceous rocks was measured using water under bottled-nitrogen pressure as flow medium. Flow rates changed more with temperature than would be expected from the normal changes of water viscosity with temperature. It was concluded that the water in the rocks has a different structure than bulk water.

PHYSICOCHEMICAL PROPERTIES STUDIES

C449. ALEXANDER, K. M., "A Study of Concrete Strength and Mode of Fracture in Terms of Matrix, Bond and Aggregate Strengths." Tewksbury Symposium on Fracture, Univ. of Melbourne (Aug. 1963) 27 pp.

Surveys current investigations aimed at relating strength and mode of concrete fracture to properties of component elements such as paste, bond, and aggregate, and describes procedures for measuring strength of components. Alexander concludes that reliable information can be obtained only if control is exercised over factors such as surface drying during testing, temperature change between casting and curing, vibration, and surface contamination of the aggregate.

A450. BREWER, H. W., "Moisture Migration—Concrete Slab-on-Ground Construction." *Jour. Res. and Devel. Labs.*, Portland Cement Assn., No. 2, 7:2-17 (May 1965).

Reports data on 141 specimens cast from 29 mixes covering a wide range of concrete quality, and demonstrates that concrete of good quality has better resistance to moisture migration than concrete of lower quality, regardless of time or type of exposure.

E451. CADY, P. D., "Mechanisms of Frost Destruction in Concrete." Ph.D. thesis, The Pennsylvania State Univ. (1967) 128 pp.

Investigates basic mechanisms of frost action in concrete, in the light of Powers' hydraulic pressure theory and the adsorbed (ordered) water theory proposed by Dunn and Hudec, which conflict sharply on several fundamental points regarding frost destruction. Adsorption isotherms were determined for 24 aggregates of widely varying frost sensitivity. To evaluate freezing quantitatively, nine of the aggregates were submitted to differential thermal analysis while encased in concrete. Both mechanisms were found to operate simultaneously in frost destruction, but hydraulic pressure due to freezing usually predominates. The dominance of one or the other appears to be a function of pore characteristics and mineralogical composition of the rock.

B452. CHEKHOVSKOI, YU. V., KAZANSKII, V. M., and LEIRIKH, V. E., "The Pore Structure and Types of Water Bonding in Hydrated Cements." *Chemical Abstracts*, Vol. 59 Col. 3633 (1963).

Results of a study of pore structure and types of water bonding in portland cement, showing that data obtained from water thermograms, drying curves, and Hg pore measurements agree within the limits of experimental error. Provides a basis for correlating sorption properties with pore structure of the hydrated-cement mass.

C453. DUNN, J. R., and HUDEC, P. P., "Rock Breakup Theory." *Rensselaer Review*, No. 1, 3:13-17 (Mar. 1966).

Discusses their theory of ordered water and its mechanism in breaking up rock.

A454. DUNN, J. R., and HUDEC, P. P., "Water, Clay, and Rock Soundness." *Ohio Jour. of Science*, No. 2, 66: 153-168 (Mar. 1966).

Cold quantitative differential thermal analysis and adsorption experiments are used to explain disintegration of clay-bearing carbonate rocks by wetting, drying, and frost action. The unsoundness of frost-sensitive carbonate rocks appears to be related not to ice but to expansion of ordered water. This ordered water is believed to be associated with clay rejected by dolomite.

C455. HANSEN, T. C., and NIELSEN, K. E. C., "Influence of Aggregate Properties on Concrete Shrinkage." *Jour. Amer. Conc. Inst.*, No. 7, 62:783-794 (July 1965).

Presents a theory for the influence of aggregate properties on concrete shrinkage. An equation is derived for computing the shrinkage of concrete from fractional volume, modulus of elasticity, and shrinkage of cement paste and aggregate.

C456. HANSEN, W. C., "Anhydrous Minerals and Organic Materials as Sources of Distress in Concrete." *Hwy. Res. Record No. 43* (1963) pp. 1-7.

Describes several classes of minerals and organic materials found in mineral aggregates that are deleterious to concrete properties, including frost resistance.

A457. MASO, J. C., "Primary Factor in the Damage of Concrete by Freezing." *Building Science Abstracts*, No. 9, 38:258 (Sept. 1965).

Results of freeze-thaw cycles (20 to —20 C) show that only hydrostatic pressure developed during the freezing of water is responsible for the damage to concrete by frost action. Differences between the coefficients of thermal expansion of aggregates (limestone or granite) and hydrated cement paste have negligible influence on disruption.

A458. NEPPER-CHRISTENSEN, P., "The Contact Between Cement Paste and Aggregates and Its Effect on Rupture Phenomena in Concrete." *Building Science Abstracts*, No. 6, 38:163 (June 1965).

Briefly mentions theories of concrete failure, and presents results of an experimental investigation of rupture phenomena in concrete subjected to tension. Size, shape, and mineralogical type of the coarse aggregate, as well as the strength of the mortar, were varied with the tests.

A459. PODVAL'NYI, A. M., "Creep of Freezing Concrete." *Building Science Abstracts*, No. 9, 36:Art. 1338 (Sept. 1963).

Creep in frozen concrete was investigated by observing the movement of concrete under compression and bending. Samples ($2.5 \times 2.5 \times 25.0$ cm) were impregnated with water, which was frozen at —40 C and the ice was melted at 30 C. Explanation of the results is attempted on the basis of the mechanism of rupture (hydraulic pressure, internal forces, elasticity), micro-fissures formed at the time of freezing, and the results of earlier work.

C460. TOKUDA, H., and ITO, T., "Some Experimental Results on Thermal Properties of Concrete." *Proc. Cong. on Testing Materials*, Japan (1964) pp. 122-123.

Discusses the importance of stabilizing concrete structure thermally and volumetrically, and describes test to evaluate effects of type of coarse aggregate and mix quantity of aggregate on properties like thermal diffusity, thermal conductivity, and coefficient of thermal expansion.

B461. VENUAT, M., "Resistance of Cement to Freezing." *Chemical Abstracts*, Vol. 60, Col. 291 (1964).

Dilation was found to be the most effective nondestructive indicator of frost action. High freeze-thaw resistance was associated with high cement fineness, optimum SO_3 content (2-4%), free CaO (1%), low free MgO, low $3CaO \cdot Al_2O_3$ and $3CaO \cdot SiO_2$, slag (50% in clinker-slag mixtures), high cement content in concrete, low w/c ratio, entrained air (4-6%), low capillary absorption, low

bleeding tendency, and maximum water retention. The capillary absorption test was useful as an indicator of relative frost resistance.

UNCONFINED FREEZING-AND-THAWING TESTS

E506. BAKR, T. A., "Volume Stability of Concrete Aggregates as Measure of Frost Susceptibility." M.S. thesis, The Pennsylvania State Univ. (1967) 102 pp.

Describes determination of the volumetric expansion of saturated aggregate particles during freezing, using a mercury-displacement dilatometer. Twenty-two aggregate types of widely varying frost susceptibility and mineralogical type were tested. The volume percent expansion during freezing was found to correlate very well with frost susceptibility of concrete made with the aggregates.

E507. ESHBACH, R. M., "The Single-Particle Expansion Test as a Method for Determining the Frost Susceptibility of Concrete Aggregate." M.S. thesis, The Pennsylvania State Univ. (1967) 150 pp.

Freezing-and-thawing tests were performed with individual aggregate particles, both unconfined and encapsulated in mortar. Twenty-two aggregate fractions of widely varying mineralogical type and frost susceptibility were used. Expansion during freezing and permanent length change were measured, and both were found to correlate significantly with frost susceptibility.

A508. HOLUBEC, I., and DE LORY, F. A., "A Study of Shaley Gravel." *Ontario Joint Hwy. Res. Program Report 19* (Mar. 1964) 63 pp.

Shale particles in shaley gravel deteriorated severely in freezing-and-thawing tests. Frost action caused these particles to split into thin plates through fine-grained strata. Dye-penetration tests revealed that fine-grained strata are more absorbent. Beneficiation of this aggregate by flotation methods was found to be practical.

A509. SCOTT, J. W., and LAUGHLIN, G. R., "A Study of the Effects of Quick Freezing on Saturated Fragments of Rock." *Res. Report KYHPR-64-6,* Kentucky Dept. of Hwys. (Feb. 1964) 59 pp.

Describes a test for frost resistance of aggregate particles, entailing immersion of particles in cold mercury (—30 to —38 C). Stream-wet aggregates were used. This test was reported to be capable of producing destructive volume changes in one freezing cycle. Some of the more important conclusions: frost resistance is not related to particle size; although most failures occur in materials with low specific gravity, specific gravity is not the sole indicator of durability; for saturated aggregate, absorption or porosity could be used to discern durability; igneous rocks are more resistant than sedimentary. Theoretical analysis showed that failure of aggregate particles could be expected at 1.0 to 2.5 percent porosity. Test values closely approximated theoretical values.

FREEZING-AND-THAWING TESTS

C634. CORDON, W. A., "Freezing and Thawing of Concrete—Mechanisms and Control." *Jour. Am. Conc. Inst.* 63: 613-618 (May 1966).

Discusses types of freezing-and-thawing deterioration, exposure conditions in concrete structures, mechanisms of freezing-and-thawing deterioration, influence of concrete aggregates and air entrainment, laboratory evaluation of freeze-thaw deterioration, and requirements and recommendations for producing durable concrete.

A635. IVANOV, F. M., BAKLANOV, A. S., and MORSEEVA, V. V., "Effect of Conditions of Hardening and Additions of Air-Entraining Substances on Frost Resistance of Concrete." *Building Science Abstracts,* No. 11, 36:Art. 1773 (Nov. 1963).

Concrete specimens were exposed to cycles of severe freezing followed by thawing in fresh water or sea water. Concrete withstanding the exposure conditions for the first two to three years was characterized as frost resistant. Measures of importance for improved frost resistance include the use of cement with reduced C_3A content, dense concrete from mixes with a water-cement ratio of less than 0.50, air-entraining admixtures, together with provision of moist conditions of hardening. Marked reduction of frost resistance may result if one of these measures is omitted.

A636. LANG, C. H., and WALSH, R. J., "Concrete Exposure Tests—Phase I." *Hwy. Res. Record No. 62* (1964) pp. 1-6.

Fifteen test slabs of portland cement concrete were subjected to outdoor exposure, and a series of freeze-thaw cycles was induced by high concentrations of NaCl and calcium chloride. Surprisingly, results showed that air-cured slabs deteriorated less than wet-cured slabs. The best sealant tested was a mixture of 50 percent boiled linseed oil and 50 percent mineral spirits. It was more effective when applied at 14 days than when applied at 1 day.

B637. MATHER, B., "Laboratory Freezing-and-Thawing Tests of Concrete." Miscellaneous Paper 6-716, U.S. Waterways Experiment Station (Apr. 1965) 18 pp.

Describes tests performed to select combinations of aggregate and cement that would yield concrete of good resistance to rapid freezing and thawing in the laboratory. Alternative methods of calculating results of such tests are given, and differences are indicated. Variations in results from tests of presumably similar concrete specimens are regarded as caused by differences in the cements used rather than the aggregates.

A638. MEININGER, R. C., FOX, J. F., and LEPPER, H. A., "A Single Particle Freezing Resistance Test for Concrete Aggregate." *Proc. ASTM,* 65:801 (1965).

Single particles of three types of coarse aggregate, two chert gravels and crushed limestone, were embedded in cylinders of air-entrained mortar. Specimens were subjected to freezing (0 F in air) and thawing (40 F in water). Changes in length and weight were measured. Chert samples expanded in varying degrees, limestone did not.

A639. MICHAELS, E. L., VOLIN, M. E., and RUOTSALA, A. P., "The Properties of Chert Aggregates in Relation to Their Deleterious Effect in Concrete." Final Report, Project R-121, Inst. of Mineral Res., Michigan Technical Univ. (July 1965) 122 pp.

In one of many tests on cherts, the relationship between particle size and freeze-thaw durability was tested by freezing and thawing saturated cherts of four separate size classes in mortar cylinders. No apparent relationship was indicated.

A640. WALKER, R. D., "Identification of Aggregates Causing Poor Concrete Performance When Frozen." *NCHRP Report 12* (1965) 48 pp.

Specimens were exposed to alternate cycles of freezing and thawing in water. It was concluded that the use of a Whittemore strain gage, a simple deep-freeze unit, and a timing device has merit for quick preliminary evaluation of coarse aggregates.

A641. WILLS, M. H., LEPPER, H. A., JR., GAYNOR, R. D., and WALKER, S., "Volume Change as a Measure of Freezing-and-Thawing Resistance of Concrete Made with Different Aggregates." *Proc. ASTM,* 63:946-965 (1963).

Specimens of air-entrained concretes containing

either a chert or a crushed-limestone coarse aggregate were subjected to rapid freeze-thaw cycles (Powers test). The results indicated that the period of immersion required to produce measurable dilation is a significant measure of frost resistance; that measurement of residual length changes alone may give an adequate measure of frost resistance; that short periods of drying are beneficial to frost resistance; and that a good correlation exists between loss in dynamic modulus for specimens subjected to the rapid cycle and dilation of specimens subjected to the slow cycle.

TEST METHOD PROPOSED BY T. C. POWERS

E721. CADY, P. D., "Frost Action in Concrete and a Method for Evaluation." M.S. thesis, The Pennsylvania State Univ. (1964) 122 pp.

An evaluation of Powers' laboratory test for frost resistance. Experiments investigated the effects of aggregate size ratio, extended periods at low temperatures, curing procedure, and casting position. Micro-cracking with increasing cooling cycles was also investigated. Dilation proved to be the most sensitive measure of frost damage in concrete. The deterioration function, based on dilation, follows the general relation $D=BA^n$, where D is total dilation in microinches, A and B are constants for a given aggregate-curing combination, and n is the number of cooling cycles. The deterioration function can be defined completely by repeating cooling cycles until the change in dilation with cycle number starts to increase. High correlation was found between rate of saturation of a specimen and the deterioration function.

A722. LARSON, T., BOETTCHER, A., CADY, P., FRANZEN, M., and REED, J., "Identification of Aggregates Exhibiting Frost Susceptibility." *NCHRP Report 15* (1965) 66 pp.

Four approaches to identification of aggregate particles that undergo destructive volume change when frozen in concrete were investigated: aggregate pore systems, aggregate particle expansion during freezing, petrographic evaluation, and the Powers slow-cooling cycle for mass aggregates. A porosity-permeability index was found to correlate well with durability. Expansion of individual aggregate particles during freezing and dilation of concrete specimens in the Powers cycles were also good measures of durability. Petrographic studies revealed certain features of aggregates that helped to explain their behavior in the tests and provided information for predicting the frost susceptibility of untested aggregates. It was concluded that no one of the methods tested combines the attributes of speed, simplicity, and ability to discriminate by degree, but further study was recommended. Time and cost data are given for the various tests.

B723. POWERS, T. C., "The Mechanism of Frost Action in Concrete." Stanton Walker Lecture No. 3, presented at Univ. of Maryland (Nov. 18, 1965) 35 pp.

Discusses the composition of concrete and the performance that can be expected of it under both field and lab conditions, pointing out various critical factors (size, saturation, paste structure) that cannot be ignored. Differences in effects of freezing on rocks and concrete are considered, and also effects of de-icers or chemicals.

MISCELLANEOUS POSSIBLE APPROACHES

C815. CARLSON, B. C., CURTIS, D. F., and HEDLUND, R. C., "Development of a Concrete Admixture to Improve Freeze-Thaw Durability." *Hwy. Res. Record 62* (1964) pp. 13-30.

Describes the use of a silicone admixture to improve scaling resistance of concrete subject to freezing and thawing and salt solutions. Trap rock and silica sand were used as aggregates, so the frost destruction was limited to the paste phase. The admixture improved scaling resistance appreciably.

B816. CORDON, W. A., and MERRILL, D., "Requirements for Freezing and Thawing Durability for Concrete." *Proc. ASTM,* 63:1026-1035 (1963).

A compendium of current thinking about the production of frost-resistant concrete. Basically, this deals with the use of low w/c ratios, good quality coarse aggregates, and AEA. Special precautions recommended for concrete slabs include minimum finishing, a drying period after curing, adequate drainage, and elimination of inferior aggregate particles.

B817. DE PAREDES GAIBREIS, P. G., "Durability of Concrete." *Monografias No. 232,* Instituto Eduardo Torroja de la Construccion y del Cemento, Madrid (1963) 138 pp.

Reviews various studies and reports on concrete durability. Compiles information on concrete components (aggregates, air, water, cement) and the most frequently met aggressive agents. One appendix describes methods for testing the strength of cements against the action of sulfates; another reviews the work being done on concrete durability at the Institute. A bibliography covers papers on durability published from 1952 to 1962.

C818. GRIEB, W. E., and WERNER, G., "Natural Weathering of Concrete Specimens Prepared with Cements Used in the Long-Time Study." *Public Roads,* No. 4, 33:57-67 (Oct. 1964).

With the same cements used by PCA in the long-time study of natural weathering of concrete, the Bureau of Public Roads prepared box-type specimens and exposed them to outdoor conditions for more than 15 years. Among the more important conclusions: concretes made with Types II, IV, and V and air-entraining cements were usually more durable than those prepared with Types I and III; concretes prepared with cements having more than 10 percent C_3A had poorer durability than those with less than 10 percent C_3A.

C819. IDORN, G. M., "A Concrete Jetty with Frost Damage." *Magazine of Conc. Res.,* No. 47, 16:89-92 (June 1964).

Describes severe popouts and surface scaling on a concrete jetty in Denmark, attributed to pure and silicified limestones and opaline and chalcedonic porous cherts that make up 20 to 40 percent of ordinary Danish gravel aggregates. Three types of frost damage dependent on physicochemical properties of the coarse aggregate are described: cretaceous limestones (porous) can cause popouts on exposure to freezing and thawing; cretaceous cherts and silicified limestones (porous) can cause popouts both on exposure to freezing and thawing and by alkali-aggregate reaction; dense flints and igneous rocks can create popouts by causing scaling of mortar in thin flakes or laitance.

C820. IVANOV, F. M., ROYAK, G. S., GLADKOV, V. S., and BAKLANOV, A. S., "Frost Resistance of Concrete under Corrosive Action of Salty Medium." *Gidrotekhnicheskoe Stroitel'stvo,* 36:13-16 (Feb. 1966).

Results of long-term experiments conducted to study effects of type of cement, hydraulic and organic admixtures, structure of concrete, hardening conditions, and environment of manufacture, on frost resistance of concretes.

C821. WALKER, S., "Quality Requirements for Concrete Aggregate." *Engineering Experiment Station Bull. 68,* Univ. of Kentucky (June 1963) pp. 52-56.

Discusses durability of concrete in terms of fine and coarse aggregates, especially the problem of

chert aggregates. Stresses the importance of a drying period to prevent disruption due to saturated aggregates, and suggests that the vacuum saturated condition is too severe for realistic testing of aggregates in concrete. Walker notes that reducing the size of the coarse aggregate will improve its frost resistance; also that most chert gravels, if used judiciously and with proper precautions, will perform satisfactorily in concrete.

C822. WARRIS, B., "The Influence of Air-Entrainment on the Frost-Resistance of Concrete." *Proc. Swedish Cement and Conc. Inst.*, 35:46 (1963); 36:134 (1964).

Part A, Void Distribution, presents an experimental and theoretical study of the distribution of air bubbles in concrete. Void distribution in general is discussed, and void parameters are given for different concretes. Part B, Hypothesis and Freezing Experiments, presents definitions and methods of measuring frost resistance. A review of theoretical studies places the many hypotheses within a general pattern. The new hypothesis introduces the so-called "critical degree of saturation," which depends on void distribution, freezing rate, permeability, and strength. To be valid for concrete, the hypothesis must also include a function of the paste content, based on the adopted measuring and statistical methods. Corroborates the experience that the water-cement ratio influences frost resistance.

APPENDIX H

COOPERATIVE TEST PROGRAM

The objectives of both NCHRP Projects 4-3(1) and 4-3(2) were addressed to the same general problem, that of identifying deleterious particles and predicting performance of aggregates when used in portland cement concrete. Free interchange of information was maintained throughout the studies by the involved research personnel at The Penn State University and Virginia Polytechnic Institute. In addition to the over-all cooperative attitude, tests were conducted on several specific aggregate fractions by both agencies and the results are reported herein. (The cooperative test program is also included as Appendix C in *NCHRP Report 65*.)

Six aggregate fractions were selected for the cooperative effort and all test samples were prepared by Penn State with representative portions being supplied to V.P.I. Tests conducted on the cooperative aggregate samples at V.P.I. were ASTM C290 and the V.P.I. slow freeze. The results are given in Table H-1. The Penn State adaptation of the slow-cooling method and a number of other tests on individual particles were conducted on the selected fractions by Penn State. The resulting data are given in Table H-2.

On the basis of the durability factors being above 80 and $b_t > +1.0$, the V.P.I. tests would indicate that all six aggregates are satisfactory for use in concrete subjected to freeze-thaw. Using the Penn State criteria selected from the slow-cooling method, with a dilation of less than 5 μ in. per cycle indicating a very sound aggregate and a dilation greater than 100 μ in. per cycle a very frost-susceptible aggregate, two of the cooperative aggregates are very sound and the remaining four are in the intermediate range of frost susceptibility.

As indicated in Table H-3, agreement between the Penn State and V.P.I. methods does not appear to be good, possibly because of the narrow frost-susceptibility range of the cooperative aggregate fractions. However, it should also be recognized that the V.P.I. method was not developed for use with aggregate fractions, whereas all of the Penn State research did involve fractions. Because the cooperative aggregates were fractions, no observed field performance information is available for comparison with either the V.P.I. or Penn State methods. Table H-3 does show that the relative rating of the cooperative aggregates by the Penn State rapid test methods agrees quite well with Penn State slow-cooling method ratings.

TABLE H-1

SUMMARY OF V.P.I. TESTS ON COOPERATIVE AGGREGATE FRACTIONS

AGGREGATE	DURABILITY FACTOR ASTM C290, DF_{100}	V.P.I. SLOW FREEZE	
		DF_{100}	b_t
02SLs1	95	97	+2.4
14SSt1+2	98	99	+4.8
16SSs1	98	99	+3.0
18IS+IT	99	99	+3.0
38MGn2	97	100	+7.5
34MAm1	100	100	+3.9

TABLE H-2

SUMMARY OF PENN STATE TESTS ON COOPERATIVE AGGREGATE FRACTIONS

AGGREGATE	VACUUM SATURATED ABSORPTION (%)	SINGLE PARTICLE DILATION (μ IN./IN.)	VOLUMETRIC PARTICLE EXPANSION (%)	AVERAGE PERMEABILITY (DARCYS)	LOG_{10} (PERM. $\times 10^6$) $\times$ V.S. ABS.	$\times \Delta L$	$\times$ VOL. % DIL.	DILATION PER CYCLE, SLOW-COOLING METHOD (μ IN./IN.)
02SLs1	2.502	225.	0.33	0.353×10^{-4}	6.319	568.	0.783	48.66
14SSt1+2	1.586	137.5	—	3.764×10^{-5}	2.499	217.	—	11.64
16SSs1	1.391	169.5	0.30	2.053×10^{-5}	1.826	213.	0.394	10.00
18IS+IT	1.995	176.8	—	7.732×10^{-6}	1.737	157.	—	6.09
38MGn2	1.712	246.8	0.17	2.941×10^{-6}	0.802	116.	0.079	3.08
34MAm1	0.221	23.8	0.08	5.663×10^{-7}	−0.056	−6.	−0.018	0.87

TABLE H-3

RATING OF COOPERATIVE TEST FRACTIONS BY PENN STATE AND V.P.I. METHODS

TEST METHOD	FROST-SUSCEPTIBILITY RATING [a] 02SLs1	14SSt1+2	16SSs1	18IS+IT	38MGn2	34MAm1
Penn State:						
Slow-cooling method, concrete specimens	1	2	3	4	5	6
Rapid tests:						
Log_{10} (perm. $\times 10^6$)						
$\times \Delta$ length change	1	2	3	4	5	6
$\times$ V.S. absorption	1	2	3	4	5	6
V.S. absorption	1	4	5	2	3	6
Vol. percent dilation	1	—	3	—	5	6
$\times \log_{10}$ (perm. $\times 10^6$)	1	—	3	—	5	6
V.P.I.:						
ASTM C290	1	3–4	3–4	5	2	6
Slow-freeze method	1	5	2–3	2–3	6	4

[a] Decreases from 1 to 6.

Published reports of the

NATIONAL COOPERATIVE HIGHWAY RESEARCH PROGRAM

are available from:

Highway Research Board
National Academy of Sciences
2101 Constitution Avenue
Washington, D.C. 20418

Rep. No.	*Title*
—*	A Critical Review of Literature Treating Methods of Identifying Aggregates Subject to Destructive Volume Change When Frozen in Concrete and a Proposed Program of Research—Intermediate Report (Proj. 4-3(2)), 81 p., $1.80
1	Evaluation of Methods of Replacement of Deteriorated Concrete in Structures (Proj. 6-8), 56 p., $2.80
2	An Introduction to Guidelines for Satellite Studies of Pavement Performance (Proj. 1-1), 19 p., $1.80
2A	Guidelines for Satellite Studies of Pavement Performance, 85 p.+9 figs., 26 tables, 4 app., $3.00
3	Improved Criteria for Traffic Signals at Individual Intersections—Interim Report (Proj. 3-5), 36 p., $1.60
4	Non-Chemical Methods of Snow and Ice Control on Highway Structures (Proj. 6-2), 74 p., $3.20
5	Effects of Different Methods of Stockpiling Aggregates—Interim Report (Proj. 10-3), 48 p., $2.00
6	Means of Locating and Communicating with Disabled Vehicles—Interim Report (Proj. 3-4), 56 p. $3.20
7	Comparison of Different Methods of Measuring Pavement Condition—Interim Report (Proj. 1-2), 29 p., $1.80
8	Synthetic Aggregates for Highway Construction (Proj. 4-4), 13 p., $1.00
9	Traffic Surveillance and Means of Communicating with Drivers—Interim Report (Proj. 3-2), 28 p., $1.60
10	Theoretical Analysis of Structural Behavior of Road Test Flexible Pavements (Proj. 1-4), 31 p., $2.80
11	Effect of Control Devices on Traffic Operations—Interim Report (Proj. 3-6), 107 p., $5.80
12	Identification of Aggregates Causing Poor Concrete Performance When Frozen—Interim Report (Proj. 4-3(1)), 47 p., $3.00
13	Running Cost of Motor Vehicles as Affected by Highway Design—Interim Report (Proj. 2-5), 43 p., $2.80
14	Density and Moisture Content Measurements by Nuclear Methods—Interim Report (Proj. 10-5), 32 p., $3.00
15	Identification of Concrete Aggregates Exhibiting Frost Susceptibility—Interim Report (Proj. 4-3(2)), 66 p., $4.00
16	Protective Coatings to Prevent Deterioration of Concrete by Deicing Chemicals (Proj. 6-3), 21 p., $1.60
17	Development of Guidelines for Practical and Realistic Construction Specifications (Proj. 10-1,) 109 p., $6.00
18	Community Consequences of Highway Improvement (Proj. 2-2), 37 p., $2.80
19	Economical and Effective Deicing Agents for Use on Highway Structures (Proj. 6-1), 19 p., $1.20
20	Economic Study of Roadway Lighting (Proj. 5-4), 77 p., $3.20
21	Detecting Variations in Load-Carrying Capacity of Flexible Pavements (Proj. 1-5), 30 p., $1.40
22	Factors Influencing Flexible Pavement Performance (Proj. 1-3(2)), 69 p., $2.60
23	Methods for Reducing Corrosion of Reinforcing Steel (Proj. 6-4), 22 p., $1.40
24	Urban Travel Patterns for Airports, Shopping Centers, and Industrial Plants (Proj. 7-1), 116 p., $5.20
25	Potential Uses of Sonic and Ultrasonic Devices in Highway Construction (Proj. 10-7), 48 p., $2.00
26	Development of Uniform Procedures for Establishing Construction Equipment Rental Rates (Proj. 13-1), 33 p., $1.60
27	Physical Factors Influencing Resistance of Concrete to Deicing Agents (Proj. 6-5), 41 p., $2.00
28	Surveillance Methods and Ways and Means of Communicating with Drivers (Proj. 3-2), 66 p., $2.60
29	Digital-Computer-Controlled Traffic Signal System for a Small City (Proj. 3-2), 82 p., $4.00
30	Extension of AASHO Road Test Performance Concepts (Proj. 1-4(2)), 33 p., $1.60
31	A Review of Transportation Aspects of Land-Use Control (Proj. 8-5), 41 p., $2.00
32	Improved Criteria for Traffic Signals at Individual Intersections (Proj. 3-5), 134 p., $5.00
33	Values of Time Savings of Commercial Vehicles (Proj. 2-4), 74 p., $3.60
34	Evaluation of Construction Control Procedures—Interim Report (Proj. 10-2), 117 p., $5.00
35	Prediction of Flexible Pavement Deflections from Laboratory Repeated-Load Tests (Proj. 1-3(3)), 117 p., $5.00
36	Highway Guardrails—A Review of Current Practice (Proj. 15-1), 33 p., $1.60
37	Tentative Skid-Resistance Requirements for Main Rural Highways (Proj. 1-7), 80 p., $3.60
38	Evaluation of Pavement Joint and Crack Sealing Materials and Practices (Proj. 9-3), 40 p., $2.00
39	Factors Involved in the Design of Asphaltic Pavement Surfaces (Proj. 1-8), 112 p., $5.00
40	Means of Locating Disabled or Stopped Vehicles (Proj. 3-4(1)), 40 p., $2.00
41	Effect of Control Devices on Traffic Operations (Proj. 3-6), 83 p., $3.60

* Highway Research Board Special Report 80.

Rep. No.	Title
42	Interstate Highway Maintenance Requirements and Unit Maintenance Expenditure Index (Proj. 14-1), 144 p., $5.60
43	Density and Moisture Content Measurements by Nuclear Methods (Proj. 10-5), 38 p., $2.00
44	Traffic Attraction of Rural Outdoor Recreational Areas (Proj. 7-2), 28 p., $1.40
45	Development of Improved Pavement Marking Materials—Laboratory Phase (Proj. 5-5), 24 p., $1.40
46	Effects of Different Methods of Stockpiling and Handling Aggregates (Proj. 10-3), 102 p., $4.60
47	Accident Rates as Related to Design Elements of Rural Highways (Proj. 2-3), 173 p., $6.40
48	Factors and Trends in Trip Lengths (Proj. 7-4), 70 p., $3.20
49	National Survey of Transportation Attitudes and Behavior—Phase I Summary Report (Proj. 20-4), 71 p., $3.20
50	Factors Influencing Safety at Highway-Rail Grade Crossings (Proj. 3-8), 113 p., $5.20
51	Sensing and Communication Between Vehicles (Proj. 3-3), 105 p., $5.00
52	Measurement of Pavement Thickness by Rapid and Nondestructive Methods (Proj. 10-6), 82 p., $3.80
53	Multiple Use of Lands Within Highway Rights-of-Way (Proj. 7-6), 68 p., $3.20
54	Location, Selection, and Maintenance of Highway Guardrail and Median Barriers (Proj. 15-1(2)), 63 p., $2.60
55	Research Needs in Highway Transportation (Proj. 20-2), 66 p., $2.80
56	Scenic Easements—Legal, Administrative, and Valuation Problems and Procedures (Proj. 11-3), 174 p., $6.40
57	Factors Influencing Modal Trip Assignment (Proj. 8-2), 78 p., $3.20
58	Comparative Analysis of Traffic Assignment Techniques with Actual Highway Use (Proj. 7-5), 85 p., $3.60
59	Standard Measurements for Satellite Road Test Program (Proj. 1-6), 78 p., $3.20
60	Effects of Illumination on Operating Characteristics of Freeways (Proj. 5-2) 148 p., $6.00
61	Evaluation of Studded Tires—Performance Data and Pavement Wear Measurement (Proj. 1-9), 66 p., $3.00
62	Urban Travel Patterns for Hospitals, Universities, Office Buildings and Capitols (Proj. 7-1), 144 p., $5.60
63	Economics of Design Standards for Low-Volume Rural Roads (Proj. 2-6), 93 p., $4.00
64	Motorists' Needs and Services on Interstate Highways (Proj. 7-7), 88 p., $3.60
65	One-Cycle Slow-Freeze Test for Evaluating Aggregate Performance in Frozen Concrete (Proj. 4-3(1)), 21 p., $1.40
66	Identification of Frost-Susceptible Particles in Concrete Aggregates (Proj. 4-3(2)), 62 p., $2.80

THE NATIONAL ACADEMY OF SCIENCES is a private, honorary organization of more than 700 scientists and engineers elected on the basis of outstanding contributions to knowledge. Established by a Congressional Act of Incorporation signed by President Abraham Lincoln on March 3, 1863, and supported by private and public funds, the Academy works to further science and its use for the general welfare by bringing together the most qualified individuals to deal with scientific and technological problems of broad significance.

Under the terms of its Congressional charter, the Academy is also called upon to act as an official—yet independent—adviser to the Federal Government in any matter of science and technology. This provision accounts for the close ties that have always existed between the Academy and the Government, although the Academy is not a governmental agency and its activities are not limited to those on behalf of the Government.

THE NATIONAL ACADEMY OF ENGINEERING was established on December 5, 1964. On that date the Council of the National Academy of Sciences, under the authority of its Act of Incorporation, adopted Articles of Organization bringing the National Academy of Engineering into being, independent and autonomous in its organization and the election of its members, and closely coordinated with the National Academy of Sciences in its advisory activities. The two Academies join in the furtherance of science and engineering and share the responsibility of advising the Federal Government, upon request, on any subject of science or technology.

THE NATIONAL RESEARCH COUNCIL was organized as an agency of the National Academy of Sciences in 1916, at the request of President Wilson, to enable the broad community of U. S. scientists and engineers to associate their efforts with the limited membership of the Academy in service to science and the nation. Its members, who receive their appointments from the President of the National Academy of Sciences, are drawn from academic, industrial and government organizations throughout the country. The National Research Council serves both Academies in the discharge of their responsibilities.

Supported by private and public contributions, grants, and contracts, and voluntary contributions of time and effort by several thousand of the nation's leading scientists and engineers, the Academies and their Research Council thus work to serve the national interest, to foster the sound development of science and engineering, and to promote their effective application for the benefit of society.

THE DIVISION OF ENGINEERING is one of the eight major Divisions into which the National Research Council is organized for the conduct of its work. Its membership includes representatives of the nation's leading technical societies as well as a number of members-at-large. Its Chairman is appointed by the Council of the Academy of Sciences upon nomination by the Council of the Academy of Engineering.

THE HIGHWAY RESEARCH BOARD, organized November 11, 1920, as an agency of the Division of Engineering, is a cooperative organization of the highway technologists of America operating under the auspices of the National Research Council and with the support of the several highway departments, the Bureau of Public Roads, and many other organizations interested in the development of highway transportation. The purposes of the Board are to encourage research and to provide a national clearinghouse and correlation service for research activities and information on highway administration and technology.

HIGHWAY RESEARCH BOARD
NATIONAL ACADEMY OF SCIENCES—NATIONAL RESEARCH COUNCIL
2101 Constitution Avenue Washington, D. C. 20418

ADDRESS CORRECT

DP-8,9,11,12,MC,19,22,S,38
Materials Engineer
Idaho Dept. of Highways
P.O. Box 7129
Boise, Idaho 83707